



Molecular and physiological responses during thermal acclimation of leaf photosynthesis and respiration in rice

Journal:	<i>Plant, Cell & Environment</i>
Manuscript ID	PCE-19-1106.R1
Wiley - Manuscript type:	Original Article
Date Submitted by the Author:	n/a
Complete List of Authors:	Rashid, Fatimah; Australian National University, Research School of Biology; Sultan Idris education University, Department of Biology Crisp, Peter; University of Minnesota, Department of Plant and Microbial Biology Zhang, You; CSIRO Plant Industry Berkowitz, Oliver; La Trobe University, Dept. of Animal, Plant and Soil Science / ARC Centre of Excellence in Plant Energy Biology Pogson, Barry; Australian National University, Research School of Biology Day, David A.; Flinders University, College of Science & Engineering Masle, Josette; Australian National University, Research School of Biology Dewar, Roderick; Australian National University, Research School of Biology Whelan, James; La Trobe University, Dept. Animal, Plant and Soil Sciences Atkin, Owen; Australian National University, ARC Centre of Excellence in Plant Energy Biology, Division of Plant Sciences Scafaro, Andrew; Australian National University, Research School of Biology
Environment Keywords:	heat, cold
Physiology Keywords:	respiration, photosynthesis: carbon reactions
Other Keywords:	acclimation, cytochrome c oxidase (COX), rice, RNA-seq
Abstract:	To further our understanding of how sustained changes in temperature affect the carbon economy of rice (<i>Oryza sativa</i>), hydroponically-grown plants of the IR64 cultivar were developed at 30/25°C (day/night) before being shifted to 25/20°C or 40/35°C. Leaf mRNA and protein abundance, sugar and starch concentration, gas-exchange and elongation rates were measured on pre-existing leaves (PE) already developed at 30/25°C, or leaves newly-developed (ND) subsequent to temperature transfer. Following a shift in growth temperature, there was a transient adjustment in metabolic gene transcript abundance of PE leaves before homeostasis was reached within 24 h, aligning with R_{dark} (leaf dark respiratory CO ₂ release) and A_n (net CO ₂ assimilation) changes. With longer exposure, the central respiratory protein CYTOCHROME C OXIDASE (COX) declined in abundance at 40/35°C. In contrast to R_{dark} ,

	<p>A_n was maintained across the three growth temperatures in ND leaves. Soluble sugars did not differ significantly with growth temperature, and growth was fastest with extended exposure at 40/35°C. The results highlight that acclimation of photosynthesis and respiration is asynchronous in rice, with heat-acclimated plants exhibiting a striking ability to maintain net carbon gain and growth when exposed to heat-wave temperatures, even while reducing investment in energy-conserving respiratory pathways.</p>

SCHOLARONE™
Manuscripts

Molecular and physiological responses during thermal acclimation of leaf photosynthesis and respiration in rice

Fatimah Azzahra Ahmad Rashid^{1,2}, Peter A. Crisp³, You Zhang⁴, Oliver Berkowitz⁵, Barry J. Pogson^{1#}, David A. Day^{6,7}, Josette Masle⁸, Roderick C. Dewar⁸, James Whelan^{5#}, Owen K. Atkin^{1#}, Andrew P. Scafaro¹

¹ Australian Research Council Centre of Excellence in Plant Energy Biology, Research School of Biology, The Australian National University, Canberra, ACT, 2601, Australia

² Current address: Department of Biology, Faculty of Science and Mathematics, Sultan Idris education University, 35900 Tanjung Malim, Perak, Malaysia

³ Department of Plant and Microbial Biology, University of Minnesota, Saint Paul, MN, 55108 USA

⁴ CSIRO Plant Industry, GPO Box 1700, Canberra, ACT, 2601, Australia

⁵ Australian Research Council Centre of Excellence in Plant Energy Biology, School of Life Science, AgriBio Building, La Trobe University, Bundoora, Victoria, 3083, Australia

⁶ College of Science and Engineering, Flinders University, South Australia, 5001, Australia

⁷ Department of Animal, Plant and Soil Sciences, AgriBio Building, La Trobe University, 5 Ring Road, Bundoora, VIC, 3086, Australia

⁸ Research School of Biology, The Australian National University, Canberra, ACT, 2601, Australia

The support of the Australian Research Council (ARC) Centre of Excellence in Plant Energy Biology (CE140100008) is acknowledged

Abstract

To further our understanding of how sustained changes in temperature affect the carbon economy of rice (*Oryza sativa*), hydroponically-grown plants of the IR64 cultivar were developed at 30/25°C (day/night) before being shifted to 25/20°C or 40/35°C. Leaf mRNA and protein abundance, sugar and starch concentrations, gas-exchange and elongation rates were measured on pre-existing leaves (PE) already developed at 30/25°C, or leaves newly-developed (ND) subsequent to temperature transfer. Following a shift in growth temperature, there was a transient adjustment in metabolic gene transcript abundance of PE leaves before homeostasis was reached within 24 h, aligning with R_{dark} (leaf dark

34 respiratory CO₂ release) and A_n (net CO₂ assimilation) changes. With longer exposure, the central
35 respiratory protein CYTOCHROME C OXIDASE (COX) declined in abundance at 40/35°C. In
36 contrast to R_{dark} , A_n was maintained across the three growth temperatures in ND leaves. Soluble sugars
37 did not differ significantly with growth temperature, and growth was fastest with extended exposure
38 at 40/35°C. The results highlight that acclimation of photosynthesis and respiration is asynchronous
39 in rice, with heat-acclimated plants exhibiting a striking ability to maintain net carbon gain and growth
40 when exposed to heat-wave temperatures, even while reducing investment in energy-conserving
41 respiratory pathways.

42

43 **Keywords:** rice, thermal stress, acclimation, respiration, photosynthesis, heat, cold, CYTOCHROME
44 C OXIDASE (COX)

45

46 **Introduction**

47

48 The response of net CO₂ assimilation (A_n) and leaf respiration in the dark (R_{dark}) to changes in
49 temperature (T) is often dynamic. Acclimation – i.e. physiological changes that enable adjustments in
50 the rate of A_n and R_{dark} at a given measuring T in response to sustained changes in growth T – occurs
51 in many species, in natural and controlled environments (Atkin, Bruhn, Hurry, & Tjoelker, 2005; Berry
52 & Bjorkman, 1980; Campbell et al., 2007; Reich et al., 2016; Smith & Dukes, 2017; Tjoelker, Oleksyn,
53 & Reich, 2001). Acclimation can also lead to metabolic homeostasis, where similar rates of A_n and
54 R_{dark} are exhibited by hot- and cold-acclimated plants, when compared at their respective growth T s.
55 Determining the extent to which R_{dark} and A_n acclimate to sustained changes in T is of growing interest,
56 as global warming is resulting in plants of natural and managed ecosystems experiencing higher
57 average growth T s, often in conjunction with more frequent and severe heat waves (CSIRO & BOM,
58 2018; Hartmann et al., 2013). The impact of heat on A_n and R_{dark} of cereal crops, including rice (*Oryza*
59 *sativa*), is of particular interest given the need to increase food production to meet the requirements of
60 a growing and more affluent world population (Godfray et al., 2010). Rice contributes substantially to
61 global food demand, particularly in Asia where it makes up more than 30% of all dietary energy intake
62 (Seck, Diagne, Mohanty, & Wopereis, 2012). However, in recent years rice yields have declined in
63 regions such as South-East Asia, with the declines being more strongly correlated with nightly
64 minimum than daytime maximum T s (Peng et al., 2004; Welch et al., 2010). Reduced yields and grain
65 quality were also observed for rice in North America when exposed to warmer night T (Lanning,
66 Siebenmorgen, Counce, Ambardekar, & Mauromoustakos, 2011). Given this, and the likely
67 importance of A_n and R_{dark} for biomass and grain production (Posch et al., 2019; Yoshida, 1972), it is

68 crucial that we develop a better understanding of how changes in T affect these key metabolic
69 processes in rice.

70 In rice and a range of other crops, RNA sequencing analysis has shown large scale
71 perturbations to the transcript profile of plants exposed to colder or warmer T , with the changes
72 occurring over a period of hours to days and across multiple functional categories, but especially in
73 genes involved in primary metabolism (Bhardwaj et al., 2015; Hu, Sun, Zhang, Nevo, & Fu, 2014;
74 Shen et al., 2014). The vast gene expression response to T -perturbations is likely mediated through
75 heat shock transcription factors, which regulate changes in transcriptional networks. These are induced
76 by heat stress and other abiotic stimuli, changing the protein complement of a cell (Morimoto, 1998;
77 Ohama, Sato, Shinozaki, & Yamaguchi-Shinozaki, 2017). However, changes in protein abundance
78 may not necessarily match changes in transcript abundance due to transcription and RNA turnover
79 rates being influenced by T (Sidaway-Lee, Costa, Rand, Finkenstadt, & Penfield, 2014), and post-
80 transcriptional regulation. In cases where heat stress results in changes in protein abundance, the
81 greatest changes are seen in proteins associated with primary metabolism, with about 50% of all leaf
82 protein abundance changes seeming to be in A_n and R_{dark} metabolic pathways (Scafaro & Atkin, 2016).
83 In rice, cold-stress similarly perturbs a large proportion of energy metabolism pathways (Neilson,
84 Mariani, & Haynes, 2011), emphasising the importance of changes in protein abundance in
85 chloroplasts and mitochondria as part of the thermal acclimation process. There is growing evidence
86 that plants can acclimate to T variations by stimulating energy metabolism at colder T and suppressing
87 energy metabolism at warmer T , either through regulation of enzymatic velocities or changes in
88 enzyme abundance (Armstrong et al., 2008; Badger, Björkman, & Armond, 1982; Campbell et al.,
89 2007; Hikosaka, Ishikawa, Borjigidai, Muller, & Onoda, 2006; Scafaro et al., 2017; Strand et al., 1999;
90 Yamori, Noguchi, & Terashima, 2005). Whether the same is true for rice remains unclear, both for
91 pre-existing (PE) leaves that experience a sustained change in growth T , and in newly-developed (ND)
92 leaves that form under a new thermal regime. In species other than rice, the extent of changes
93 underpinning thermal acclimation (including changes in leaf structure, nitrogen partitioning and
94 organelle abundance), is typically greater in ND than PE leaves (Armstrong et al., 2008; Gorsuch,
95 Pandey, & Atkin, 2010; O'Leary, Asao, Millar, & Atkin, 2018; Tjoelker, Reich, & Oleksyn, 1999;
96 Yamori et al., 2005).

97 Past studies on rice conducted during the vegetative (Glaubitz et al., 2014; Kurimoto, Day,
98 Lambers, & Noguchi, 2004) and reproductive (Bahuguna, Solis, Shi, & Jagadish, 2017; Mohammed,
99 Cothren, & Tarpley, 2013) phases of development have reported limited and variable levels of
100 acclimation of R_{dark} . By contrast, A_n of rice shows strong thermal acclimation, with rates of net CO_2
101 uptake measured at the prevailing growth T being homeostatic or increasing as growth T is increased

102 from 15 to 37°C (Nagai & Makino, 2009; Yamori, Noguchi, Hikosaka, & Terashima, 2010). Such
103 studies point to a possible asynchrony in rice acclimation, with a more dynamic A_n than R_{dark} response,
104 although further work simultaneously comparing A_n and R_{dark} in rice is needed. Interestingly, a range
105 of other crops and non-crop species show the opposite – greater R_{dark} than A_n acclimation capacity
106 (Campbell et al., 2007; Drake et al., 2016; Way & Oren, 2010). Although such studies detail the
107 physiological acclimation of energy metabolism in plants, including rice, less is known about the
108 molecular and biochemical responses that underpin this phenotypic T acclimation.

109 It is with the above issues in mind that we conducted a study using the IR64 cultivar of *Oryza*
110 *sativa* to address the following aims: (1) characterise the extent of thermal acclimation of R_{dark} and A_n ;
111 and, (2) link physiological acclimation to the underlying processes through analysis of leaf transcript,
112 protein, sugar, and starch abundance, following changes in growth T . We hypothesized that: (1) initial
113 exposure to very high growth T increases and decreases the rates of respiratory CO_2 release and net
114 photosynthetic CO_2 uptake, respectively; (2) subsequent acclimation is associated with recovery of A_n ,
115 and reduced rates of R_{dark} ; and (3) thermal acclimation of R_{dark} and A_n is associated with dynamic
116 changes in gene expression and protein abundance in key pathways associated with energy capture
117 and use.

118

119 **Materials and methods**

120

121 *Plant material and temperature treatments*

122 Rice (*Oryza sativa*) cultivar IR64 plants were grown hydroponically in a glasshouse facility at the
123 Research School of Biology, Australian National University in Canberra between October and
124 December 2015. Seeds were initially incubated at 40-42°C for two days before soaking in water for
125 eight hours, placed on wet Whatman filter papers in petri dishes and kept in the dark at 30°C for five
126 days. The germinated seedlings were then transferred to trays of vermiculite and placed in temperature-
127 controlled glasshouses (30°C day and 25°C night) under natural sunlight and photoperiod, with
128 photosynthetically active radiation (PAR) between 400 and 1200 $\mu\text{mol m}^{-2} \text{s}^{-1}$. When the third leaf had
129 emerged, seedlings were transplanted from vermiculite to a hydroponic system. Individual plants were
130 placed within PVC tubes with a 3.7 cm diameter and 13 cm height. Tubes were then suspended at the
131 top of 20 L capacity hydroponic tanks (12 tanks in total), with each tank holding a maximum of 20
132 plants. Each tank was filled with hydroponic solution (Table S1) (Hubbart, Peng, Horton, Chen, &
133 Murchie, 2007). The nutrient solution was replaced weekly. Sulphuric acid or sodium hydroxide were
134 used to adjust the pH to 5-6, with pH monitored using a portable pH meter (Rowe Scientific Pty. Ltd.,

135 NSW, Australia). The hydroponic solution was aerated continuously using Infinity AP-950 air pumps
136 (Kong's Pty. Ltd., Ingleburn, Australia).

137 After two weeks of hydroponic growth at 30/25°C ('warm' treatment), the most recently fully-
138 expanded leaves were labelled as pre-existing (PE) leaves. Following labelling, four tanks were
139 randomly chosen and shifted to an adjacent glasshouse room set to 25°C day and 20°C night (25/20°C –
140 'cold' treatment), and four other tanks were moved to a room set at 40°C day and 35°C night (40/35°C
141 – 'hot' treatment); four tanks were retained at 30/25°C as controls. Relative humidity was not
142 controlled. Newly-developed (ND) leaves that emerged under each thermal regime were labelled, with
143 all measurements reported on ND leaves made 21 days after *T*-transfer.

144

145 *Determination of transcript abundance*

146 Plants were transferred to new thermal regimes three hours after sunrise. To quantify transcript
147 abundance, the labelled pre-existing (PE) leaves were harvested during the photoperiod: two, six and
148 24 h after *T*-transfer. For each time-point and temperature treatment, approximately 8 cm long
149 segments (less than 100 mg of fresh mass) were sampled half-way along the leaf blade, and
150 immediately frozen in liquid N₂ and stored at -80°C until RNA extraction. Total RNA was extracted
151 using the RNeasy plant mini protocol (Qiagen, Doncaster, VIC, AU) and treated with DNase I (Qiagen,
152 Doncaster, VIC, AU) to remove any contaminating DNA.

153 For qPCR analysis, 1 µg of total RNA in a 10 µL volume was reverse-transcribed into cDNA
154 using SuperScript III First-Strand cDNA Synthesis Kit (Invitrogen, Carlsbad, CA, USA), according to
155 the manufacturer's instructions. The reverse-transcribed cDNA samples were diluted 10-fold.
156 Transcript levels of six selected genes and one reference gene (refer to Table S2 for gene accession
157 numbers and primer sequences) were analysed using a Light-Cycler® 480 System (Roche Holding
158 AG, Basel, Switzerland) with SYBR Green I Dye (QIAGEN, Doncaster, Victoria, AU). cDNA
159 samples from each biological replicate were assayed in two technical duplicates. The reaction-mix in
160 each qPCR contained 0.4 µM of each pair of primers, 5 µL of SYBR Master Mix, and 4.6 µL of the
161 diluted cDNA sample in a 10 µL total reaction volume. The raw fluorescence data were analysed using
162 LinRegPCR (Ramakers, Ruijter, Deprez, & Moorman, 2003; Ruijter et al., 2009). Data were
163 normalized to the reference gene, eukaryotic initiation factor 5c (*EIF5C*; LOC_Os11g21990.1), and
164 were expressed as fold-changes against control conditions.

165 RNAseq libraries were prepared using the Illumina Stranded Total RNAseq kit with RiboZero
166 rRNA depletion as per the manufacturer's guidelines (Illumina). Libraries were pooled and sequenced
167 on a HiSeq1500 for 61 cycles in single end mode at the Centre for AgriBioscience, University of
168 LaTrobe. Analysis pipelines for pre-processing and mapping of sequence data are available online on

169 GitHub (<https://github.com/pedrocrisp/NGS-pipelines>). Quality control was performed with *FastQC*
170 v.0.11.2. Adapters were removed using *scythe* v.0.991 with flags -p 0. and reads were quality trimmed
171 with *sickle* v.1.33 with flags -q 20 (quality threshold), and -l 20 (minimum read length after trimming).
172 The trimmed and quality-filtered reads were aligned to the rice reference genome Os-Nipponbare-
173 Reference-IRGSP-1.0 from the MSU Rice Genome Annotation Project Database v7
174 (<http://rice.plantbiology.msu.edu/>) using the *subjunc* aligner v1.5.0-p1 with -u and -H flags to report
175 only reads with a single unambiguous best mapping location, -P 3 for phred+33 encoding (Liao, Smyth,
176 & Shi, 2013b). Reads were then sorted, indexed and compressed using *samtools* v1.1-26-g29b0367
177 (Li et al., 2009) and strand-specific bigwig files were generated using *bedtools genomecov* v2.16.1
178 (Quinlan & Hall, 2010) and the UCSC utility *bedGraphToBigWig* for viewing in IGV (Robinson et
179 al., 2011). Summary statistics for each sample are provided in Supplementary Dataset S1: Summary
180 of transcriptomic datasets.

181 For standard differential gene expression testing, the number of reads mapping per IRGSP-
182 1.0 gene loci was summarised using *featureCounts* v1.5.0-p1 (Liao, Smyth, & Shi, 2013a) with flags
183 -P and -c to discard read pairs mapping to different chromosomes and the -s flag set to 2 for strand
184 specificity for a strand specific library, multimapping reads and multioverlapping reads were not
185 counted. Reads were summarised to parent IRGSP-1.0 gene loci rather than individual splice variants
186 by summarising to the genomic coordinates defined by the feature "gene" in the IRGSP-1.0.gff
187 reference (last modified 7/2/2012
188 ftp://ftp.plantbiology.msu.edu/pub/data/Eukaryotic_Projects/o_sativa/annotation_dbs/pseudomolecules/version_7.0/all.dir/all.gff3). Only loci
189 with an abundance of at least 1 CPM (approximately 5 reads) in at least 4 samples were retained.
190 Statistical testing for relative gene expression was performed in R following the “*edgeR-limma-*
191 *voom*” approach (<https://www.bioconductor.org/help/workflows/RNAseq123/>); using, *edgeR* v.3.4.2
192 (McCarthy, Chen, & Smyth, 2012; Robinson & Oshlack, 2010; Robinson & Smyth, 2007a, 2007b),
193 and *voom* in the *limma* package 3.20.1 (Law, Chen, Shi, & Smyth, 2014; Smyth, Michaud, & Scott,
194 2005).

195

196 *Determination of protein abundance*

197 Samples of frozen PE leaf material six and 24 h after *T* transfer, as well as frozen ND leaf material,
198 were ground to a fine powder using a chilled mortar and pestle, and protein was extracted in extraction
199 buffer containing 100 mM tricine pH 8.0, 1 mM EDTA, 1 mM PMSF, 1x protease inhibitor cocktail,
200 2% (w/v) PVPP, 10 mM (w/v) ascorbate, 5 mM DTT, and distilled water. The sample was then
201 solubilized in a NuPAGE LDS Sample Buffer (Invitrogen, Carlsbad, CA, USA) with 10% (v/v) DTT,
202 then heated for 10 minutes at 95°C, and centrifuged for 30 sec at 12,000 RPM. Thereafter, supernatant

203 was collected and 8 μ L were loaded and separated on 4-12% NuPAGE Bis-Tris gel (Invitrogen,
204 Carlsbad, CA, USA) using the MOPS-based buffer system. To blot, proteins from the gel were
205 transferred to Immobilon-P Polyvinylidene fluoride (PVDF) membranes (Merck Millipore, Kilsyth,
206 VIC, AU) using an XCell II Blot module (Invitrogen, Carlsbad, CA, USA). Membranes were then
207 blocked for 2 h with 5% (w/v) skim-milk powder in Tris-buffered saline containing 0.1% (v/v) Tween-
208 20 (TBST). To probe for cytochrome *c* oxidase (*COX*) subunit II, alternative oxidase (*AOX*),
209 uncoupling protein (*UCP*) and voltage-dependent anion-selective channel protein (*VDAC1*-porin), the
210 membranes were incubated for 2 h in primary antibody solution (5% w/v skim milk powder in TBST)
211 containing commercially available polyclonal antibodies (Agrisera, Vännäs, Västerbotten, Sweden).
212 All antibodies were diluted 1:5000. An antibody for ribulose-1,5-bisphosphate carboxylase/oxygenase
213 (Rubisco) was received from Assoc. Prof. Spencer Whitney (Research School of Biology, Australian
214 National University, Canberra, ACT, AU) and used at a dilution of 1:10 000. After washing with TBST,
215 the membranes were incubated for 1 h in goat anti-rabbit antibody solution (5% w/v skim milk powder
216 in TBST) at a dilution of 1:8000. Proteins were then visualized using the AttoPhos AP fluorescent
217 substrate system (Promega, Madison, WI, USA), imaged using a Versa-Doc (Bio-Rad, Hercules, CA,
218 USA) imaging system and quantified using Image Lab software (Bio-Rad, Hercules, CA, USA).
219 Protein concentrations were determined by the Bradford method using Bovine Serum Albumin (BSA)
220 as a standard.

221

222 *Determination of soluble sugar and starch concentrations*

223 Starch and soluble sugars of PE leaves transferred from 30/25°C to 25/20°C or 40/35°C for one and
224 seven days, and ND leaves at the prevailing *T* were collected from separate, previously unsampled
225 plants. Samples were collected at 9:30 to 10:00 am, corresponding to 3 h into the light period, frozen
226 and stored at -80°C before freeze-drying at -105°C for two days (Virtis Benchtop™ “K”, SP, Scientific,
227 Gardiner, NY, USA), then ground to a fine powder from which a 5-10 mg aliquot was taken. Five-
228 hundred μ L of 80% (v/v) ethanol was added and vortexed for 20 sec. Thereafter, leaf tissues were
229 incubated at 80°C while being centrifuged at 500 RPM for 20 min. Following further centrifugation at
230 12,000 RPM for 5 min, the resulting pellet and supernatant were separated. This procedure was
231 repeated a two more times, and the three pellets and three supernatants were pooled. The pooled
232 supernatants and pellets were used for determination of soluble sugars and starch concentrations, using
233 a Fructose Assay Kit (Sigma-Aldrich, St Louis, MO, USA) and a Total Starch Assay Kit (Megazyme,
234 Chicago, IL, USA), respectively. Following manufacturer’s instructions, measurements were made in
235 triplicate, at a wavelength of 340 nm, using a microtitre plate reader (Infinite® M1000 Pro; Tecan US,

236 Morrisville, NC) and standard curves were generated for soluble sugars using sucrose, glucose and
237 fructose (Sigma-Aldrich, St Louis, MO, USA) at known concentrations.

238

239 *Gas exchange measurements using Licor 6400XT 6 cm² cuvettes*

240 Gas-exchange was measured on fully-expanded pre-existing (PE) leaves just prior to- and one, two,
241 three, five and seven days after *T* transfer, as well as on fully-expanded newly-developed (ND) leaves
242 21 days after transfer, using two matched LI-6400 instruments equipped with 6 cm² cuvettes and a
243 6400-02B red-blue light source (Li-Cor, Lincoln, NE, USA). At each time point, light-saturated net
244 CO₂ assimilation rates (A_n) and then dark respiration rates (R_{dark}) were measured during the light period
245 (between 10 am and 2 pm) in the glasshouses, at the prevailing day-time *T* of each treatment as well
246 as at a common temperature of 30°C for ND leaves. In call cases, A_n was measured first, with the
247 following settings: 1000 $\mu\text{mol m}^{-2} \text{s}^{-1}$ photosynthetic photon flux density (PPFD), relative humidity
248 of 60–70%, 400 ppm reference CO₂, and a flow rate of 500 $\mu\text{mol s}^{-1}$. Photosynthesis was measured
249 when CO₂ concentrations in the sample IRGA had stabilized, typically within 10 minutes of exposure
250 to 1000 $\mu\text{mol m}^{-2} \text{s}^{-1}$ PPFD. Thereafter, R_{dark} was measured as above but with the flow rate slowed to
251 300 $\mu\text{mol s}^{-1}$ and turning off the light source for at least 30 minutes of darkness before taking
252 measurements.

253

254 *Gas exchange measurements using using Walz chambers*

255 High resolution temperature response curves of R_{dark} and light-saturated A_n were made on intact ND
256 leaves using two matched LI-6400XT portable gas exchange systems (Li-Cor, Lincoln, NE, USA)
257 each connected to a 14 x 10 cm well-mixed, temperature-controlled Walz Gas-Exchange Chamber
258 3010-GWK1 (Heinz Walz GmbH, Effeltrich, Germany). For each temperature-response curve, leaf *T*
259 was measured with a small-gauge wire copper constantan thermocouple pressed against the lower
260 surface of the leaf and attached to a LI-6400 external thermocouple adaptor (LI6400-13, Li-Cor Inc.,
261 Lincoln, NE, USA) that enabled leaf temperature to be recorded by the LI-6400XT. As leaves were
262 heated, net CO₂ exchange was recorded at 30 s intervals using the LI-6400XT portable gas exchange
263 systems fitted with an empty and closed 6 cm² chamber that was plumbed into the airstream exiting
264 the Walz leaf chamber (Fig. S1). A_n was measured as described for the 6 cm² cuvette but using a Walz
265 LED-Panel RGBW-L084 light source (Heinz Walz GmbH, Effeltrich, Germany). A_n was monitored
266 as leaves were heated at 1°C min⁻¹ from 20 to 45°C. A water trap was used to remove water vapour,
267 as transpiration from whole intact leaves was incompatible with Licor instrumentation. Therefore,
268 stomatal conductance (g_s) and associated water parameters were not recorded. For R_{dark} , on separate
269 leaves to those used for measuring A_n , the flow rate was reduced to 300 $\mu\text{mol s}^{-1}$, the light source was

270 turned off, and the chamber was covered with a black cloth, before increasing the leaf temperature in
271 steps of $1^{\circ}\text{C min}^{-1}$, from 20 to 60°C . In parallel to quantifying the temperature-response of R_{dark} , we
272 measured minimal chlorophyll *a* fluorescence (F_o) in the presence of a low-intensity far-red light pulse
273 (necessary to maintain PSII in the oxidized state) every 30 sec using a Mini-PAM portable chlorophyll
274 fluorometer (Heinz Walz, Effeltrich, Germany) fitted above the glass surface of the leaf chamber. The
275 temperature at which F_o increased was used as an indication of heat-induced damage to photosystem
276 II, which we hereafter refer to as T_{crit} , calculated using the template of O'Sullivan *et al.* (2013). At the
277 cessation of measurements, leaves were photographed and analysed for leaf area using ImageJ
278 software (Abramoff, Magelhaes, & Ram, 2004). Leaves were stored in paper bags, oven-dried at 70°C
279 for two days and weighed to obtain the dry mass. Quadratic equations were fit to A_n temperature curves
280 and the x- and y-axis values corresponding to the vertex taken as the T -optimum (T_{opt}) and A_n -optimum
281 (A_{opt}) of net assimilation, respectively. For the R_{dark} temperature curves, the x- and y-axis values
282 corresponding to the maximum recorded R_{dark} were taken as the T at which R_{dark} reached a maximum
283 (T_{max}) and the maximum R_{dark} value recorded (R_{max}), respectively.

284

285 *Leaf elongation rates*

286 The leaf elongation rates (LER) of four leaves from separate plants from each temperature regime were
287 measured at five separate time-points over a 24 h period. Measurements were made using a ruler,
288 starting from the ligule of the second youngest leaf to its tip.

289

290 *Statistical analysis*

291 For all T -treatments and collection times, four separate leaves from four separate previously unsampled
292 plants, one plant from each of the four hydroponic tanks (pot replicates) were sampled. One-way
293 Analysis of Variance (ANOVA) was performed on R_{dark} and A_n gas-exchange experiments comparing
294 temperature treatments. Two-way ANOVA was performed on LMA and protein, starch, and sugar
295 concentrations comparing time of sampling and temperature treatments. Gas-exchange and leaf
296 biochemical statistical analysis was performed using GraphPad Prism (v 7) software. Statistical
297 analysis of transcript abundance was performed using *R* statistical software (v 3.6.1) and packages as
298 mentioned above.

299

300 *Data availability*

301 RNA-seq data is available under the GEO identifier GSE136045.

302

303 **Results**

304

305 *Molecular and biochemical responses of leaves to T*

306 Quantitative PCR was performed on specific genes of interest to elucidate the genetic response of pre-
307 existing (PE) leaves exposed to a change in *T* (Fig. 1). Apart from a sharp rise 6 h into the 40/35°C *T*-
308 transfer, there was a general reduction in transcript abundance of *cytochrome c oxidase (cox)*, a gene
309 encoding the central respiratory electron transport chain. This reduction occurred in leaves transferred
310 to 25/20°C and 40/35°C, over the seven days post-transfer period, . Two genes encoding respiratory
311 proteins that potentially reduce the production of ATP – *alternative oxidase (aox)* and *uncoupling*
312 *protein (ucp)* – both showed an initial increase in expression within the first 24 h of transfer to the
313 hotter 40/35°C, followed by a decline to 30/25°C levels by 48 h. The photosynthetic electron transport
314 gene *ferredoxin NADP reductase (fnr)*, and the Calvin/Benson cycle gene *phosphoribulokinase (prk)*
315 generally showed an increase in expression in the first 48 h at 40/35°C before being suppressed for up
316 to 5 days post-transfer. *Sucrose phosphate synthase (sps)*, involved in the synthesis of sucrose from its
317 precursors, also initially spiked in the first 24 h following transfer to 40/35°C, before being transiently
318 suppressed. Both *sps* and the respiratory and photosynthetic genes – apart from *aox* – followed a
319 similar expression profile when heat-treated, suggesting that assimilate production/consumption and
320 sucrose synthesis were coordinated in response to heat perturbations. In general, the greatest
321 perturbation to gene expression occurred within the first 24 h after transfer.

322 Based on the qPCR results, we conducted RNA-seq at two, six and 24 h after transfer of PE
323 leaves to new *T*. Following data quality control and filtering, transcript abundance of 19,308 rice genes
324 were retained for differential expression testing. Around 20 M reads were obtained per sample, which
325 were aligned to the Os-Nipponbare-Reference-IRGSP-1.0 rice reference genome (Data Set S1).
326 Principal component analysis showed a substantial treatment effect on gene expression for the heat-
327 exposed leaves (40/35°C) during the first six hours after *T*-transfer compared to the other two 30/25°C
328 and 25/20°C growth regimes (Fig. 2). Globally, there was little gene expression variation between the
329 cold (25/20°C) and the warm (30/25°C) control conditions. After 24 h of growth at new *T*-regimes,
330 limited variation in gene expression was observed between all of the three *T*s (Table S3).

331 To assess changes in the expression of individual genes to the hot or cold treatments,
332 differentially expressed genes were identified at each time point by comparison to the warm control
333 expression levels (Data Set S2). There were very few genes differentially expressed under the cold
334 conditions, only six genes in total (Table S3). By contrast, under hot conditions, there were 1,818 and
335 1,465 genes differentially expressed after two and six hours, respectively. After 24 hours, there were
336 no differentially expressed genes under the hot conditions compared to the control plants. There was

337 a significant overlap between the genes differentially expressed after two and six hours of heat
338 treatment, (Fig. 3a, b). In total, 30% of the genes upregulated after six hours were already upregulated
339 by two hours, and 38% of genes downregulated after six hours were already downregulated by two
340 hours. Many of the remaining genes that were significantly different in transcript abundance only after
341 six hours were already trending in the same direction at the two-hour time point, but the difference
342 compared to the controls did not pass the significance threshold (Fig. 3 c). Overall, these results show
343 that there are significant short-term changes in transcript abundance in rice plants exposed to heat
344 stress. The expression profiles of samples exposed for two and six hours show consistent changes;
345 however, some of the changes peak at two hours and others peak at six hours and most changes
346 dissipate within 24 hours.

347 In total, the heat treatment led to the up- and down-regulation of 1,337 and 1,446 genes,
348 respectively. To investigate the extent to which these genes have a photosynthetic or respiratory
349 function, we first examined expression of genes involved in photosynthesis, glycolysis, TCA and
350 mitochondrial electron transport using MapMan pathway annotations (Fig. S2-4) (Thimm et al., 2004).
351 This qualitative analysis revealed that the expression of only a small number of
352 photosynthetic/respiratory genes were affected. To extract a list of high-confidence differentially
353 expressed respiration-related genes, we manually curated a list of rice loci with homology to
354 Arabidopsis respiration genes (Data Set S3). Using this list, we found that eight genes were
355 differentially expressed at high temperature, with two genes downregulated more than 2-fold: *aox* and
356 ATP-dependent *phosphofructokinase* (Table 1). The seemingly conflicting result of an initial increase
357 in *aox* from the qPCR results, but a decline in *aox* during the same period from the RNA-seq results,
358 can be explained by our qPCR primers targeting the *aox1a* isoform while the RNA-seq identified a
359 decline in the *aox1c* isoform (Data Set S3).

360 It is interesting that in addition to the increase in *aox* and *ucp* gene expression, the expression
361 of an external NAD(P)H dehydrogenase also increased, while that of Complex II decreased
362 significantly (Table 1). Together these changes suggest that an increase in non-phosphorylating
363 electron transport occurred in response to exposure to higher *T*, at the expense of electron transport
364 coupled to ATP synthesis, at least in the short term. The increase in external NAD(P)H dehydrogenase
365 gene expression may also indicate an increased need for mitochondrial oxidation of excess reductant
366 produced in the chloroplast at higher *T*.

367 Given the relatively small effect of the heat treatment on the expression of respiration- or
368 photosynthesis-related genes, we next performed Gene Ontology enrichment analysis. This revealed a
369 notable enrichment for genes involved in primary metabolism (eg GO:0044238) and response to
370 abiotic stimuli (eg GO:0050896), as well as in many biosynthetic pathways (Fig 4).

371 Protein abundance (expressed on a leaf area basis) of key mitochondrial electron transport
372 components – CYTOCHROME C OXIDASE (COX) subunit II, ALTERNATIVE OXIDASE (AOX)
373 and UNCOUPLING PROTEIN (UCP) – were determined by Western blots in PE leaves 6 h and one-
374 day after *T*-transfer, and in newly developed (ND) leaves that formed under each prevailing growth *T*
375 (Fig. 5, Fig. S4). The cold (20/25°C) and heat (40/35°C) treatments did not affect the total protein
376 concentration of leaves, at any time after *T*-transfer (Table S4). As was the case for gene expression,
377 there was a significant decline in COX subunit II protein abundance after 24 h. COX subunit II also
378 declined in abundance in ND leaves when grown at 40/35°C compared to 25/20°C (Fig. 5a). We
379 assume the changes observed in COX subunit II reflect changes in abundance of the entire complex.
380 The abundance of AOX and UCP protein did not vary in response to growth *T* or duration of exposure
381 to heat for either PE or ND leaves, despite the initial spike in *aox* and *ucp* gene expression after transfer
382 to 40/35°C (Fig. 1). Interestingly two bands of AOX that varied relative to one another with
383 temperature treatment were evident in the Western blot (Fig. S5). This is consistent with the
384 fluctuations in expression of different *aox* genes noted above. Patterns of protein abundance were
385 similar when the analysis was standardised to dry mass or porin abundance (Fig. S6). Porin is a voltage-
386 dependent channel protein located at the outer membrane of mitochondria and is widely used as a
387 proxy for mitochondrial surface area due to its stability under a wide range of environmental conditions
388 (Noguchi, Taylor, Millar, Lambers, & Day, 2005; Shane et al., 2004). Thus, the matching results using
389 leaf area, dry mass or porin abundance indicate that the decline in COX abundance with increased *T*
390 was not a result of changes in Leaf Mass to Area ratio (LMA) or reduced mitochondria per unit area
391 of leaf. There was a trend for the abundance of Rubisco to decline with the amount of time a leaf
392 developed under 40/35°C (Fig. 5d), although there were no statistically significant *T* or developmental
393 stage effect.

394 LMA and starch, glucose, fructose and sucrose concentrations were measured in PE leaves one
395 and seven days after *T*-transfer, and in ND leaves at the prevailing temperature (Table 2). LMA did
396 not change significantly in response to *T*, for either transferred PE leaves or ND leaves, similar to
397 previous observations in rice over a similar *T* range (Nagai & Makino, 2009). However, ND leaves
398 did exhibit significantly greater LMA than PE transferred leaves, suggesting an effect of leaf rank on
399 LMA. Transferred PE and subsequently formed ND leaves exhibited consistently lower starch
400 concentrations with increasing *T* and significantly lower starch with extended duration of development
401 at the prevailing *T*. Unlike the dynamic responses of leaf starch concentrations to *T* change,
402 concentrations of soluble sugars were remarkably stable across both PE and ND leaves, in terms of
403 both *T*-regime and exposure time. Negative correlations between R_{dark} and soluble sugars were

404 observed among leaves within each individual T treatment but not among the three T treatments (Table
405 S5).

406

407 *CO₂ flux in responses to T*

408 How molecular changes altered the physiological performance of rice carbon metabolism at differing
409 growth T was investigated through gas-exchange measurements. Rates of A_n and R_{dark} are here
410 presented on a dry mass (DM) basis, noting that the patterns are similar when expressed on a leaf area
411 basis (Fig S7), reflecting the fact that growth T had no significant effect on LMA (Table 2). A
412 significant change in both A_n and R_{dark} (using mid-sections of leaves placed in Licor 6400 3 x 2 cm
413 chambers) occurred within the first 24 h of transfer to a 40/35°C T -regime for PE leaves, with A_n
414 falling and R_{dark} increasing when measured at the prevailing growth T (Fig. 6). This was followed by
415 stabilisation at the new rate over the subsequent six days. By contrast, A_n and R_{dark} remained relatively
416 constant at both 30/25°C and 25/20°C over a seven-day period monitoring period. Interestingly, rates
417 of R_{dark} for the 30/25°C treated plants decreased from day 3 to 7, compared to the first three days,
418 resulting in slightly lower rates of R_{dark} than for the 25/20°C treated plants by day 7. This possibly
419 reflects temperature-dependent differences in leaf senescence rates. As it could not be controlled,
420 relative humidity in the 40/35°C glasshouse room (Fig. S8) was substantially lower than the other two
421 rooms, leading to reduced humidity during gas-exchange measurements (Fig. 6c). As a consequence,
422 the vapour pressure deficit between the leaf and surrounding air (VPD_{Leaf}) increased over the first
423 seven days in PE leaves transferred to 40/35°C, resulting in a dramatic difference by day seven (Fig.
424 6d). The higher VPD_{Leaf} coincided with lower g_s in 40/35°C treated leaves at days three, five and seven,
425 and lower intercellular to ambient CO_2 concentration ratios (C_i/C_a) at days five and seven (Fig. 6e, f).
426 However, for the first two days post transfer both VPD_{Leaf} and g_s were similar between the three growth
427 T s. Therefore, the decline in A_n and changes in transcript abundance within one day of transfer to
428 40/35°C were not attributable to water relations. Over the longer-term, water relations may have
429 contributed to a slight reduction in C_i/C_a , but not enough to influence A_n , with A_n being stable from
430 one to seven days after transfer irrespective of changes in g_s and C_i/C_a (Fig. 6b). The changes in g_s
431 were not substantive enough to change leaf T , which was stable over the seven days, with both air T
432 and leaf T deviating by less than 2°C from the set room T (Fig. S8).

433 Short-term temperature response curves of entire ND leaves that formed at each prevailing
434 growth T regime were quantified over a 20 to 60°C range using the Walz large leaf chamber (Fig. 7;
435 refer to Figure S9 for area-based rates and Table S6 for quadratic equations fit to curves). Over most
436 of the range of measuring T s, leaves developed at 25/20°C exhibited higher rates of R_{dark} than those

437 developed under the other two T -regimes. Rates were lowest in leaves developed at 40/35°C (Fig. 7a).
438 When normalised to rates at 30°C, differences in R_{dark} were less pronounced (Fig. 7b), indicating that
439 while R_{dark} at a given measuring T was affected by growth T , the general shape of the $R_{\text{dark}}-T$ curves
440 remained largely similar across the three treatments. These observations are consistent with a Type II
441 (changes in baseline) rather than Type I (changes in Q_{10} , the increase in R_{dark} with a 10°C increase in
442 T) respiratory acclimation response (Atkin & Tjoelker, 2003). Importantly, while respiratory thermal
443 acclimation occurred, it was not sufficient to result in R_{dark} being homeostatic across the three growth
444 T treatments. As a result, R_{dark} measured at the growth T was significantly greater in the leaves
445 developed under hot conditions than under the other two treatments (Table 3). Growth T also had a
446 significant effect on the measuring T at which R_{dark} and A_n reached their maximum rates, with leaves
447 developed under high T exhibiting higher T -maxima than control 30/25°C leaves (Table 3). When
448 measured at the prevailing growth T of each treatment, mass-based rates of light-saturated A_n were
449 stable (i.e. homeostatic), further supporting the occurrence of strong thermal acclimation of A_n in ND
450 leaves (Fig. 7), contrary to PE leaves (Fig. 6). The temperature at which PSII lost functionality (T_{crit})
451 tended to increase with growth T (being 3.8°C higher in the hot-grown plants compared to those grown
452 at 25/20°C), although the differences were not statistically significant at $p < 0.05$ (Table 3). The high
453 degree of thermal acclimation exhibited by photosynthesis resulted in the ratio of R_{dark} to A_n being
454 lowest in the hot-grown plants, particularly at high measuring T (Fig. 8a); at a measuring T of 40°C,
455 hot-acclimated plants exhibited R_{dark}/A_n ratios that were 50% lower than those measured for their cold-
456 grown counterparts. Further evidence that rice acclimated to heat is seen in the fact that leaf elongation
457 rates – taken over the day and night period – were faster for the 40/35°C grown plants at all times (Fig.
458 8b). Interestingly, A_n of PE leaves ranged from 1.2 to 1.8 $\mu\text{mol g}^{-1} \text{DM s}^{-1}$ (Fig. 6), substantially faster
459 than the 0.6 $\mu\text{mol g}^{-1} \text{DM s}^{-1}$ in ND leaves (Fig. 7). The former were obtained from measurements on
460 mid-leaf sections placed in a 6 cm² chamber, while the latter were obtained from whole leaves placed
461 in a 14 x 10 cm Walz chamber. The lower A_n rates in the latter might reflect a lower proportion of
462 mesophyll cells per unit of area or DM across whole blades compared to the mid-blade section.

463

464 Discussion

465

466 Our study investigated the response of photosynthetic and respiratory metabolism to short- and long-
467 term changes in growth T – the highest of which is indicative of heat-wave T s – to explore: (1) the
468 extent of thermal acclimation of photosynthesis and respiration; and, (2) what underlying changes in
469 gene expression and protein abundance occur during the acclimation process. The results demonstrate

470 that the process of acclimation begins with abrupt changes in gene expression in PE leaves within the
471 first 24 h of heat exposure, followed by a return to homeostatic gene expression (Fig. 1). Importantly,
472 the abundance of the key energy-conserving respiratory protein, COX, declines in abundance when
473 pre-existing leaves are heat-treated for 24 hours, with this phenotype being maintained in newly-
474 developed leaves formed at 40/35°C (Fig. 5). This decline in COX was linked to a slight decline in
475 overall rates of R_{dark} (Fig. 7). The results support the hypothesis that acclimation of photosynthesis
476 and dark respiration are asynchronous in rice, but contrary to observations in non-crop species
477 (Campbell et al., 2007), light-saturated A_n acclimated to a greater extent than R_{dark} (Fig. 7; Table 3).
478 This ability to maintain photosynthetic carbon gain at 40°C is likely to be of crucial importance in
479 helping rice maintain growth during heat-wave conditions.

480
481 *Acclimation to changes in T are rapid and involve a multitude of genes*

482 There was a substantial change in the gene expression profile of rice leaves shifted from 30°C to 40°C
483 within the first 24 h of transfer (Figs. 1, 2, 3, and 4). As might be expected, the largest number of gene
484 expression perturbations were in primary and cellular metabolic processes (Fig. 4). This extensive
485 metabolic response aligns with the instability in R_{dark} and A_n fluxes over the initial 24 h post T -transfer
486 (Fig. 6), which would have contributed to a metabolic imbalance through changes in assimilate supply
487 and demand. Interestingly, the most responsive genes to the initial exposure to heat among upregulated
488 genes were genes involved in biosynthetic processes (Fig. 4) suggesting a stimulation of growth. This
489 is supported by the longer-term increase in leaf elongation rates observed in the 40/35°C grown plants.

490 When analysed in more detail, we observed that heat induced genes linked to energy dissipation
491 (*aox* and *ucp*) over the first 24 h of 40°C heat exposure (Fig. 1, Table 1). AOX and UCP are involved
492 in the diversion of electrons for formation of proton gradients and subsequent ATP synthesis (Krauss,
493 Zhang, & Lowell, 2005; Vanlerberghe, 2013). Past work has shown that overexpressing *aox* in young
494 rice seedlings imparts a benefit on growth under a T of 37°C for eight days, which was attributed to a
495 reduction of excessive proton motive force and reactive oxygen species (Murakami & Toriyama, 2008).
496 Given that AOX and UCP both divert electrons away from ATP synthesis under conditions of high
497 reductant supply, the rapid upregulation of these genes following the initial changes in growth T – with
498 rapid stimulation of R_{dark} and presumably greater reduction of ubiquinone pools (UQ) – indicates that
499 there may have been a temporary imbalance between NAD(P)H supply and demand for ATP. The
500 initial increases in *aox* and *ucp* gene expression (Fig. 1) did not translate into increased total AOX and
501 UCP protein abundance (Fig. 5). However, qPCR results indicate upregulation of the *aox1a* isoform,
502 responsive to abiotic stress in Arabidopsis mitochondria (Clifton, Millar, & Whelan, 2006; Shapiguzov

503 et al., 2019), while over the same period RNA-seq analysis indicated a significant decline in a separate
504 *aox1c* isoform. It is possible that the AOX1C isoform is less tolerant of high temperatures and therefore
505 is partially replaced by the AOX1a isoform. In this context it is interesting that in *Arabidopsis* AOX1a
506 is the major stress-inducible isoform. Since AOX operates as a non-covalently linked dimer (Siedow
507 & Umbach, 2000), the change in the relative expressions of *aox1a* and *1c* isoforms may also indicate
508 a change in the conformation of the AOX dimer, with a different mix of homo- and hetero-dimers in
509 response to heat. This suggests that AOX may have shifted to a more heat-tolerant conformation at
510 40/35°C, at least when the initial shock was imposed. This is an illustration that enzyme isoforms can
511 be an important part of abiotic stress responses that can be easily overlooked when only considering
512 total protein abundance.

513 The limited gene induction when leaves were transferred from 30 to 25°C (Fig. 3c) suggests
514 that a shift to this colder growth T did not significantly perturb metabolic processes in rice leaves,
515 consistent with the limited PE leaf response of R_{dark} or A_n when exposed to the cold (Fig. 6). However,
516 cold-responsive transcriptional regulators and associated changes in metabolism expected from cold
517 exposure (Zhu, Dong, & Zhu, 2007) must have been triggered by the colder T s. Regulatory adjustments
518 did indeed occur in ND rather than PE leaves, with R_{dark} at a given T being higher in the cold-grown
519 ND leaves (Fig. 7), and homeostasis of A_n being reached in ND leaves when measured at the prevailing
520 growth T (Table 3, Fig. 7).

521

522 *The most evident longer-term acclimation response is reduced COX abundance*

523 The clearest biochemical response to increasing growth T , both in PE and ND leaves, was a decline in
524 the abundance of COX (Fig. 5). A decline in COX has been reported for rice roots when grown at
525 25°C relative to 15°C (Kurimoto, Millar, Lambers, Day, & Noguchi, 2004). Conversely, COX content
526 increased in *Arabidopsis thaliana* leaves grown at 5°C relative to 21°C (Armstrong et al., 2008). In
527 all these cases, COX protein content and rates of respiration at a common measuring T (including in
528 our study; Fig. 5 and Fig. 7) decreased when plants grew at hotter T , suggesting that thermal
529 acclimation results in changes not only in overall rates of respiration but also in the capacity to produce
530 ATP. The acclimation response was rapid as COX declined in abundance by 24 h after 40°C T transfer
531 in PE leaves (Fig. 5).

532 The decline in COX abundance with hotter growth T is intriguing. If COX activity became
533 rate-limiting, it is likely that more ROS would be produced as the UQ pool would quickly become
534 over-reduced. However, other reports suggest that the UQ redox state is relatively stable, including
535 during changes in T , despite higher R_{dark} (Covey-Crump et al., 2007; Wagner & Wagner, 1995). If we

536 assume that UQ redox poise was also stable during the greater R_{dark} at the hottest growth T in our
537 experiments, there are two possible explanations. (1) The absolute flux of electrons through COX
538 actually increased despite the decrease in protein abundance. This could be due to COX capacity being
539 far greater than the capacity of the overall mETC. But since increasing T s stimulates the relative
540 activity of enzymes (Copeland, 2000), it is possible that the smaller amount of COX protein had higher
541 activity. In other words, the plants could make do with less COX at hotter T . (2) Alternatively,
542 activation of AOX at the higher T may have occurred to supplement COX activity thereby preventing
543 overload of the UQ pool. Measuring T -dependent *in vivo* ^{18}O fluxes through COX and AOX, as well
544 as leaf ATP content is required to determine terminal oxidase activity and ATP synthesis.
545 Understanding what, if any, biological benefit arises from synthesising less COX at warmer growth T
546 is another important consideration. Alternatively, a reduction in COX might be a consequence of heat
547 directly interfering with its synthesis. In support of this, a recent report shows that COX abundance
548 and capacity in Arabidopsis is significantly reduced by knocking out a HSP70 isoform, suggesting that
549 heat in some way interacts with COX formation (Wei et al., 2019).

550

551 *Acclimation of R_{dark} and A_n is asynchronous in rice*

552 The R_{dark}/A_n ratio increased with short-term increases in measuring T (Fig. 8), reflecting the fact that
553 R_{dark} is more temperature dependent than is A_n . R_{dark}/A_n ratios were similar in 25 and 30°C grown leaves,
554 when measured at the prevailing growth T of each treatment (i.e. R_{dark}/A_n was homeostatic). Thus, the
555 acclimation process led to the balance between carbon gain and release being maintained across this
556 moderate range of growth T s (Fig. 8). Acclimation was not, however, sufficient to maintain
557 homeostasis of R_{dark}/A_n in 40°C grown plants (Fig. 8). Similar results of R_{dark}/A_n ratios in leaves and
558 whole plants remaining relatively stable over moderate but not extremely high T have been reported
559 (Atkin, Scheurwater, & Pons, 2006, 2007; Campbell et al., 2007; Drake et al., 2016; Loveys et al.,
560 2003). Different to past studies, our findings in rice show that homeostasis of R_{dark}/A_n is largely the
561 result of maintenance of A_n more than through a marked reduction in rates of R_{dark} . Our results
562 categorically show A_n acclimates to a greater extent than R_{dark} in rice, supporting previous studies of
563 rice that collectively point to greater A_n than R_{dark} acclimation capacity (Bahuguna et al., 2017;
564 Glaubitz et al., 2014; Kurimoto, Millar, et al., 2004; Mohammed et al., 2013; Nagai & Makino, 2009;
565 Yamori et al., 2010), and field studies that infer limited rice R_{dark} acclimation capacity (Peng et al.,
566 2004; Welch et al., 2010). However, for many plant functional types, including temperate grasses, the
567 opposite occurs; R_{dark} acclimates to a greater extent than A_n (Campbell et al., 2007; Ow, Griffin,
568 Whitehead, Walcroft, & Turnbull, 2008; Way & Oren, 2010; Way & Sage, 2008; Yamori et al., 2005).
569 In this context, it should be noted that the previous studies are of species from temperate rather than

570 tropical habitats, raising the question of whether, beyond rice, tropical grasses generally have
571 asynchronous acclimation favouring A_n . The homeostasis of A_n and superior LER of hot-grown ND
572 rice leaves was more remarkable when viewed alongside evidence that prolonged exposure to drier air
573 was closing stomata and presenting slight reductions in CO_2 availability, at least in PE leaves (Fig. 6).
574 There is evidence that stomata close following a T -dependent increase in VPD_{Leaf} , with the mechanism
575 yet uncharacterised but likely involving guard cell sensing of water potential below the epidermis
576 (Peak & Mott, 2010; Shope, Peak, & Mott, 2008). It seems that declining VPD_{Leaf} triggers stomatal
577 closure in rice, even with unlimited root water supply.

578 As noted earlier, in recent years, rice yields have declined in response to increased daily mean
579 T_s , with the decline being more strongly correlated with increasing night rather than day T_s (Peng et
580 al., 2004; Welch et al., 2010). Our finding that A_n is homeostatic across growth T , whereas R_n is not
581 (Table 3) – underpinned by greater acclimation of photosynthesis than respiration – suggests that one
582 reason why yields are declining with increasing night temperatures is because high temperatures
583 stimulate respiratory CO_2 release. This would have a negative effect on daily net carbon gain, and thus
584 the ability to accumulate biomass in the lead up to anthesis.

585

586 *Potential implications of rice leaf acclimation and starch concentration on crop yield*

587 We found that soluble sugar concentrations of rice leaves were remarkably stable, irrespective of
588 growth T or developmental time at each growth T (Table 2). Maintaining soluble sugar homeostasis is
589 an important physiological requirement for many plant species, achieved through balancing CO_2
590 uptake and release in source leaves with sugar export to sink tissues (Rolland, Moore, & Sheen, 2002).
591 Homeostasis of sucrose concentrations in rice leaves has been observed even when carbon demand by
592 sink tissues is limited [e.g. reduced partitioning of sugars to grain (Wang et al., 2008)]. In our study,
593 homeostasis of soluble sugar concentrations occurred even at 40°C , where rates of R_{dark} were
594 significantly higher than in plants at the cooler growth T_s . Associated with the maintenance of sugar
595 concentrations was a T -dependent decline in starch concentration, both in PE and ND leaves (Table
596 2). For PE leaves exposed to 40°C , assimilate supply declined, particularly for 40°C transferred leaves,
597 due to a marked increase in R_{dark} and a decline in A_n (Fig. 6). Starch content also significantly declined
598 with developmental duration under high T , contrary to soluble sugar concentrations (Table 2). It seems
599 likely, therefore, that the reason soluble sugars did not significantly decline at warmer T for PE leaves
600 – even though assimilate supply fell – was a greater draw-down in the starch pool to maintain soluble
601 sugar concentrations (i.e. a reliance on stored assimilate). Other studies [e.g. on the temperate tree
602 *Populus tremula* (Hüve et al., 2012)] have highlighted the importance of starch degradation in

603 maintaining soluble sugar concentrations, particularly under conditions that stimulate CO₂ release by
604 respiration. Interestingly, in our study, ND leaves exhibited reduced starch concentrations while also
605 maintaining assimilate supply; one explanation for this might be that the decline in starch and
606 maintenance of sugars of ND leaves was linked to the increased leaf elongation rates we observed for
607 40°C ND leaves (Fig. 8b), with increased growth (i.e. sink demand) necessitating a greater supply of
608 sugars mediated by the starch pool (Stitt & Zeeman, 2012).

609 The decline in starch concentrations for PE and ND leaves at 40°C (Table 2) has interesting
610 implications for rice development and yield. Starch is stored in the stems in the late vegetative stage
611 of rice, and accounts for a large proportion of the carbon accumulated in seeds, a process that is
612 detrimentally affected by heat stress (Blum, Sinmena, Mayer, Golan, & Shpiler, 1994; Impa et al.,
613 2018; Morita & Nakano, 2011; Yang & Zhang, 2005). Other studies using the IR64 cultivar exposed
614 to hot night temperatures have shown an increase in R_{dark} and associated cost to vegetative growth and
615 starch content of panicles, ultimately reducing yield (Bahuguna et al., 2017; Glaubitz et al., 2014). The
616 reduced storage of starch in leaves with increasing T that we observed at the vegetative stage –
617 assuming it did not reflect diversion of starch to stems – would suggest reduced potential for the storage
618 of starch in stems and a penalty to yield of rice growing in warmer environments. This would be
619 particularly true for rice plants exposed to transient extreme T – such as during heat waves – as we
620 postulate the reduction in starch for PE leaves was due to a reduction in assimilate acquisition due to
621 stimulated R_{dark} and suppressed A_n . However, ND leaves did show reduced starch concentration, not as
622 a result of reduced assimilate acquisition, but most likely associated with an increase in growth rates
623 (Table 2; Fig. 8). Thus, it is likely that rice will experience different limitations on yield depending on
624 the duration of thermal changes, with shorter-term exposure to rising T – over a period in which tissue
625 cannot develop anew – likely leading to a greater suppression of yield than leaves developed under the
626 prevailing growth T . Rice may even experience increased yield with sustained mild warming of both
627 night and particularly day T . However, yield potential is dependent on whether heat-dependent changes
628 in growth at the vegetative stage of rice positively contributes to yield, which may be true (Glaubitz et
629 al., 2014; Scafaro et al., 2018), and not simply accelerate development and shorten the time to
630 flowering.

631

632 *Conclusions*

633 Overall, the results we present here demonstrate that both leaf respiration and photosynthesis can
634 acclimate in rice but the extent of acclimation is asynchronous and dependent on the timeframe of T
635 exposure. Warmer growth T of 40°C relative to 25°C will have a greater impact on rice CO₂ flux,

636 metabolic pathways, starch concentration and ultimately growth. Consequently, rice growing in a
 637 warmer climate with more extreme heating events will likely experience T -dependent alterations in
 638 growth and yield. The duration and intensity of T changes, together with complex interactions between
 639 assimilate acquisition, storage and utilisation will determine if this warmer environment will be
 640 beneficial or detrimental to rice productivity over the coming decades. We suggest that enhancing the
 641 acclimation capacity of R_{dark} for rice at warmer growth T – potentially through COX, AOX and UCP
 642 regulation – could be a key target for improving rice productivity in a warmer world.

643

644 **Acknowledgements**

645

646 We thank Assoc. Prof Spencer Whitney for providing Rubisco antibody. The support of the Australian
 647 Research Council (ARC) Centre of Excellence in Plant Energy Biology (CE140100008) to OA, BP
 648 and JM is acknowledged. The authors have no conflict of interest to declare.

649

650

651 **References**

652

- 653 Abramoff, M. D., Magelhaes, P. J., & Ram, S. J. (2004). Image Processing with ImageJ.
 654 *Biophotonics International*, 11(7), 36-42.
- 655 Armstrong, A. F., Badger, M. R., Day, D. A., Barthet, M. M., Smith, P. M. C., Millar, A. H., . . .
 656 Atkin, O. K. (2008). Dynamic changes in the mitochondrial electron transport chain
 657 underpinning cold acclimation of leaf respiration. *Plant, Cell & Environment*, 31(8), 1156-
 658 1169.
- 659 Atkin, O. K., Bruhn, D., Hurry, V. M., & Tjoelker, M. G. (2005). Evans Review No. 2: The hot and
 660 the cold: unravelling the variable response of plant respiration to temperature. *Functional*
 661 *Plant Biology*, 32(2), 87-105.
- 662 Atkin, O. K., Scheurwater, I., & Pons, T. L. (2006). High thermal acclimation potential of both
 663 photosynthesis and respiration in two lowland *Plantago* species in contrast to an alpine
 664 congeneric. *Global Change Biology*, 12(3), 500-515.
- 665 Atkin, O. K., Scheurwater, I., & Pons, T. L. (2007). Respiration as a percentage of daily
 666 photosynthesis in whole plants is homeostatic at moderate, but not high, growth temperatures.
 667 *New Phytologist*, 174(2), 367-380.
- 668 Atkin, O. K., & Tjoelker, M. G. (2003). Thermal acclimation and the dynamic response of plant
 669 respiration to temperature. *Trends in Plant Science*, 8(7), 343-351.
- 670 Badger, M. R., Björkman, O., & Armond, P. A. (1982). An analysis of photosynthetic response and
 671 adaptation to temperature in higher plants: temperature acclimation in the desert evergreen
 672 *Nerium oleander* L*. *Plant, Cell & Environment*, 5(1), 85-99.
- 673 Bahuguna, R. N., Solis, C. A., Shi, W., & Jagadish, K. S. V. (2017). Post-flowering night respiration
 674 and altered sink activity account for high night temperature-induced grain yield and quality
 675 loss in rice (*Oryza sativa* L.). *Physiologia Plantarum*, 159(1), 59-73.
- 676 Berry, J., & Bjorkman, O. (1980). Photosynthetic response and adaptation to temperature in higher
 677 plants. *Annual Review of Plant Physiology*, 31(1), 491-543.

- 678 Bhardwaj, A. R., Joshi, G., Kukreja, B., Malik, V., Arora, P., Pandey, R., . . . Agarwal, M. (2015).
679 Global insights into high temperature and drought stress regulated genes by RNA-Seq in
680 economically important oilseed crop Brassica juncea. *BMC Plant Biology*, *15*(1), 9.
- 681 Blum, A., Sinmena, B., Mayer, J., Golan, G., & Shpiller, L. (1994). Stem reserve mobilisation
682 supports wheat-grain filling under heat stress. *Functional Plant Biology*, *21*(6), 771-781.
- 683 Campbell, C., Atkinson, L., Zaragoza-Castells, J., Lundmark, M., Atkin, O., & Hurry, V. (2007).
684 Acclimation of photosynthesis and respiration is asynchronous in response to changes in
685 temperature regardless of plant functional group. *New Phytologist*, *176*(2), 375-389.
- 686 Clifton, R., Millar, A. H., & Whelan, J. (2006). Alternative oxidases in Arabidopsis: A comparative
687 analysis of differential expression in the gene family provides new insights into function of
688 non-phosphorylating bypasses. *Biochimica et Biophysica Acta (BBA) - Bioenergetics*,
689 *1757*(7), 730-741.
- 690 Copeland, R. A. (2000). *Enzymes: A Practical Introduction to Structure, Mechanism, and Data*
691 *Analysis* (Second Edition ed.). New York, NY: JOHN WILEY & SONS.
- 692 Covey-Crump, E. M., Bykova, N. V., Affourtit, C., Hoefnagel, M. H. N., Gardeström, P., & Atkin,
693 O. K. (2007). Temperature-dependent changes in respiration rates and redox poise of the
694 ubiquinone pool in protoplasts and isolated mitochondria of potato leaves. *Physiologia*
695 *Plantarum*, *129*(1), 175-184.
- 696 CSIRO, & BOM. (2018). *State of the Climate 2018*. Retrieved from Canberra, Australia:
697 [https://www.csiro.au/en/Research/OandA/Areas/Assessing-our-climate/State-of-the-Climate-](https://www.csiro.au/en/Research/OandA/Areas/Assessing-our-climate/State-of-the-Climate-2018)
698 [2018](https://www.csiro.au/en/Research/OandA/Areas/Assessing-our-climate/State-of-the-Climate-2018)
- 699 Drake, J. E., Tjoelker, M. G., Aspinwall, M. J., Reich, P. B., Barton, C. V. M., Medlyn, B. E., &
700 Duursma, R. A. (2016). Does physiological acclimation to climate warming stabilize the ratio
701 of canopy respiration to photosynthesis? *New Phytologist*, *211*(3), 850-863.
- 702 Glaubitz, U., Li, X., Köhl, K. I., van Dongen, J. T., Hinch, D. K., & Zuther, E. (2014). Differential
703 physiological responses of different rice (*Oryza sativa*) cultivars to elevated night
704 temperature during vegetative growth. *Functional Plant Biology*, *41*(4), 437-448.
- 705 Godfray, H. C. J., Beddington, J. R., Crute, I. R., Haddad, L., Lawrence, D., Muir, J. F., . . . Toulmin,
706 C. (2010). Food security: the challenge of feeding 9 billion people. *Science*, *327*(5967), 812-
707 818.
- 708 Gorsuch, P. A., Pandey, S., & Atkin, O. K. (2010). Temporal heterogeneity of cold acclimation
709 phenotypes in Arabidopsis leaves. *Plant, Cell & Environment*, *33*(2), 244-258.
- 710 Hartmann, D. L., A.M.G. Klein Tank, M. Rusticucci, L.V. Alexander, S. Brönnimann, Y.
711 Charabi, . . . Zhai, P. M. (2013). *Observations: Atmosphere and Surface*. In: *Climate Change*
712 *2013: The Physical Science Basis. Contribution of Working Group I to the Fifth Assessment*
713 *Report of the Intergovernmental Panel on Climate Change*. Retrieved from Cambridge,
714 United Kingdom and New York, NY, USA:
- 715 Hikosaka, K., Ishikawa, K., Borjigidai, A., Muller, O., & Onoda, Y. (2006). Temperature
716 acclimation of photosynthesis: mechanisms involved in the changes in temperature
717 dependence of photosynthetic rate. *Journal of Experimental Botany*, *57*(2), 291-302.
- 718 Hu, T., Sun, X., Zhang, X., Nevo, E., & Fu, J. (2014). An RNA sequencing transcriptome analysis of
719 the high-temperature stressed tall fescue reveals novel insights into plant thermotolerance.
720 *BMC Genomics*, *15*(1), 1147.
- 721 Hubbart, S., Peng, S., Horton, P., Chen, Y., & Murchie, E. H. (2007). Trends in leaf photosynthesis
722 in historical rice varieties developed in the Philippines since 1966. *Journal of Experimental*
723 *Botany*, *58*(12), 3429-3438.
- 724 Hüve, K., Bichele, I., Ivanova, H., Keerberg, O., Pärnik, T., Rasulov, B., . . . Niinemets, Ü. (2012).
725 Temperature responses of dark respiration in relation to leaf sugar concentration. *Physiologia*
726 *Plantarum*, *144*(4), 320-334.

- 727 Impa, S. M., Sunoj, V. S. J., Krassovskaya, I., Bheemanahalli, R., Obata, T., & Jagadish, S. V. K.
728 (2018). Carbon balance and source-sink metabolic changes in winter wheat exposed to high
729 night-time temperature. *Plant, Cell & Environment*, 0(ja).
- 730 Krauss, S., Zhang, C.-Y., & Lowell, B. B. (2005). The mitochondrial uncoupling-protein
731 homologues. *Nature Reviews Molecular Cell Biology*, 6, 248.
- 732 Kurimoto, K., Day, D. A., Lambers, H., & Noguchi, K. (2004). Effect of respiratory homeostasis on
733 plant growth in cultivars of wheat and rice. *Plant, Cell & Environment*, 27(7), 853-862.
- 734 Kurimoto, K., Millar, A. H., Lambers, H., Day, D. A., & Noguchi, K. (2004). Maintenance of growth
735 rate at low temperature in rice and wheat cultivars with a high degree of respiratory
736 homeostasis is associated with a high efficiency of respiratory ATP production. *Plant and
737 Cell Physiology*, 45(8), 1015-1022.
- 738 Lanning, S. B., Siebenmorgen, T. J., Counce, P. A., Ambardekar, A. A., & Mauromoustakos, A.
739 (2011). Extreme nighttime air temperatures in 2010 impact rice chalkiness and milling
740 quality. *Field Crops Research*, 124(1), 132-136.
- 741 Law, C. W., Chen, Y., Shi, W., & Smyth, G. K. (2014). voom: precision weights unlock linear model
742 analysis tools for RNA-seq read counts. *Genome Biology*, 15(2), R29.
- 743 Li, H., Handsaker, B., Wysoker, A., Fennell, T., Ruan, J., Homer, N., . . . Genome Project Data
744 Processing, S. (2009). The Sequence Alignment/Map format and SAMtools. *Bioinformatics*,
745 25(16), 2078-2079.
- 746 Liao, Y., Smyth, G. K., & Shi, W. (2013a). featureCounts: an efficient general purpose program for
747 assigning sequence reads to genomic features. *Bioinformatics*, 30(7), 923-930.
- 748 Liao, Y., Smyth, G. K., & Shi, W. (2013b). The Subread aligner: fast, accurate and scalable read
749 mapping by seed-and-vote. *Nucleic Acids Research*, 41(10), e108-e108.
- 750 Loveys, B. R., Atkinson, L. J., Sherlock, D. J., Roberts, R. L., Fitter, A. H., & Atkin, O. K. (2003).
751 Thermal acclimation of leaf and root respiration: an investigation comparing inherently fast-
752 and slow-growing plant species. *Global Change Biology*, 9(6), 895-910.
- 753 McCarthy, D. J., Chen, Y., & Smyth, G. K. (2012). Differential expression analysis of multifactor
754 RNA-Seq experiments with respect to biological variation. *Nucleic Acids Research*, 40(10),
755 4288-4297.
- 756 Mohammed, R., Cothren, J. T., & Tarpley, L. (2013). High night temperature and abscisic acid affect
757 rice productivity through altered photosynthesis, respiration and spikelet fertility. *Crop
758 Science*, 53(6), 2603-2612.
- 759 Morimoto, R. I. (1998). Regulation of the heat shock transcriptional response: cross talk between a
760 family of heat shock factors, molecular chaperones, and negative regulators. *Genes &
761 Development*, 12(24), 3788-3796.
- 762 Morita, S., & Nakano, H. (2011). Nonstructural carbohydrate content in the stem at full heading
763 contributes to high performance of ripening in heat-tolerant rice cultivar Nikomaru. *Crop
764 Science*, 51(2), 818-828.
- 765 Murakami, Y., & Toriyama, K. (2008). Enhanced high temperature tolerance in transgenic rice
766 seedlings with elevated levels of alternative oxidase, OsAOX1a. *Plant Biotechnology*, 25(4),
767 361-364.
- 768 Nagai, T., & Makino, A. (2009). Differences Between Rice and Wheat in Temperature Responses of
769 Photosynthesis and Plant Growth. *Plant & Cell Physiology*, 50(4), 744-755.
- 770 Neilson, K. A., Mariani, M., & Haynes, P. A. (2011). Quantitative proteomic analysis of cold-
771 responsive proteins in rice. *Proteomics*, 11(9), 1696-1706.
- 772 Noguchi, K. O., Taylor, N. L., Millar, A. H., Lambers, H., & Day, D. A. (2005). Response of
773 mitochondria to light intensity in the leaves of sun and shade species. *Plant, Cell &
774 Environment*, 28(6), 760-771.
- 775 O'Leary, B. M., Asao, S., Millar, A. H., & Atkin, Owen K. (2018). Core principles which explain
776 variation in respiration across biological scales. *New Phytologist*, 0(0).

- 777 O'sullivan, O. S., Weerasinghe, K. W. L. K., Evans, J. R., Egerton, J. J. G., Tjoelker, M. G., & Atkin,
778 O. K. (2013). High-resolution temperature responses of leaf respiration in snow gum
779 (*Eucalyptus pauciflora*) reveal high-temperature limits to respiratory function. *Plant, Cell &*
780 *Environment*, 36(7), 1268-1284.
- 781 Ohama, N., Sato, H., Shinozaki, K., & Yamaguchi-Shinozaki, K. (2017). Transcriptional Regulatory
782 Network of Plant Heat Stress Response. *Trends in Plant Science*, 22(1), 53-65.
- 783 Ow, L. F., Griffin, K. L., Whitehead, D., Walcroft, A. S., & Turnbull, M. H. (2008). Thermal
784 acclimation of leaf respiration but not photosynthesis in *Populus deltoides* × *nigra*. *New*
785 *Phytologist*, 178(1), 123-134.
- 786 Peak, D., & Mott, K. A. (2010). A new, vapour-phase mechanism for stomatal responses to humidity
787 and temperature. *Plant, Cell & Environment*, 34(1), 162-178.
- 788 Peng, S., Huang, J., Sheehy, J. E., Laza, R. C., Visperas, R. M., Zhong, X., . . . Cassman, K. G.
789 (2004). Rice yields decline with higher night temperature from global warming. *Proceedings*
790 *of the National Academy of Sciences of the United States of America*, 101(27), 9971-9975.
- 791 Posch, B. C., Kariyawasam, B. C., Bramley, H., Coast, O., Richards, R. A., Reynolds, M. P., . . .
792 Atkin, O. K. (2019). Exploring high temperature responses of photosynthesis and respiration
793 to improve heat tolerance in wheat. *Journal of Experimental Botany*, 70(19), 5051-5069.
- 794 Quinlan, A. R., & Hall, I. M. (2010). BEDTools: a flexible suite of utilities for comparing genomic
795 features. *Bioinformatics*, 26(6), 841-842.
- 796 Ramakers, C., Ruijter, J. M., Deprez, R. H. L., & Moorman, A. F. M. (2003). Assumption-free
797 analysis of quantitative real-time polymerase chain reaction (PCR) data. *Neuroscience*
798 *Letters*, 339(1), 62-66.
- 799 Reich, P. B., Sendall, K. M., Stefanski, A., Wei, X., Rich, R. L., & Montgomery, R. A. (2016).
800 Boreal and temperate trees show strong acclimation of respiration to warming. *Nature*,
801 531(7596), 633-636.
- 802 Robinson, J. T., Thorvaldsdóttir, H., Winckler, W., Guttman, M., Lander, E. S., Getz, G., & Mesirov,
803 J. P. (2011). Integrative genomics viewer. *Nature Biotechnology*, 29(1), 24-26.
- 804 Robinson, M. D., & Oshlack, A. (2010). A scaling normalization method for differential expression
805 analysis of RNA-seq data. *Genome Biology*, 11(3), R25.
- 806 Robinson, M. D., & Smyth, G. K. (2007a). Moderated statistical tests for assessing differences in tag
807 abundance. *Bioinformatics*, 23(21), 2881-2887.
- 808 Robinson, M. D., & Smyth, G. K. (2007b). Small-sample estimation of negative binomial dispersion,
809 with applications to SAGE data. *Biostatistics*, 9(2), 321-332.
- 810 Rolland, F., Moore, B., & Sheen, J. (2002). Sugar Sensing and Signaling in Plants. *The Plant Cell*,
811 14, S185-S205.
- 812 Ruijter, J. M., Ramakers, C., Hoogaars, W. M. H., Karlen, Y., Bakker, O., van den Hoff, M. J. B., &
813 Moorman, A. F. M. (2009). Amplification efficiency: linking baseline and bias in the analysis
814 of quantitative PCR data. *Nucleic Acids Research*, 37(6), e45-e45.
- 815 Scafaro, A. P., & Atkin, O. K. (2016). The Impact of Heat Stress on the Proteome of Crop Species.
816 In G. H. Salekdeh (Ed.), *Agricultural Proteomics Volume 2: Environmental Stresses* (pp.
817 155-175). Cham: Springer International Publishing.
- 818 Scafaro, A. P., Atwell, B. J., Muylaert, S., Reusel, B. V., Ruiz, G. A., Van Rie, J., & Gallé, A.
819 (2018). A thermotolerant variant of rubisco activase from a wild relative improves growth
820 and seed yield in rice under heat stress. *Frontiers in Plant Science*, 9, 1663.
- 821 Scafaro, A. P., Xiang, S., Long, B. M., Bahar, N. H. A., Weerasinghe, L. K., Creek, D., . . . Atkin, O.
822 K. (2017). Strong thermal acclimation of photosynthesis in tropical and temperate wet-forest
823 tree species: the importance of altered Rubisco content. *Global Change Biology*, 23(7), 2783-
824 2800.
- 825 Seck, P. A., Diagne, A., Mohanty, S., & Wopereis, M. C. S. (2012). Crops that feed the world 7:
826 Rice. *Food Security*, 4(1), 7-24.

- 827 Shane, M. W., Cramer, M. D., Funayama-Noguchi, S., Cawthray, G. R., Millar, A. H., Day, D. A., &
828 Lambers, H. (2004). Developmental physiology of cluster-root carboxylate synthesis and
829 exudation in *harsh hakea*. Expression of phosphoenolpyruvate carboxylase and the
830 alternative oxidase. *Plant Physiology*, *135*(1), 549.
- 831 Shapiguzov, A., Vainonen, J. P., Hunter, K., Tossavainen, H., Tiwari, A., Järvi, S., . . . Kangasjärvi,
832 J. (2019). Arabidopsis RCD1 coordinates chloroplast and mitochondrial functions through
833 interaction with ANAC transcription factors. *eLife*, *8*, e43284.
- 834 Shen, C., Li, D., He, R., Fang, Z., Xia, Y., Gao, J., . . . Cao, M. (2014). Comparative transcriptome
835 analysis of RNA-seq data for cold-tolerant and cold-sensitive rice genotypes under cold
836 stress. *Journal of Plant Biology*, *57*(6), 337-348.
- 837 Shope, J. C., Peak, D., & Mott, K. A. (2008). Stomatal responses to humidity in isolated epidermes.
838 *Plant, Cell & Environment*, *31*(9), 1290-1298.
- 839 Sidaway-Lee, K., Costa, M. J., Rand, D. A., Finkenstadt, B., & Penfield, S. (2014). Direct
840 measurement of transcription rates reveals multiple mechanisms for configuration of the
841 Arabidopsis ambient temperature response. *Genome Biology*, *15*(3), R45.
- 842 Siedow, J. N., & Umbach, A. L. (2000). The mitochondrial cyanide-resistant oxidase: structural
843 conservation amid regulatory diversity. *Biochimica et Biophysica Acta (BBA) -*
844 *Bioenergetics*, *1459*(2), 432-439.
- 845 Smith, N. G., & Dukes, J. S. (2017). Short-term acclimation to warmer temperatures accelerates leaf
846 carbon exchange processes across plant types. *Global Change Biology*, *23*(11), 4840-4853.
- 847 Smyth, G. K., Michaud, J., & Scott, H. S. (2005). Use of within-array replicate spots for assessing
848 differential expression in microarray experiments. *Bioinformatics*, *21*(9), 2067-2075.
- 849 Stitt, M., & Zeeman, S. C. (2012). Starch turnover: pathways, regulation and role in growth. *Current*
850 *Opinion in Plant Biology*, *15*(3), 282-292.
- 851 Strand, A., Hurry, V., Henkes, S., Huner, N., Gustafsson, P., Gardestrom, P., & Stitt, M. (1999).
852 Acclimation of Arabidopsis leaves developing at low temperatures. Increasing cytoplasmic
853 volume accompanies increased activities of enzymes in the calvin cycle and in the sucrose-
854 biosynthesis pathway. *Plant Physiology*, *119*(4), 1387-1398.
- 855 Thimm, O., Bläsing, O., Gibon, Y., Nagel, A., Meyer, S., Krüger, P., . . . Stitt, M. (2004). mapman: a
856 user-driven tool to display genomics data sets onto diagrams of metabolic pathways and other
857 biological processes. *The Plant Journal*, *37*(6), 914-939.
- 858 Tjoelker, M. G., Oleksyn, J., & Reich, P. B. (2001). Modelling respiration of vegetation: evidence
859 for a general temperature-dependent Q_{10} . *Global Change Biology*, *7*(2), 223-230.
- 860 Tjoelker, M. G., Reich, P. B., & Oleksyn, J. (1999). Changes in leaf nitrogen and carbohydrates
861 underlie temperature and CO₂ acclimation of dark respiration in five boreal tree species.
862 *Plant, Cell & Environment*, *22*(7), 767-778.
- 863 Vanlerberghe, C. G. (2013). Alternative oxidase: A mitochondrial respiratory pathway to maintain
864 metabolic and signaling homeostasis during abiotic and biotic stress in plants. *International*
865 *Journal of Molecular Sciences*, *14*(4).
- 866 Wagner, A. M., & Wagner, M. J. (1995). Measurements of *in vivo* ubiquinone reduction levels in
867 plant cells. *Plant Physiology*, *108*(1), 277.
- 868 Wang, E., Wang, J., Zhu, X., Hao, W., Wang, L., Li, Q., . . . He, Z. (2008). Control of rice grain-
869 filling and yield by a gene with a potential signature of domestication. *Nature Genetics*, *40*,
870 1370.
- 871 Way, D. A., & Oren, R. (2010). Differential responses to changes in growth temperature between
872 trees from different functional groups and biomes: a review and synthesis of data. *Tree*
873 *Physiology*, *30*(6), 669-688.
- 874 Way, D. A., & Sage, R. F. (2008). Thermal acclimation of photosynthesis in black spruce [*Picea*
875 *mariana* (Mill.) B.S.P.]. *Plant, Cell & Environment*, *31*(9), 1250-1262.

- 876 Wei, S.-S., Niu, W.-T., Zhai, X.-T., Liang, W.-Q., Xu, M., Fan, X., . . . Li, B. (2019). Arabidopsis
877 mtHSC70-1 plays important roles in the establishment of COX-dependent respiration and
878 redox homeostasis. *Journal of Experimental Botany*, 70(20), 5575-5590.
- 879 Welch, J. R., Vincent, J. R., Auffhammer, M., Moya, P. F., Dobermann, A., & Dawe, D. (2010).
880 Rice yields in tropical/subtropical Asia exhibit large but opposing sensitivities to minimum
881 and maximum temperatures. *Proceedings of the National Academy of Sciences*, 107(33),
882 14562-14567.
- 883 Yamori, W., Noguchi, K., Hikosaka, K., & Terashima, I. (2010). Phenotypic plasticity in
884 photosynthetic temperature acclimation among crop species with different cold tolerances.
885 *Plant Physiology*, 152(1), 388-399.
- 886 Yamori, W., Noguchi, K., & Terashima, I. (2005). Temperature acclimation of photosynthesis in
887 spinach leaves: analyses of photosynthetic components and temperature dependencies of
888 photosynthetic partial reactions. *Plant, Cell & Environment*, 28(4), 536-547.
- 889 Yang, J., & Zhang, J. (2005). Grain filling of cereals under soil drying. *New Phytologist*, 169(2),
890 223-236.
- 891 Yoshida, S. (1972). Physiological aspects of grain yield. *Annual review of Plant Physiology*, 23, 437-
892 464.
- 893 Zhu, J., Dong, C.-H., & Zhu, J.-K. (2007). Interplay between cold-responsive gene regulation,
894 metabolism and RNA processing during plant cold acclimation. *Current Opinion in Plant*
895 *Biology*, 10(3), 290-295.
- 896
- 897
- 898
- 899
- 900
- 901
- 902
- 903
- 904
- 905
- 906
- 907
- 908
- 909
- 910
- 911
- 912
- 913
- 914

Table 1. Differential expression of respiration genes in leaves after exposure to *T* of 40°C relative to 30°C. Differential expression defined as FDR < 0.05, marked as '*'. Electron transport chain (ETC), Pentose Phosphate Pathway (PPP). No TCA cycle genes were differentially expressed.

Pathway	Gene_name	locus	Log2 fold-change	
			2 hours	6 hours
ETC	Complex II (Succinate dehydrogenase)	LOC_Os08g02640	-0.55*	-0.58*
ETC	External NAD(P)H dehydrogenase	LOC_Os06g47000	0.72*	0.44
ETC	Uncoupling protein	LOC_Os11g48040	0.81*	0.46
ETC	Alternative oxidase	LOC_Os02g47200	-0.99*	-1.91*
glycolysis	ATP-dependent phosphofructokinase	LOC_Os01g53680	-0.11	-1.13*
glycolysis	Phosphoglycerate kinase	LOC_Os02g07260	0.78*	0.39
glycolysis	Enolase	LOC_Os10g08550	0.61*	0.34
PPP	Ribulose 5-phosphate 3-epimerase	LOC_Os09g32810	0.53*	0.87*

915
916
917
918
919
920
921
922
923
924
925
926
927
928
929
930
931
932

Table 2. Leaf mass per unit area (LMA), starch and soluble sugars of pre-existing (PE) leaves transferred from 30/25°C to 25/20°C or 40/35°C for one and seven days, and leaves newly-developed (ND) at the prevailing *T*. Data represents mean of three or four separate leaves from separate previously unsampled plants \pm SE. The *F*-values and *P*-values of a two-way ANOVA comparing *T*, developmental stage (*D*) and any interaction (*T* \times *D*) are reported with asterisks indicating significance at *P*<0.05.

		LMA (g m ⁻²)	Starch (mg g ⁻¹ DM)	Soluble sugar (mg g ⁻¹ DM)
25/20°C	Day 1	20 \pm 3	11.3 \pm 1.9	13.5 \pm 0.2
	Day 7	19 \pm 2	5.5 \pm 0.3	11.2 \pm 0.1
	ND	30 \pm 2	14.4 \pm 3.0	11.1 \pm 0.2
30/25°C	Day 1	19 \pm 2	14.9 \pm 2.1	13.0 \pm 0.5
	Day 7	21 \pm 2	4.9 \pm 1.0	10.5 \pm 0.2
	ND	28 \pm 0.4	9.6 \pm 1.6	11.0 \pm 0.6
40/35°C	Day 1	18 \pm 2	8.5 \pm 0.4	11.9 \pm 0.2
	Day 7	23 \pm 2	3.5 \pm 0.3	10.9 \pm 0.3
	ND	29 \pm 1	6.7 \pm 0.5	11.6 \pm 0.3
<i>T</i> \times <i>D</i>		<i>F</i> =0.7, <i>P</i> =0.6	<i>F</i> =1.7, <i>P</i> =0.14	<i>F</i> =0.01, <i>P</i> =0.99
<i>D</i>		<i>F</i> =28, <i>P</i> <0.001*	<i>F</i> =13, <i>P</i> <0.001*	<i>F</i> =0.14, <i>P</i> =0.94
<i>T</i>		<i>F</i> =0.1, <i>P</i> =0.9	<i>F</i> =4.2, <i>P</i> =0.03*	<i>F</i> =0.01, <i>P</i> =0.99

933

934

935

936

937

938

939

940

941

942

943

944

945

946

947

948

949

950

951

952

953

Table 3. Summary of key photosynthetic and respiratory parameters generated from temperature-response curves. Parameters are: leaf mass per area; the temperature at which R_{dark} and A_n exhibited maximum rates (T_{max} and T_{opt} , respectively); the maximum rates of R_{dark} and A_n reached (R_{max} and A_{opt} , respectively); rates of R_{dark} and A_n at the prevailing growth temperature; and, the temperature at which PSII lost functionality as determined by an increase in basal fluorescence (T_{crit}). Data represents means of three or four separate leaves from separate plants \pm SE and statistical data (F -value and P -value) based on one-way ANOVA of temperature treatment effect. Superscript letters show significant differences between the T treatments according to a Tukey test.

	25/20°C	30/25°C	40/30°C	F -value	P -value
LMA (g m^{-2})	33 \pm 2	30 \pm 2	35 \pm 3	1.4	0.31
T_{max} (°C)	51 \pm 1 ^a	54 \pm 1 ^{a,b}	55 \pm 1 ^b	4.7	0.04*
T_{opt} (°C)	29 \pm 1 ^a	31 \pm 1 ^{a,b}	33 \pm 0.3 ^b	6.1	0.04*
R_{max} ($\mu\text{mol g}^{-1} \text{DM s}^{-1} \times 10^{-3}$)	120 \pm 5	117 \pm 6	121 \pm 2	0.16	0.86
A_{opt} ($\mu\text{mol g}^{-1} \text{DM s}^{-1}$)	0.65 \pm 0.05	0.67 \pm 0.02	0.69 \pm 0.04	0.28	0.76
R_{dark} ($\mu\text{mol g}^{-1} \text{DM s}^{-1} \times 10^{-3}$)	24 \pm 3 ^a	27 \pm 3 ^a	57 \pm 2 ^b	35	<0.001*
A_n ($\mu\text{mol m}^{-2} \text{s}^{-1}$)	0.62 \pm 0.04	0.67 \pm 0.02	0.65 \pm 0.04	0.52	0.62
T_{crit} (°C)	46.0 \pm 0.6	46.9 \pm 0.9	49.8 \pm 1.5	3.726	0.089

954

955

956

957

958

959

960

961

962

963

964

965

966

967

968

969

970

971

972 **Figure Legends**

973

974 **Figure 1.** Quantitative PCR analysis of gene expression over the first 168 hours (7 days) after transfer
975 of leaves from 30/25°C to 25/20°C or 40/35°C. Genes analysed were: the respiratory cytochrome *c*
976 complex (*cox*) subunit II, alternative oxidase complex (*aox*) and uncoupling protein (*ucp*); the
977 photosynthetic genes ferredoxin NADH reductase (*fnr*) and phosphoribulose kinase (*prk*); and the
978 sugar metabolism gene sucrose phosphatase synthase (*sps*). Gene expression was revitalised at each
979 time-point to the non-transferred 30/25°C control.

980

981 **Figure 2.** Principal component analysis of normalised RNA-seq expression values for each sample
982 following temperature treatment for (a) 2 hours and (b) 6 hours. Samples are coloured by treatment,
983 day/night temperatures of 30/25°C (control), 40/35°C (hot), and 25/20°C (cold). The y-axis is principle
984 component 1 (PC1) and the x axis is principle component 2 (PC2); the percent of variation explained
985 by each axis is indicated. RNA-seq libraries were normalised using *edgeR* (“TMM” method) and *voom*
986 transformation, scaled by unit variance and clustered using singular value decomposition.

987

988 **Figure 3.** Identification of genes differentially expressed during temperature treatments. (a, b)
989 Common and time point specific differentially expressed genes under heat treatment (40/35°C). The
990 overlap between genes differentially expressed at 2 and 6 h under heat treatment for (a) upregulated
991 genes and (b) downregulated genes. ‘*’ indicates significant overlap $p \ll 0.001$, fisher’s one-tailed
992 exact test (hypergeometric). (c) Hierarchical clustering of differentially expressed genes. For each time
993 point (2, 6 and 24 h) differentially expressed genes were determined for both the hot (40/35°C) and
994 cold (25/20°C) temperature treatments relative to the 30/25°C control conditions (FDR < 0.05). For
995 each differentially expressed gene, the relative fold-change under each condition over the time series
996 is then displayed on a log₂ scale: red = upregulated, blue = downregulated.

997

998 **Figure 4.** Gene ontology (GO) term enrichment among genes differentially Upregulated (a) or
999 downregulated (b) genes after 2 h at 40°C. Ontological annotations downloaded from MSU and
1000 ontology enrichment tests performed with topGO in R using the Fisher standard test (on tailed fisher's
1001 exact test/ hypergeometric test) with post hoc p value correction for multiple testing using the
1002 Benjamini & Hochberg method.

1003

1004 **Figure 5.** Abundance of mitochondrial electron transport chain proteins and Rubisco determined by
1005 Western blot analysis for rice leaves sampled at different developmental stages of; PE leaves six and
1006 24 h after T transfer to 25/20°C or 40/35°C, and leaves newly developed (ND) post T -transfer. (a)
1007 Abundance of CYTOCHROME C OXIDASE (COX) subunit II, (b) ALTERNATIVE OXIDASE
1008 (AOX), (c) UNCOUPLING PROTEIN (UCP) and (d) Rubisco large subunit on a leaf area basis with
1009 data normalised by adjusting the largest value in each dataset to 100. Data represent mean \pm SE of four
1010 independent western blots, with each blot representing leaf tissue from a separate plant. The P -values
1011 of a two-way ANOVA comparing temperature (T), developmental stage (D) and the interaction
1012 between the two ($T \times D$) are reported on each graph. Representative blots are presented in Figure S5.

1013

1014 **Figure 6.** Rates of dry mass (DM) based dark respiration (R_{dark} ; a), net assimilation (A_n ; b), Relative
1015 humidity (RH; c), vapour pressure deficit between the leaf and surrounding air (VPD_{Leaf} ; d), stomatal
1016 conductance (g_s ; e), and ratio of intercellular to ambient CO_2 concentrations (Ci/Ca ; f) measured at the
1017 respective day-time growth temperature of each treatment just prior to (day 0), and 1, 2, 3, 5 and 7-
1018 days after transfer of control 30/25°C day/night grown leaves to either 25/20°C, 40/35°C or maintained
1019 at 30/25°C. Values are means of four biological replicates \pm SE.

1020

1021 **Figure 7.** Temperature-response curves (a, b) of dark respiration (R_{dark}) and (c, d) net assimilation (A_n),
1022 on a dry mass (DM) basis. Values are absolute (a, c) or normalised to values at 30°C (b, d).
1023 Measurements were made on whole newly-developed (ND) leaves growing for 21 d at day/night
1024 temperatures of 25/20°C, 30/25°C or 40/35°C. Curves fitted to R_{dark} and A_n are quadratic functions.
1025 Calculated acclimation parameters from the curves are presented in Table 3. Rates were recorded every
1026 30 sec as leaves were heated at 1°C per minute. Filled area represent standard error of three to four
1027 biological replicates.

1028

1029 **Figure 8.** The percentage of dark respiration (R_{dark}) relative to light-saturated net assimilation (A_n) (a),
1030 and leaf elongation rates (LER) over a 24 h day/night cycle (b), for ND leaves growing for 21 d at
1031 day/night temperatures of 25/20°C, 30/25°C or 40/35°C. For the R_{dark}/A_n ratio values are calculated
1032 from the absolute means presented in Figure 7. For LER the dark (night) period of the 24 h cycle is
1033 shaded in grey and values are the means \pm SE of four plant replicates.

1034

Summary statement

Leaf respiration and photosynthesis in rice (*Oryza sativa* L.) shows asynchronous acclimation capacity in favour of photosynthesis. Heat acclimation reduced the protein abundance of the respiratory protein cytochrome *c* oxidase (COX), despite respiration and growth being stimulated.

Do not distribute

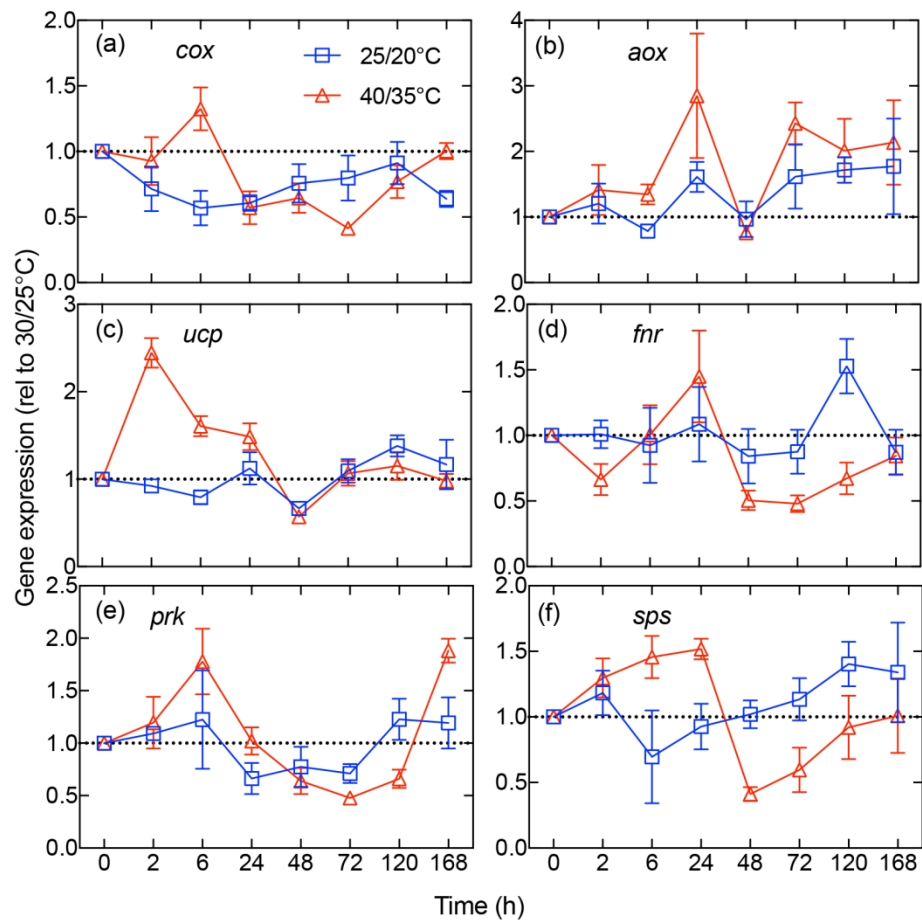


Figure 1. Quantitative PCR analysis of gene expression over the first 168 hours (7 days) after transfer of leaves from 30/25°C to 25/20°C or 40/35°C. Genes analysed were: the respiratory cytochrome c complex (*cox*) subunit II, alternative oxidase complex (*aox*) and uncoupling protein (*ucp*); the photosynthetic genes ferredoxin NADH reductase (*fnr*) and phosphoribulose kinase (*prk*); and the sugar metabolism gene sucrose phosphatase synthase (*sps*). Gene expression was revitalised at each time-point to the non-transferred 30/25°C control.

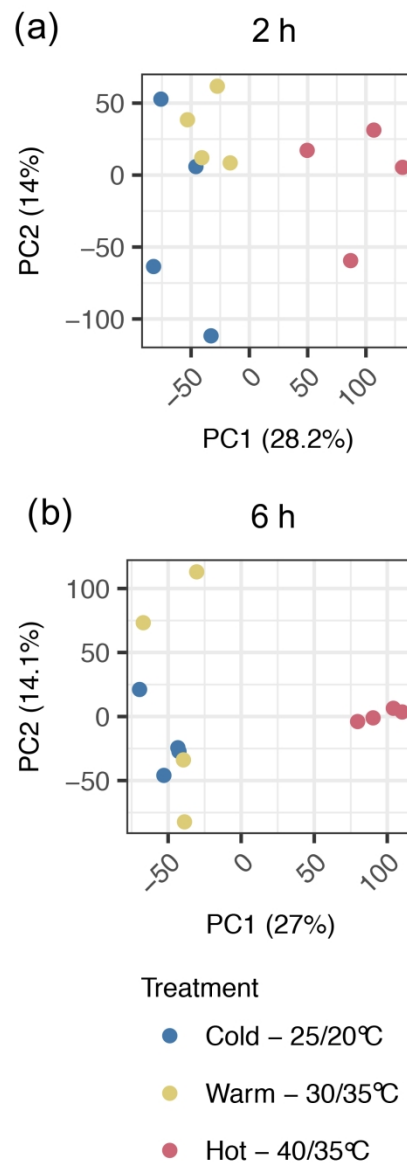


Figure 2. Principal component analysis of normalised RNA-seq expression values for each sample following temperature treatment for (a) 2 hours and (b) 6 hours. Samples are coloured by treatment, day/night temperatures of 30/25°C (control), 40/35°C (hot), and 25/20°C (cold). The y-axis is principle component 1 (PC1) and the x axis is principle component 2 (PC2); the percent of variation explained by each axis is indicated. RNA-seq libraries were normalised using edgeR ("TMM" method) and voom transformation, scaled by unit variance and clustered using singular value decomposition.

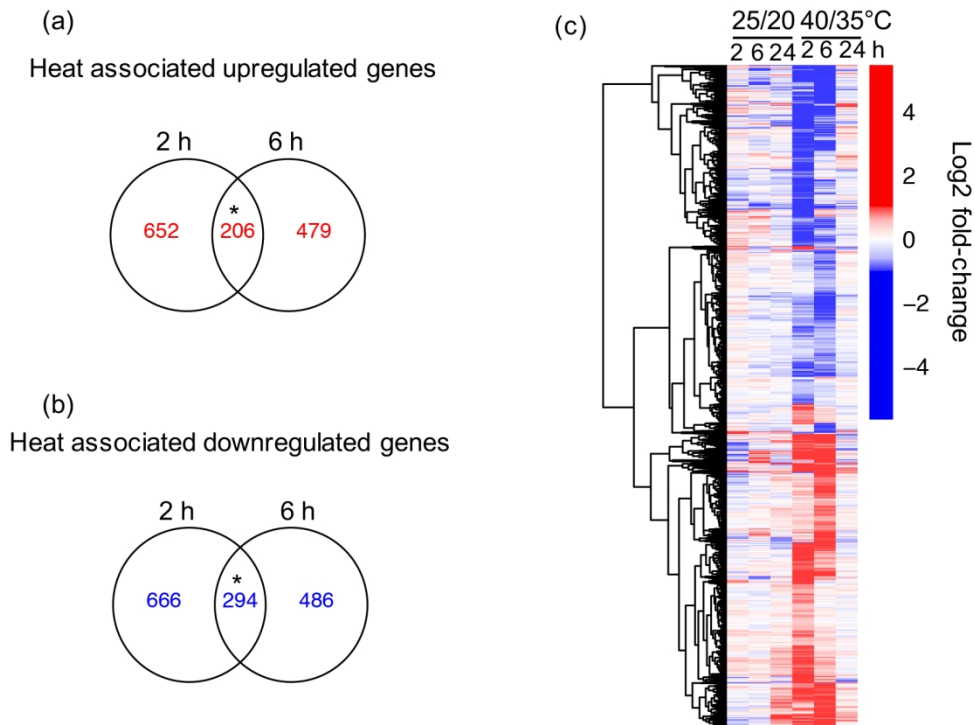


Figure 3. Identification of genes differentially expressed during temperature treatments. (a, b) Common and time point specific differentially expressed genes under heat treatment (40/35°C). The overlap between genes differentially expressed at 2 and 6 h under heat treatment for (a) upregulated genes and (b) downregulated genes. '*' indicates significant overlap $p < 0.001$, fisher's one-tailed exact test (hypergeometric). (c) Hierarchical clustering of differentially expressed genes. For each time point (2, 6 and 24 h) differentially expressed genes were determined for both the hot (40/35°C) and cold (25/20°C) temperature treatments relative to the 30/25°C control conditions (FDR < 0.05). For each differentially expressed gene, the relative fold-change under each condition over the time series is then displayed on a log₂ scale: red = upregulated, blue = downregulated.

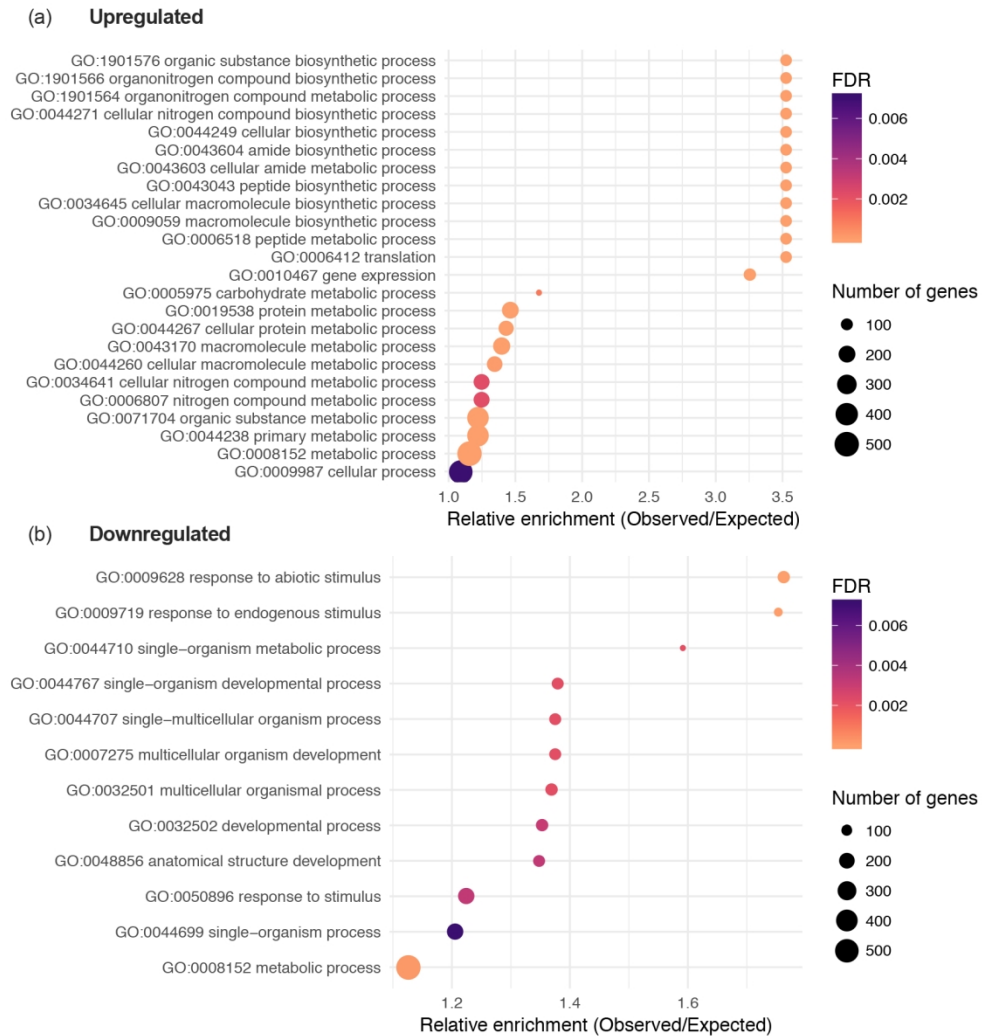


Figure 4. Gene ontology (GO) term enrichment among genes differentially Upregulated (a) or downregulated (b) genes after 2 h at 40°C. Ontological annotations downloaded from MSU and ontology enrichment tests performed with topGO in R using the Fisher standard test (on tailed fisher's exact test/hypergeometric test) with post hoc *p*-value correction for multiple testing using the Benjamini & Hochberg method.

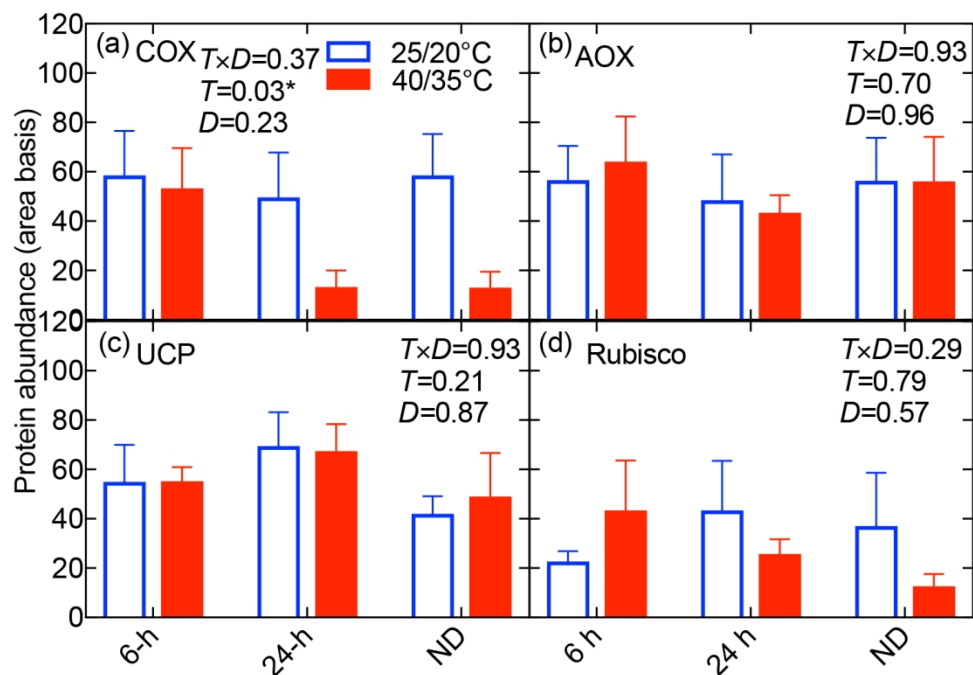


Figure 5. Abundance of mitochondrial electron transport chain proteins and Rubisco determined by Western blot analysis for rice leaves sampled at different developmental stages of; PE leaves six and 24 h after T transfer to 25/20°C or 40/35°C, and leaves newly developed (ND) post T -transfer. (a) Abundance of CYTOCHROME C OXIDASE (COX) subunit II, (b) ALTERNATIVE OXIDASE (AOX), (c) UNCOUPLING PROTEIN (UCP) and (d) Rubisco large subunit on a leaf area basis with data normalised by adjusting the largest value in each dataset to 100. Data represent mean \pm SE of four independent western blots, with each blot representing leaf tissue from a separate plant. The P -values of a two-way ANOVA comparing temperature (T), developmental stage (D) and the interaction between the two ($T \times D$) are reported on each graph. Representative blots are presented in Figure S5.

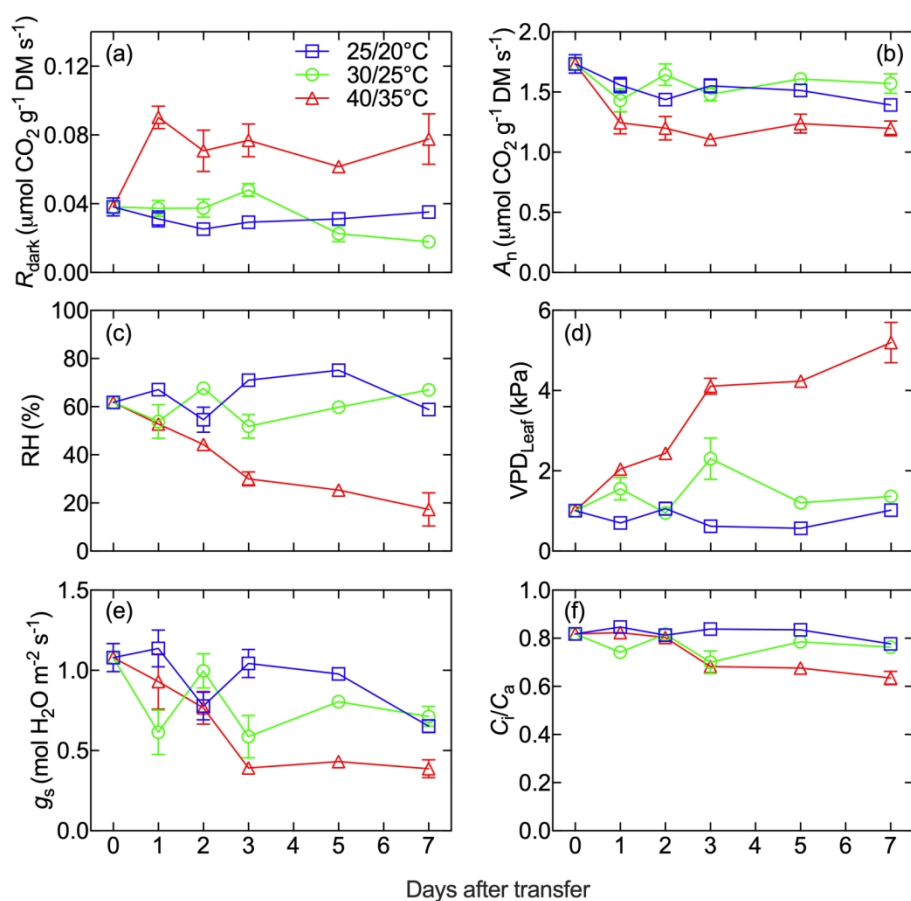


Figure 6. Rates of dry mass (DM) based dark respiration (R_{dark} ; a), net assimilation (A_n ; b), Relative humidity (RH; c), vapour pressure deficit between the leaf and surrounding air (VPD_{Leaf} ; d), stomatal conductance (g_s ; e), and ratio of intercellular to ambient CO₂ concentrations (C_i/C_a ; f) measured at the respective day-time growth temperature of each treatment just prior to (day 0), and 1, 2, 3, 5 and 7-days after transfer of control 30/25°C day/night grown leaves to either 25/20°C, 40/35°C or maintained at 30/25°C. Values are means of four biological replicates \pm SE.

152x141mm (300 x 300 DPI)

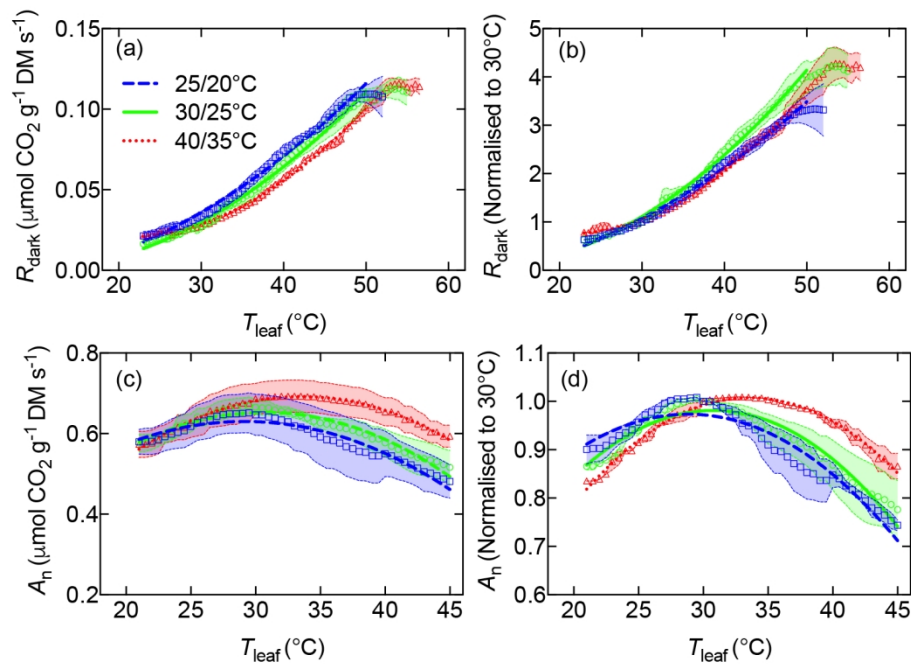


Figure 7. Temperature-response curves (a, b) of dark respiration (R_{dark}) and (c, d) net photosynthesis (A_n), on a dry mass (DM) basis. Values are absolute (a, c) or normalised to values at 30°C (b, d). Measurements were made on whole newly-developed (ND) leaves growing for 21 d at day/night temperatures of 25/20°C, 30/25°C or 40/35°C. Curves fitted to R_{dark} and A_n are quadratic functions. Calculated acclimation parameters from the curves are presented in Table 3. Rates were recorded every 30 sec as leaves were heated at 1°C per minute. Filled area represent standard error of three to four biological replicates.

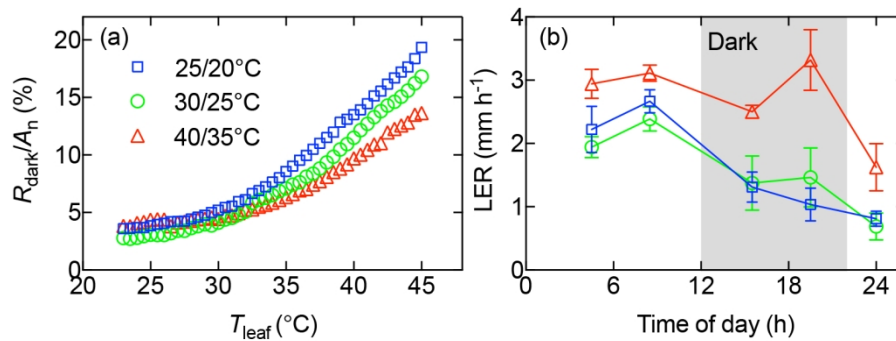


Figure 8. The percentage of dark respiration (R_{dark}) relative to light-saturated net assimilation (A_n) (a), and leaf elongation rates (LER) over a 24 h day/night cycle (b), for ND leaves growing for 21 d at day/night temperatures of 25/20°C, 30/25°C or 40/35°C. For the R_{dark}/A_n ratio values are calculated from the absolute means presented in Figure 7. For LER the dark (night) period of the 24 h cycle is shaded in grey and values are the means \pm SE of four plant replicates.

Supporting Information

Molecular and physiological responses during thermal acclimation of leaf photosynthesis and respiration in rice

Fatimah Azzahra Ahmad Rashid^{1,2}, Peter A. Crisp³, You Zhang⁴, Oliver Berkowitz⁵, Barry J. Pogson¹, David A. Day^{6,7}, Josette Masle⁸, James Whelan⁵, Owen K. Atkin¹, Andrew P. Scafaro¹

¹ Australian Research Council Centre of Excellence in Plant Energy Biology, Research School of Biology, The Australian National University, Canberra, ACT, 2601, Australia

² Current address: Department of Biology, Faculty of Science and Mathematics, Sultan Idris education University, 35900 Tanjung Malim, Perak, Malaysia

³ Department of Plant and Microbial Biology, University of Minnesota, Saint Paul, MN, 55108 USA

⁴ CSIRO Plant Industry, GPO Box 1700, Canberra, ACT, 2601, Australia

⁵ Australian Research Council Centre of Excellence in Plant Energy Biology, School of Life Science, AgriBio Building, La Trobe University, Bundoora, Victoria, 3083, Australia

⁶ College of Science and Engineering, Flinders University, South Australia, 5001, Australia

⁷ Department of Animal, Plant and Soil Sciences, AgriBio Building, La Trobe University, 5 Ring Road, Bundoora, VIC, 3086, Australia

⁸ Research School of Biology, The Australian National University, Canberra, ACT, 2601, Australia

Table S1. Concentrations of essential macro- and micro-nutrients in hydroponic solution for rice plants.

Element	Chemical formula	Concentration (mM)
Macronutrients		
Nitrogen (N)	NH_4NO_3	1.4
Phosphorus (P)	$\text{NaH}_2\text{PO}_4 \cdot 2\text{H}_2\text{O}$	0.6
Potassium (P), Sulfur (S)	K_2SO_4	0.5
Calcium (Ca)	$\text{CaCl}_2 \cdot 2\text{H}_2\text{O}$	0.2
Magnesium (Mg)	$\text{MgSO}_4 \cdot 7\text{H}_2\text{O}$	0.8
Micronutrients		
Iron (Fe)	Fe-EDTA	0.07
Boron (B)	H_3BO_3	0.037
Manganese (Mn)	$\text{MnCl}_2 \cdot 4\text{H}_2\text{O}$	0.009
Zinc (Zn)	$\text{ZnSO}_4 \cdot 7\text{H}_2\text{O}$	0.00075
Copper (Cu)	$\text{CuSO}_4 \cdot 5\text{H}_2\text{O}$	0.0003
Molybdenum (Mo)	$(\text{NH}_4)_6\text{Mo}_7\text{O}_{24} \cdot 4\text{H}_2\text{O}$	0.0001
Vanadium (V)	NH_4VO_3	0.000138
Silicon (Si)	Na_2SiO_3	0.0012963

Table S2. Primers used for qPCR gene expression analysis

Protein	Sequence (5'→3')	Length	Start	Stop	Tm	GC %	Size	location	mRNA
Ferredoxin NADP reductase	TCAGGCTCTACTCC ATCGCC	20	48 7	50 6	58 .9	60	15	exon 2	NM_001063 105.1
	ACCAGGCTTCAAGT CACAGAGG	22	63 8	61 7	60	54. 6	2	exon 3 or 4	
Phosphoribulokinase	TTTGATGCCTTCATT GATCCCC	22	86 5	88 6	56 .8	45. 5	80	exon 3 or 4	NM_001054 360.1
	TCATCAGGAATAAG CTGGGTTGG	23	94 4	92 2	58 .1	47. 8		exon 4	
Uncoupling protein	CCTCTACGAGCCCG TGAAATCC	22	34 8	36 9	60 .6	59. 1	13 4	exon 2 or 3	NM_001075 091.1
	TGACAAGGTCAGTG GGGTTGG	21	48 1	46 1	60	57. 1		exon 4	
Cytochrome oxidase (COX)	GCCATTGCAGGAGT GATGGG	20	73	92	59 .2	60	85		LOC_Os12g 33946.1
	TCCCACCAAGAATT TGATCGCC	22	15 7	13 6	59	50			
Alternative oxidase (AOX)	TGCTTTAGGCCATG GGAGACC	21	41 6	43 6	59 .9	57. 1	84	exon 1 or 2	NM_001060 293.1
	CTTGTCGAGCAGCG TCTTGG	20	49 9	48 0	59 .5	60		exon 1	
Sucrose-phosphate synthase (SPS)	ATGCGAAGCCTGAA ACCCCC	20	13 17	13 36	60 .9	60	12 4	exon 8 or 9	NM_001052 401.1
	CACACGGAGGTGCA GAAAAGG	21	14 40	14 20	59 .6	57. 1		exon 9	
eIF4-gamma/eIF5/eIF2-epsilon domain containing protein (Eukaryotic initiation factor 5C)	CTGATGGAGGCTGT TCAGTGG	21	10 35	10 55	58 .5	57. 1	81	exon 6 or 7	NM_001074 292.1
	AGCCCATGCTTTCA CCTGCC	20	11 15	10 96	61 .2	60		exon 7	

Table S3 Differentially expressed genes. At each time point, differential expressed genes were assessed for the hot and cold treated plants relative to the warm grown control plants sampled at the same time ($n = 4$). Genes were considered differentially expressed an FDR adjusted p (p_{adj}) < 0.05 .

Treatment	Time point	Upregulated	Downregulated
Cold	2 hr	4	0
Hot	2 hr	858	960
Cold	6 hr	2	0
Hot	6 hr	685	780
Cold	24 hr	0	0
Hot	24 hr	0	0

Table S4. Protein concentrations of 25/20°C and 40/35°C day/night grown leaves. Data represents mean of three to four biological replicates \pm SE.

	Protein concentration (mg ml ⁻¹)	
	25/20°C	40/35°C
6 hr [Pre-existing (PE) leaves]	7.7 \pm 0.8	7.0 \pm 1.0
Day 1 [Pre-existing (PE) leaves]	8.8 \pm 1.9	6.9 \pm 1.3
Newly-developed (ND) leaves	8.5 \pm 0.7	7.8 \pm 0.8

Do not distribute

Table S5. Pearson's correlation coefficients between rates of dark respiration and concentration of soluble sugars for plants grown at different growth temperature regimes.

	Dark respiration x soluble sugars		
	25/20°C	30/25°C	40/35°C
Day 1			
Correlation coefficient	-0.999	-0.999	0.049
<i>P</i> -value	0.024*	0.032*	0.969
Day 7			
Correlation coefficient	-0.805	-0.990	-0.461
<i>P</i> -value	0.405	0.090	0.695
Newly developed (ND)			
Correlation coefficient	-0.420	-0.560	0.879
<i>P</i> -value	0.724	0.621	0.317

Table S6. Quadratic equations for the short-term temperature (T)-response curves of dark respiration (R_{dark}) and net assimilation (A_{n}) as presented in Figure 7. The equations were fitted to the mean values of each temperature treatment and their Absolute Sum of Squares (ASS) and goodness-of-fit (R^2) are provided. Equations for R_{dark} were only fitted in the range of 22 to 50°C. R_{dark} and A_{n} units are in $\mu\text{mol CO}_2 \text{ g}^{-1} \text{ DM s}^{-1} \times 10^{-3}$ and T is in °C.

Day/night temperatures	Equation	ASS	R^2
25/20°C	$R_{\text{dark}} = -7.2 - 0.094 \times T + 0.051 \times T^2$	2.5×10^{-5}	0.99
	$A_{\text{n}} = 60 + 39 \times T - 0.67 \times T^2$	9.0×10^{-5}	0.92
30/25°C	$R_{\text{dark}} = 2.4 - 0.096 \times T + 0.063 \times T^2$	1.7×10^{-5}	0.99
	$A_{\text{n}} = 89 + 48 \times T - 0.72 \times T^2$	6.0×10^{-5}	0.94
40/35°C	$R_{\text{dark}} = 5.8 - 3.7 \times T + 0.092 \times T^2$	1.1×10^{-5}	0.99
	$A_{\text{n}} = -240 + 56 \times T - 0.83 \times T^2$	7.3×10^{-5}	0.99



Figure S1 A photo of a LI-6400XT portable gas exchange system (top) and Walz 3010-GWK1 chamber (bottom) used in quantification of short-term temperature-response curves of R_{dark} and A_n in new-developed (ND) leaves. Airline tubes were used to connect the Walz 3010-GWK1 chamber to the LICOR Infrared gas analyser head with a water trap in between to remove excess humidity. Photos are courtesy of www.licor.com and www.walz.com.

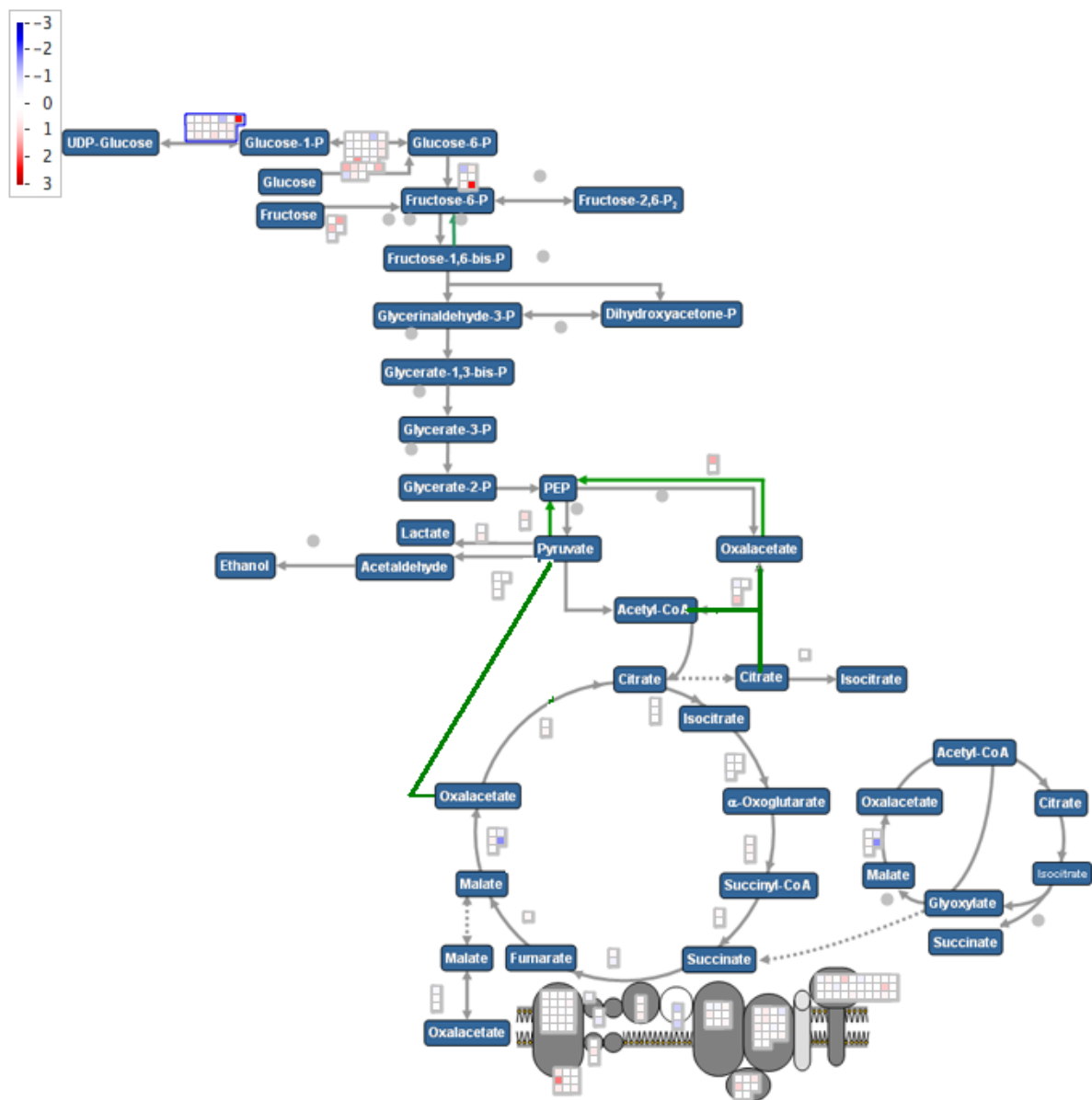


Figure S2 Differential gene expression in the Glycolysis and TCA under hot treatment
Gene expression is visualised in a MapMan pathway view of Glycolysis and the tricarboxylic acid (TCA) cycle. Each box represents a rice gene with homology to an Arabidopsis gene annotated in the MapMan pathway. Data show for the comparison of 2 hours hot treatment compared to 2 hours control treatment (warm); red shading represents up-regulation and blue shading down-regulation on a log₂ fold-change scale.

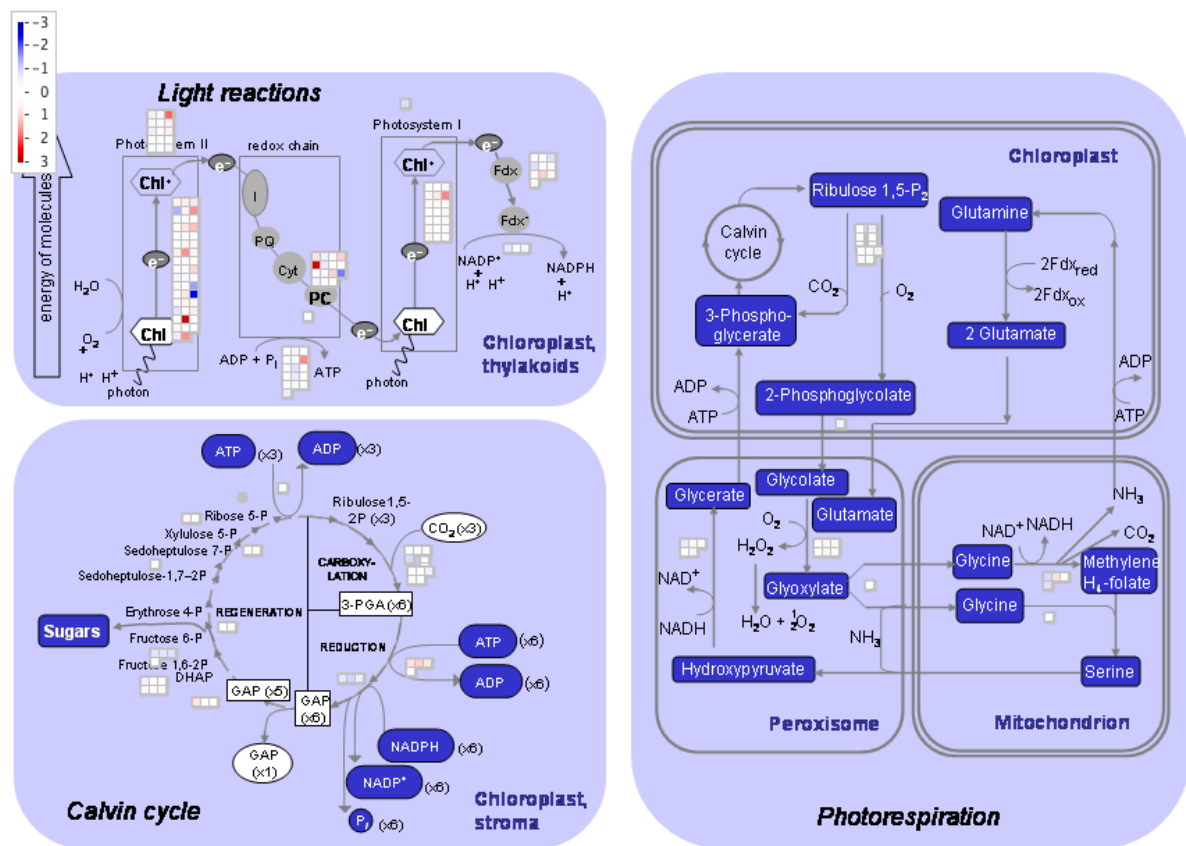


Figure S3. Differential gene expression of photosynthetic genes under hot (40/35°C) treatment. Gene expression is visualised in a MapMan pathway view of photosynthesis. Each box represents a rice gene with homology to an Arabidopsis gene annotated in the MapMan pathway. Data show for the comparison of two hours hot treatment compared to two hours control (30/25°C) treatment; red shading represents up-regulation and blue shading down-regulation on a log₂ fold-change scale.

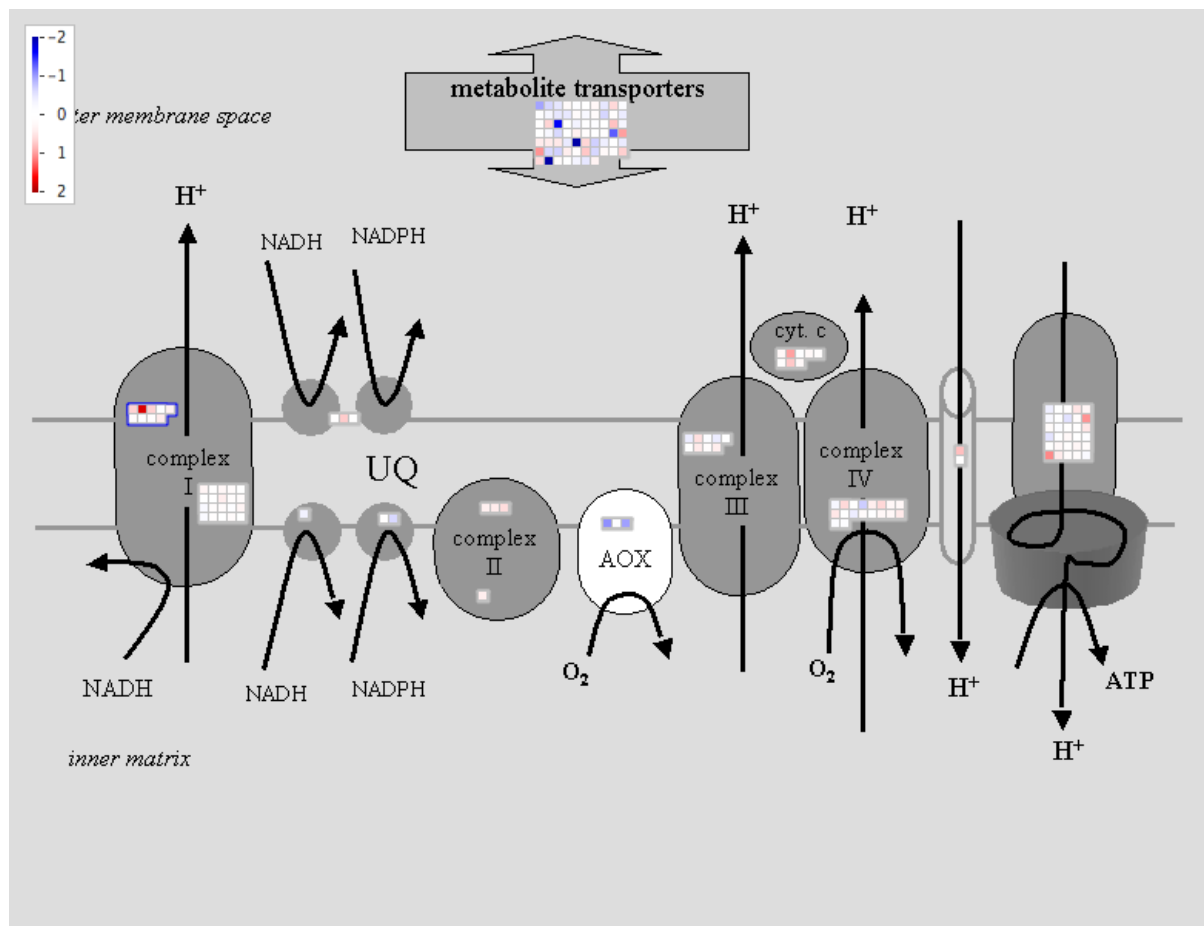


Figure S4. Differential gene expression in the mitochondrial electron transport chain under hot treatment. Gene expression is visualised in a MapMap pathway view of the mitochondrial electron transport. Each box represents a rice gene with homology to an Arabidopsis gene annotated in the MapMan pathway. Data show for the comparison of two hours hot (40/35°C) treatment compared to two hours control treatment (30/25°C); red shading represents up-regulation and blue shading down-regulation on a log₂ fold-change scale.

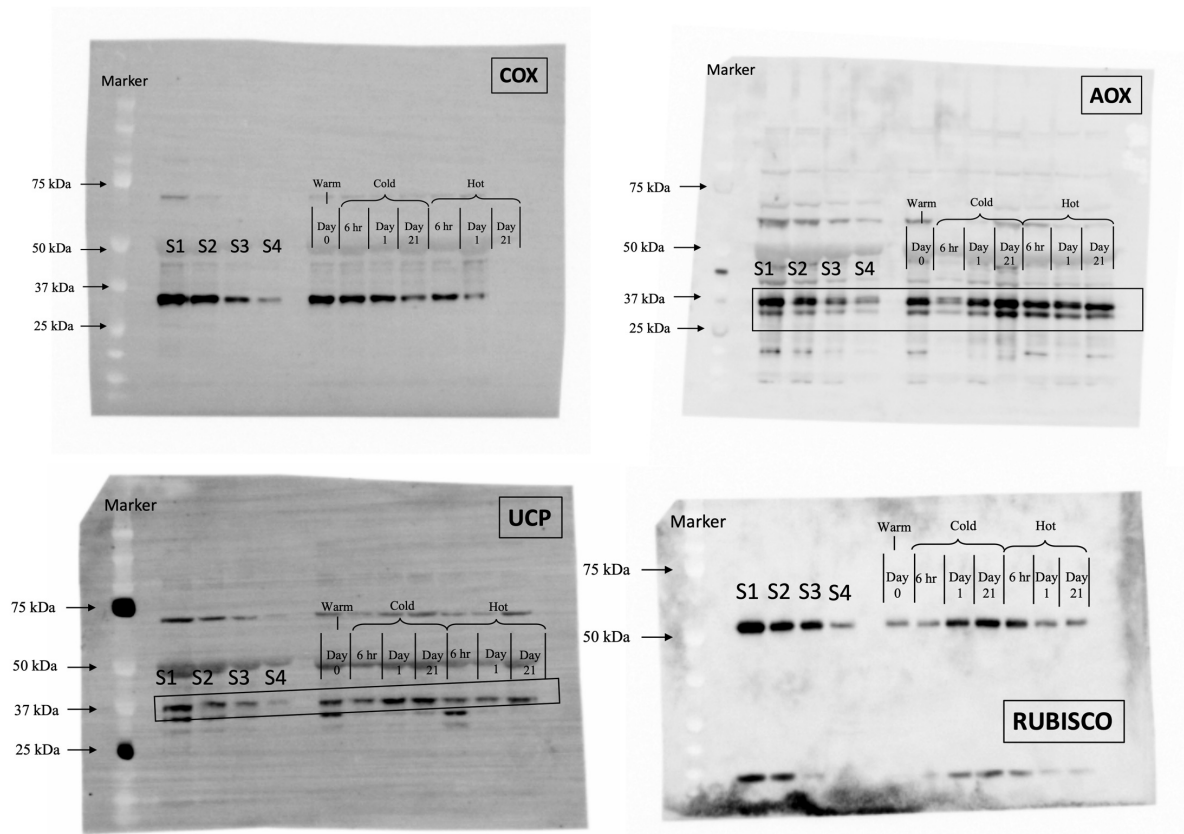


Figure S5. Representative western blots of cytochrome c oxidase (COX) subunit II, alternative oxidase (AOX), uncoupling protein (UCP), and Rubisco, used for determination of protein content of leaves. S1 to S4 is a dilution series of the warm/control (30/25°C) samples. This is followed by the initial day 0 warm leaves prior to temperature transfer, the 6-h and 1-day times after transfer of PE leaves, and ND leaves after 21 days of temperature transfer, for the cold (25/20°C) and hot (40/35°C) treatments as indicated on the images. For AOX and UCP, the bands within the box are what was classified and analysed as the proteins of interest based on the molecular weight marker markers.

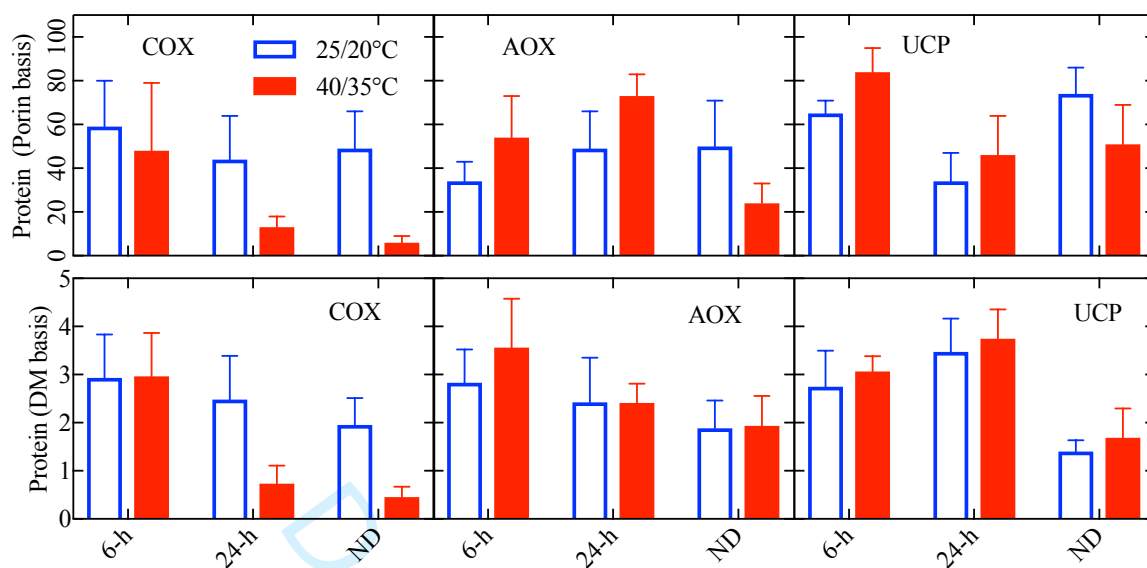


Figure S6. Abundance of mitochondrial electron transport chain proteins determined by Western blot analysis for pre-existing rice leaves sampled at; six and 24 h after *T* transfer to 25/20°C or 40/35°C, and leaves newly developed (ND) post *T*-transfer. The top three panels are protein abundance of cytochrome *c* oxidase (COX), alternative oxidase (AOX), and uncoupling protein (UCP) normalised to porin abundance and adjusting the largest value in each dataset to 100. The bottom three panels are leaf area values normalised to a dry mass (DM) basis by factoring in the leaf mass per area of pre-existing and newly developed leaves as presented in Table 2 of the text. Data represent mean \pm SE of four independent western blots, with each blot representing leaf tissue from a separate plant.

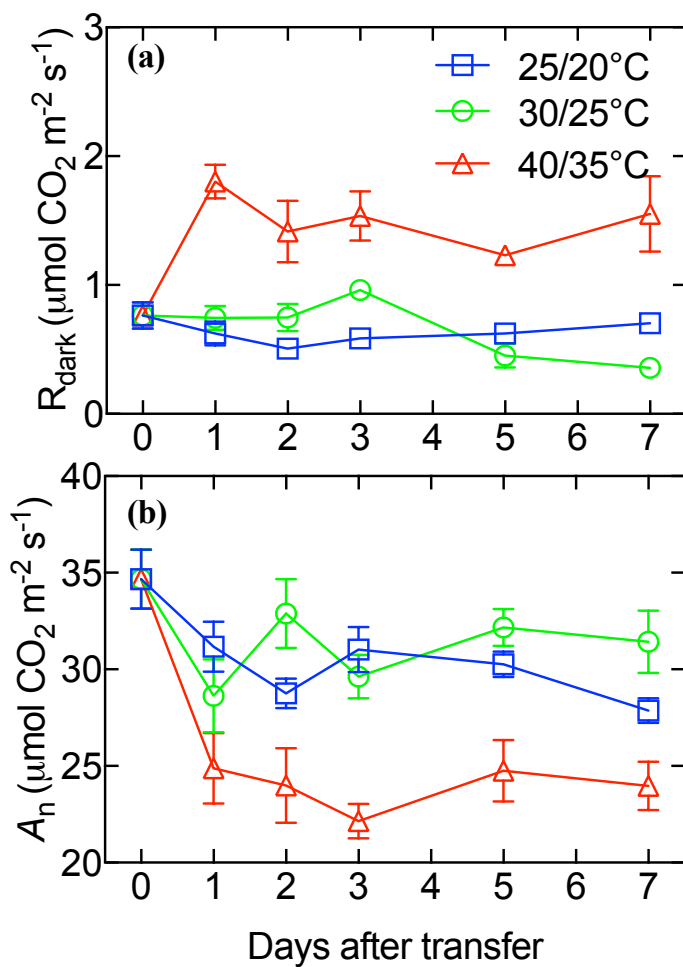


Figure S7. Rates of leaf area based dark respiration (R_{dark}) and net photosynthesis (A_n). Rates were measured at the respective day-time growth temperature of each treatment just prior to (day 0), and 1, 2, 3, 5 and 7-days after transfer of control 30/25°C day/night grown leaves to either 25/20°C, 40/35°C or maintained at 30/25°C. Values are means of four biological replicates \pm SE.

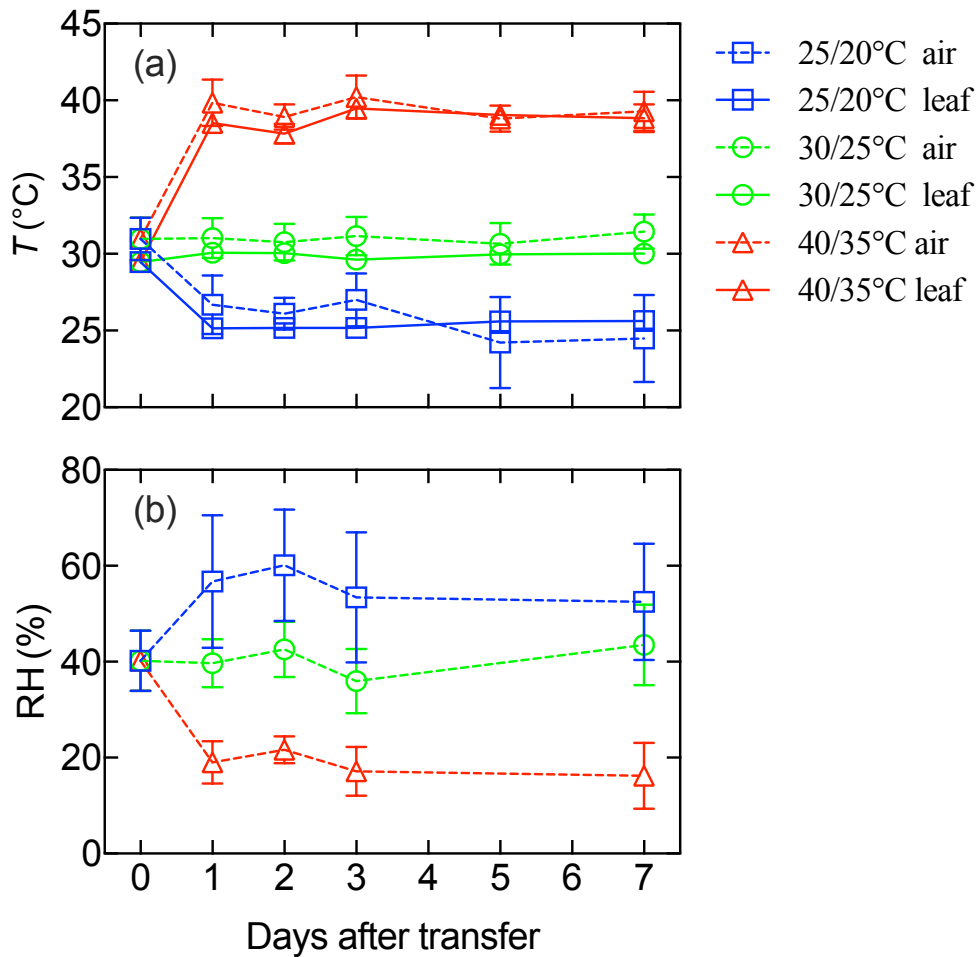


Figure S8. Room (dashed lines) and leaf (solid lines) temperatures and relative humidity (RH) over the steady-state gas exchange experimental period. Temperatures (T) were measured in the room by a thermometer and at the leaf surface by a thermocouple and relative humidity (RH) was measured in the room by a hygrometer. Values are means \pm SD.

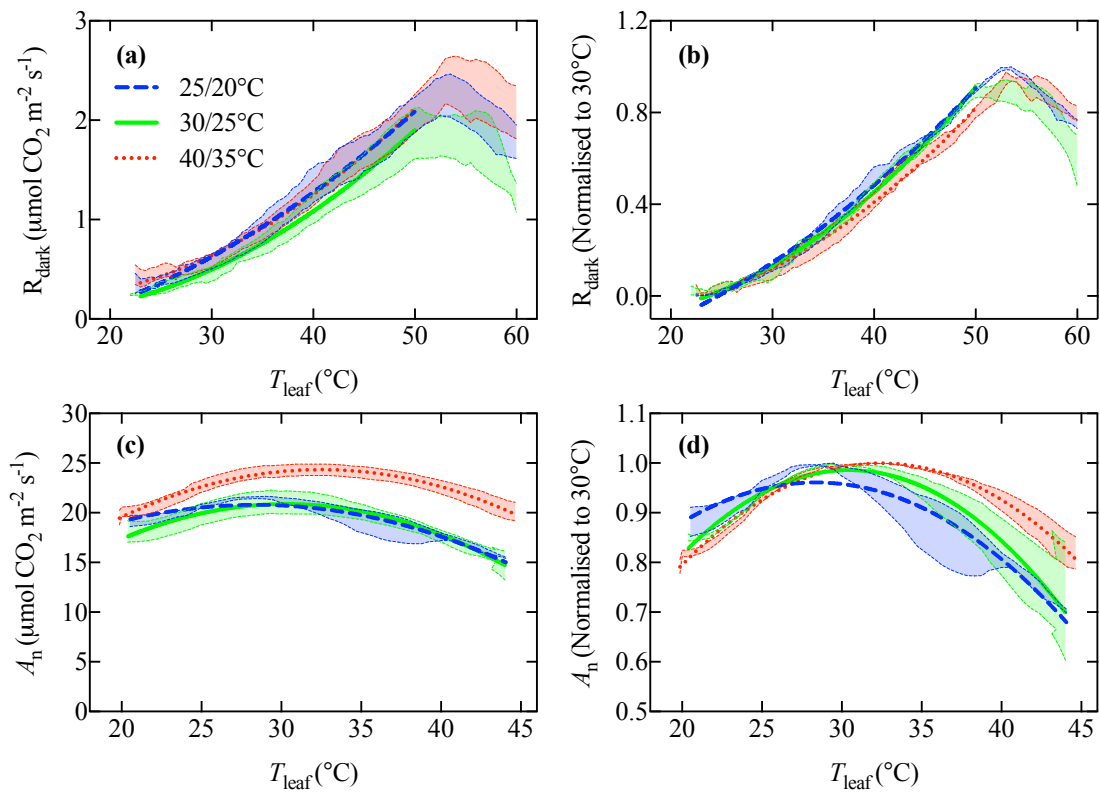


Figure S9. Temperature-response curves (a, b) of dark respiration (R_{dark}) and (c, d) net photosynthesis (A_n), on an area basis. Values are absolute (a, c) or normalised to values at 30°C (b, d). Measurements were made on whole newly-developed (ND) leaves growing for 21 d at day/night temperatures of 25/20°C, 30/25°C or 40/35°C. Curves fitted to R_{dark} and A_n are quadratic functions. Rates were recorded every 30 sec as leaves were heated at 1°C per minute. Filled area represent standard error of three to four biological replicates.

Molecular and physiological responses during thermal acclimation of leaf photosynthesis and respiration in rice

Fatimah Azzahra Ahmad Rashid^{1,2}, Peter A. Crisp³, You Zhang⁴, Oliver Berkowitz⁵, Barry J. Pogson^{1#}, David A. Day^{6,7}, Josette Masle⁸, Roderick C. Dewar⁸, James Whelan^{5#}, Owen K. Atkin^{1#}, Andrew P. Scafaro¹

¹ Australian Research Council Centre of Excellence in Plant Energy Biology, Research School of Biology, The Australian National University, Canberra, ACT, 2601, Australia

² Current address: Department of Biology, Faculty of Science and Mathematics, Sultan Idris education University, 35900 Tanjung Malim, Perak, Malaysia

³ Department of Plant and Microbial Biology, University of Minnesota, Saint Paul, MN, 55108 USA

⁴ CSIRO Plant Industry, GPO Box 1700, Canberra, ACT, 2601, Australia

⁵ Australian Research Council Centre of Excellence in Plant Energy Biology, School of Life Science, AgriBio Building, La Trobe University, Bundoora, Victoria, 3083, Australia

⁶ College of Science and Engineering, Flinders University, South Australia, 5001, Australia

⁷ Department of Animal, Plant and Soil Sciences, AgriBio Building, La Trobe University, 5 Ring Road, Bundoora, VIC, 3086, Australia

⁸ Research School of Biology, The Australian National University, Canberra, ACT, 2601, Australia

The support of the Australian Research Council (ARC) Centre of Excellence in Plant Energy Biology (CE140100008) is acknowledged

Abstract

To further our understanding of how sustained changes in temperature affect the carbon economy of rice (*Oryza sativa*), hydroponically-grown plants of the IR64 cultivar were developed at 30/25°C (day/night) before being shifted to 25/20°C or 40/35°C. Leaf mRNA and protein abundance, sugar and starch ~~content~~ concentrations, gas-exchange and elongation rates were measured on pre-existing leaves (PE) already developed at 30/25°C, or leaves newly-developed (ND) subsequent to temperature transfer. Following a shift in growth temperature, there was a transient adjustment in metabolic gene transcript abundance of PE leaves before homeostasis was reached within 24 h, aligning with R_{dark}

34 (leaf dark respiratory CO₂ release) and A_n (net CO₂ assimilation) changes. With longer exposure, the
35 central respiratory protein CYTOCHROME C OXIDASE (COX) declined in abundance at 40/35°C.
36 In contrast to R_{dark} , A_n was maintained across the three growth temperatures in ND leaves. Soluble
37 sugars did not differ significantly with growth temperature, and growth was fastest with extended
38 exposure at 40/35°C. The results highlight that acclimation of photosynthesis and respiration is
39 asynchronous in rice, with heat-acclimated plants exhibiting a striking ability to maintain net carbon
40 gain and growth when exposed to heat-wave temperatures, even while reducing investment in energy-
41 conserving respiratory pathways.

42

43 **Keywords:** rice, thermal stress, acclimation, respiration, photosynthesis, heat, cold, CYTOCHROME
44 C OXIDASE (COX)

45

46 **Introduction**

47

48 The response of net CO₂ assimilation (A_n) and leaf respiration in the dark (R_{dark}) to changes in
49 temperature (T) is often dynamic. Acclimation – i.e. physiological changes that enable adjustments in
50 the rate of A_n and R_{dark} at a given measuring T in response to sustained changes in growth T – occurs
51 in many species, in natural and controlled environments (Atkin, Bruhn, Hurry, & Tjoelker, 2005; Berry
52 & Bjorkman, 1980; Campbell et al., 2007; Reich et al., 2016; Smith & Dukes, 2017; Tjoelker, Oleksyn,
53 & Reich, 2001). Acclimation can also lead to metabolic homeostasis, where similar rates of A_n and
54 R_{dark} are exhibited by hot- and cold-acclimated plants, when compared at their respective growth T s.
55 Determining the extent to which R_{dark} and A_n acclimate to sustained changes in T is of growing interest,
56 as global warming is resulting in plants of natural and managed ecosystems experiencing higher
57 average growth T s, often in conjunction with more frequent and severe heat waves (CSIRO & BOM,
58 2018; Hartmann et al., 2013). The impact of heat on A_n and R_{dark} of cereal crops, including rice (*Oryza*
59 *sativa*), is of particular interest given the need to increase food production to meet the requirements of
60 a growing and more affluent world population (Godfray et al., 2010). Rice contributes substantially to
61 global food demand, particularly in Asia where it makes up more than 30% of all dietary energy intake
62 (Seck, Diagne, Mohanty, & Wopereis, 2012). However, in recent years rice yields have declined in
63 regions such as South-East Asia, with the declines being more strongly correlated with nightly
64 minimum than daytime maximum T s (Peng et al., 2004; Welch et al., 2010). Reduced yields and grain
65 quality were also observed for rice in North America when exposed to warmer night T (Lanning,
66 Siebenmorgen, Counce, Ambardekar, & Mauromoustakos, 2011). Given this, and the likely
67 importance of A_n and R_{dark} for biomass and grain production (Posch et al., 2019; Yoshida, 1972), it is

68 crucial that we develop a better understanding of how changes in T affect these key metabolic
69 processes in rice.

70 In rice and a range of other crops, RNA sequencing analysis has shown large scale
71 perturbations to the transcript profile of plants exposed to colder or warmer T , with the changes
72 occurring over a period of hours to days and across multiple functional categories, but especially in
73 genes involved in primary metabolism (Bhardwaj et al., 2015; Hu, Sun, Zhang, Nevo, & Fu, 2014;
74 Shen et al., 2014). The vast gene expression response to T -perturbations is likely mediated through
75 heat shock transcription factors, which regulate changes in transcriptional networks. These are induced
76 by heat stress and other abiotic stimuli, changing the protein complement of a cell (Morimoto, 1998;
77 Ohama, Sato, Shinozaki, & Yamaguchi-Shinozaki, 2017). However, changes in protein abundance
78 may not necessarily match changes in transcript abundance due to transcription and RNA turnover
79 rates being influenced by T (Sidaway-Lee, Costa, Rand, Finkenstadt, & Penfield, 2014), and post-
80 transcriptional regulation. In cases where heat stress results in changes in protein abundance, the
81 greatest changes are seen in proteins associated with primary metabolism, with about 50% of all leaf
82 protein abundance changes seeming to be in A_n and R_{dark} metabolic pathways (Scafaro & Atkin, 2016).
83 In rice, cold-stress similarly perturbs a large proportion of energy metabolism pathways (Neilson,
84 Mariani, & Haynes, 2011), emphasising the importance of changes in protein abundance in
85 chloroplasts and mitochondria as part of the thermal acclimation process. There is growing evidence
86 that plants can acclimate to T variations by stimulating energy metabolism at colder T and suppressing
87 energy metabolism at warmer T , either through regulation of enzymatic velocities or changes in
88 enzyme abundance (Armstrong et al., 2008; Badger, Björkman, & Armond, 1982; Campbell et al.,
89 2007; Hikosaka, Ishikawa, Borjigidai, Muller, & Onoda, 2006; Scafaro et al., 2017; Strand et al., 1999;
90 Yamori, Noguchi, & Terashima, 2005). Whether the same is true for rice remains unclear, both for
91 pre-existing (PE) leaves that experience a sustained change in growth T , and in newly-developed (ND)
92 leaves that form under a new thermal regime. In species other than rice, the extent of changes
93 underpinning thermal acclimation (including changes in leaf structure, nitrogen partitioning and
94 organelle abundance), is typically greater in ND than PE leaves (Armstrong et al., 2008; Gorsuch,
95 Pandey, & Atkin, 2010; O'Leary, Asao, Millar, & Atkin, 2018; Tjoelker, Reich, & Oleksyn, 1999;
96 Yamori et al., 2005).

97 Past studies on rice conducted during the vegetative (Glaubitz et al., 2014; Kurimoto, Day,
98 Lambers, & Noguchi, 2004) and reproductive (Bahuguna, Solis, Shi, & Jagadish, 2017; Mohammed,
99 Cothren, & Tarpley, 2013) phases of development have reported limited and variable levels of
100 acclimation of R_{dark} . By contrast, A_n of rice shows strong thermal acclimation, with rates of net CO_2
101 uptake measured at the prevailing growth T being homeostatic or increasing as growth T is increased

102 from 15 to 37°C (Nagai & Makino, 2009; Yamori, Noguchi, Hikosaka, & Terashima, 2010). Such
103 studies point to a possible asynchrony in rice acclimation, with a more dynamic A_n than R_{dark} response,
104 although further work simultaneously comparing A_n and R_{dark} in rice is needed. Interestingly, a range
105 of other crops and non-crop species show the opposite – greater R_{dark} than A_n acclimation capacity
106 (Campbell et al., 2007; Drake et al., 2016; Way & Oren, 2010). Although such studies detail the
107 physiological acclimation of energy metabolism in plants, including rice, less is known about the
108 molecular and biochemical responses that underpin this phenotypic T acclimation.

109 It is with the above issues in mind that we conducted a study using the IR64 cultivar of *Oryza*
110 *sativa* to address the following aims: (1) characterise the extent of thermal acclimation of R_{dark} and A_n ;
111 and, (2) link physiological acclimation to the underlying processes through analysis of leaf transcript,
112 protein, sugar, and starch abundance, following changes in growth T . We hypothesized that: (1) initial
113 exposure to very high growth T increases and decreases the rates of respiratory CO_2 release and net
114 photosynthetic CO_2 uptake, respectively; (2) subsequent acclimation is associated with recovery of A_n ,
115 and reduced rates of R_{dark} ; and (3) thermal acclimation of R_{dark} and A_n is associated with dynamic
116 changes in gene expression and protein abundance in key pathways associated with energy capture
117 and use.

118

119 **Materials and methods**

120

121 *Plant material and temperature treatments*

122 Rice (*Oryza sativa*) cultivar IR64 plants were grown hydroponically in a glasshouse facility at the
123 Research School of Biology, Australian National University in Canberra between October and
124 December 2015. Seeds were initially incubated at 40-42°C for two days before soaking in water for
125 eight hours, placed on wet Whatman filter papers in petri dishes and kept in the dark at 30°C for five
126 days. The germinated seedlings were then transferred to trays of vermiculite and placed in temperature-
127 controlled glasshouses (30°C day and 25°C night) under natural sunlight and photoperiod, with
128 photosynthetically active radiation (PAR) between 400 and 1200 $\mu\text{mol m}^{-2} \text{s}^{-1}$. When the third leaf had
129 emerged, seedlings were transplanted from vermiculite to a hydroponic system. Individual plants were
130 placed within PVC tubes with a 3.7 cm diameter and 13 cm height. Tubes were then suspended at the
131 top of 20 L capacity hydroponic tanks (12 tanks in total), with each tank holding a maximum of 20
132 plants. Each tank was filled with hydroponic solution (Table S1) (Hubbart, Peng, Horton, Chen, &
133 Murchie, 2007). The nutrient solution was replaced weekly. Sulphuric acid or sodium hydroxide were
134 used to adjust the pH to 5-6, with pH monitored using a portable pH meter (Rowe Scientific Pty. Ltd.,

135 NSW, Australia). The hydroponic solution was aerated continuously using Infinity AP-950 air pumps
136 (Kong's Pty. Ltd., Ingleburn, Australia).

137 After two weeks of hydroponic growth at 30/25°C ('warm' treatment), the most recently fully-
138 expanded leaves were labelled as pre-existing (PE) leaves. Following labelling, four tanks were
139 randomly chosen and shifted to an adjacent glasshouse room set to 25°C day and 20°C night (25/20°C –
140 'cold' treatment), and four other tanks were moved to a room set at 40°C day and 35°C night (40/35°C
141 – 'hot' treatment); four tanks were retained at 30/25°C as controls. Relative humidity was not
142 controlled. Newly-developed (ND) leaves that emerged under each thermal regime were labelled, with
143 all measurements reported on ND leaves made 21 days after *T*-transfer.

144

145 *Determination of transcript abundance*

146 Plants were transferred to new thermal regimes three hours after sunrise. To quantify transcript
147 abundance, the labelled pre-existing (PE) leaves were harvested during the photoperiod: two, six and
148 24 h after *T*-transfer. For each time-point and temperature treatment, approximately 8 cm long
149 segments (less than 100 mg of fresh mass) were sampled half-way along the leaf blade, and
150 immediately frozen in liquid N₂ and stored at -80°C until RNA extraction. Total RNA was extracted
151 using the RNeasy plant mini protocol (Qiagen, Doncaster, VIC, AU) and treated with DNase I (Qiagen,
152 Doncaster, VIC, AU) to remove any contaminating DNA.

153 For qPCR analysis, 1 µg of total RNA in a 10 µL volume was reverse-transcribed into cDNA
154 using SuperScript III First-Strand cDNA Synthesis Kit (Invitrogen, Carlsbad, CA, USA), according to
155 the manufacturer's instructions. The reverse-transcribed cDNA samples were diluted 10-fold.
156 Transcript levels of six selected genes and one reference gene (refer to Table S2 for gene accession
157 numbers and primer sequences) were analysed using a Light-Cycler® 480 System (Roche Holding
158 AG, Basel, Switzerland) with SYBR Green I Dye (QIAGEN, Doncaster, Victoria, AU). cDNA
159 samples from each biological replicate were assayed in two technical duplicates. The reaction-mix in
160 each qPCR contained 0.4 µM of each pair of primers, 5 µL of SYBR Master Mix, and 4.6 µL of the
161 diluted cDNA sample in a 10 µL total reaction volume. The raw fluorescence data were analysed using
162 LinRegPCR (Ramakers, Ruijter, Deprez, & Moorman, 2003; Ruijter et al., 2009). Data were
163 normalized to the reference gene, eukaryotic initiation factor 5c (*EIF5C*; LOC_Os11g21990.1), and
164 were expressed as fold-changes against control conditions.

165 RNAseq libraries were prepared using the Illumina Stranded Total RNAseq kit with RiboZero
166 rRNA depletion as per the manufacturer's guidelines (Illumina). Libraries were pooled and sequenced
167 on a HiSeq1500 for 61 cycles in single end mode at the Centre for AgriBioscience, University of
168 LaTrobe. Analysis pipelines for pre-processing and mapping of sequence data are available online on

169 GitHub (<https://github.com/pedrocrisp/NGS-pipelines>). Quality control was performed with *FastQC*
170 v.0.11.2. Adapters were removed using *scythe* v.0.991 with flags -p 0. and reads were quality trimmed
171 with *sickle* v.1.33 with flags -q 20 (quality threshold), and -l 20 (minimum read length after trimming).
172 The trimmed and quality-filtered reads were aligned to the rice reference genome Os-Nipponbare-
173 Reference-IRGSP-1.0 from the MSU Rice Genome Annotation Project Database v7
174 (<http://rice.plantbiology.msu.edu/>) using the *subjunc* aligner v1.5.0-p1 with -u and -H flags to report
175 only reads with a single unambiguous best mapping location, -P 3 for phred+33 encoding (Liao, Smyth,
176 & Shi, 2013b). Reads were then sorted, indexed and compressed using *samtools* v1.1-26-g29b0367
177 (Li et al., 2009) and strand-specific bigwig files were generated using *bedtools genomecov* v2.16.1
178 (Quinlan & Hall, 2010) and the UCSC utility *bedGraphToBigWig* for viewing in IGV (Robinson et
179 al., 2011). Summary statistics for each sample are provided in Supplementary Dataset S1: Summary
180 of transcriptomic datasets.

181 For standard differential gene expression testing, the number of reads mapping per IRGSP-
182 1.0 gene loci was summarised using *featureCounts* v1.5.0-p1 (Liao, Smyth, & Shi, 2013a) with flags
183 -P and -c to discard read pairs mapping to different chromosomes and the -s flag set to 2 for strand
184 specificity for a strand specific library, multimapping reads and multioverlapping reads were not
185 counted. Reads were summarised to parent IRGSP-1.0 gene loci rather than individual splice variants
186 by summarising to the genomic coordinates defined by the feature "gene" in the IRGSP-1.0.gff
187 reference (last modified 7/2/2012
188 ftp://ftp.plantbiology.msu.edu/pub/data/Eukaryotic_Projects/o_sativa/annotation_dbs/pseudomolecules/version_7.0/all.dir/all.gff3). Only loci
189 with an abundance of at least 1 CPM (approximately 5 reads) in at least 4 samples were retained.
190 Statistical testing for relative gene expression was performed in R following the “*edgeR-limma-*
191 *voom*” approach (<https://www.bioconductor.org/help/workflows/RNAseq123/>); using, *edgeR* v.3.4.2
192 (McCarthy, Chen, & Smyth, 2012; Robinson & Oshlack, 2010; Robinson & Smyth, 2007a, 2007b),
193 and *voom* in the *limma* package 3.20.1 (Law, Chen, Shi, & Smyth, 2014; Smyth, Michaud, & Scott,
194 2005).

195

196 *Determination of protein abundance*

197 Samples of frozen PE leaf material six and 24 h after *T* transfer, as well as frozen ND leaf material,
198 were ground to a fine powder using a chilled mortar and pestle, and protein was extracted in extraction
199 buffer containing 100 mM tricine pH 8.0, 1 mM EDTA, 1 mM PMSF, 1x protease inhibitor cocktail,
200 2% (w/v) PVPP, 10 mM (w/v) ascorbate, 5 mM DTT, and distilled water. The sample was then
201 solubilized in a NuPAGE LDS Sample Buffer (Invitrogen, Carlsbad, CA, USA) with 10% (v/v) DTT,
202 then heated for 10 minutes at 95°C, and centrifuged for 30 sec at 12,000 RPM. Thereafter, supernatant

203 was collected and 8 μ L were loaded and separated on 4-12% NuPAGE Bis-Tris gel (Invitrogen,
204 Carlsbad, CA, USA) using the MOPS-based buffer system. To blot, proteins from the gel were
205 transferred to Immobilon-P Polyvinylidene fluoride (PVDF) membranes (Merck Millipore, Kilsyth,
206 VIC, AU) using an XCell II Blot module (Invitrogen, Carlsbad, CA, USA). Membranes were then
207 blocked for 2 h with 5% (w/v) skim-milk powder in Tris-buffered saline containing 0.1% (v/v) Tween-
208 20 (TBST). To probe for cytochrome *c* oxidase (*COX*) subunit II, alternative oxidase (*AOX*),
209 uncoupling protein (*UCP*) and voltage-dependent anion-selective channel protein (*VDAC1*-porin), the
210 membranes were incubated for 2 h in primary antibody solution (5% w/v skim milk powder in TBST)
211 containing commercially available polyclonal antibodies (Agrisera, Vännäs, Västerbotten, Sweden).
212 All antibodies were diluted 1:5000. An antibody for ribulose-1,5-bisphosphate carboxylase/oxygenase
213 (Rubisco) was received from Assoc. Prof. Spencer Whitney (Research School of Biology, Australian
214 National University, Canberra, ACT, AU) and used at a dilution of 1:10 000. After washing with TBST,
215 the membranes were incubated for 1 h in goat anti-rabbit antibody solution (5% w/v skim milk powder
216 in TBST) at a dilution of 1:8000. Proteins were then visualized using the AttoPhos AP fluorescent
217 substrate system (Promega, Madison, WI, USA), imaged using a Versa-Doc (Bio-Rad, Hercules, CA,
218 USA) imaging system and quantified using Image Lab software (Bio-Rad, Hercules, CA, USA).
219 Protein concentrations were determined by the Bradford method using Bovine Serum Albumin (BSA)
220 as a standard.

221 222 *Determination of soluble sugar and starch ~~content~~ concentrations*

223 Starch and soluble sugars of PE leaves transferred from 30/25°C to 25/20°C or 40/35°C for one and
224 seven days, and ND leaves at the prevailing *T* were collected from separate, previously unsampled
225 plants. Samples were collected at 9:30 to 10:00 am, corresponding to 3 h into the light period, frozen
226 and stored at -80°C before freeze-drying at -105°C for two days (Virtis Benchtop™ “K”, SP, Scientific,
227 Gardiner, NY, USA), then ground to a fine powder from which a 5-10 mg aliquot was taken. Five-
228 hundred μ L of 80% (v/v) ethanol was added and vortexed for 20 sec. Thereafter, leaf tissues were
229 incubated at 80°C while being centrifuged at 500 RPM for 20 min. Following further centrifugation at
230 12,000 RPM for 5 min, the resulting pellet and supernatant were separated. This procedure was
231 repeated a two more times, and the three pellets and three supernatants were pooled. The pooled
232 supernatants and pellets were used for determination of soluble sugars and starch
233 ~~contents~~ concentrations, using a Fructose Assay Kit (Sigma-Aldrich, St Louis, MO, USA) and a Total
234 Starch Assay Kit (Megazyme, Chicago, IL, USA), respectively. Following manufacturer’s instructions,
235 measurements were made in triplicate, at a wavelength of 340 nm, using a microtitre plate reader

236 (Infinite® M1000 Pro; Tecan US, Morrisville, NC) and standard curves were generated for soluble
237 sugars using sucrose, glucose and fructose (Sigma-Aldrich, St Louis, MO, USA) at known
238 concentrations.

239
240 *Gas exchange measurements using Licor 6400XT 6 cm² cuvettes*

241 Gas-exchange was measured on fully-expanded pre-existing (PE) leaves just prior to- and one, two,
242 three, five and seven days after *T* transfer, as well as on fully-expanded newly-developed (ND) leaves
243 21 days after transfer, using two matched LI-6400 instruments equipped with 6 cm² cuvettes and a
244 6400-02B red-blue light source (Li-Cor, Lincoln, NE, USA). At each time point, light-saturated net
245 CO₂ assimilation rates (A_n) and then dark respiration rates (R_{dark}) were measured during the light period
246 (between 10 am and 2 pm) in the glasshouses, at the prevailing day-time *T* of each treatment as well
247 as at a common temperature of 30°C for ND leaves. In call cases, A_n was measured first, with the
248 following settings: 1000 $\mu\text{mol m}^{-2} \text{s}^{-1}$ photosynthetic photon flux density (PPFD), relative humidity
249 of 60–70%, 400 ppm reference CO₂, and a flow rate of 500 $\mu\text{mol s}^{-1}$. Photosynthesis was measured
250 when CO₂ concentrations in the sample IRGA had stabilized, typically within 10 minutes of exposure
251 to 1000 $\mu\text{mol m}^{-2} \text{s}^{-1}$ PPFD. Thereafter, R_{dark} was measured as above but with the flow rate slowed to
252 300 $\mu\text{mol s}^{-1}$ and turning off the light source for at least 30 minutes of darkness before taking
253 measurements.

254
255 *Gas exchange measurements using using Walz chambers*

256 High resolution temperature response curves of R_{dark} and light-saturated A_n were made on intact ND
257 leaves using two matched LI-6400XT portable gas exchange systems (Li-Cor, Lincoln, NE, USA)
258 each connected to a 14 x 10 cm well-mixed, temperature-controlled Walz Gas-Exchange Chamber
259 3010-GWK1 (Heinz Walz GmbH, Effeltrich, Germany). For each temperature-response curve, leaf *T*
260 was measured with a small-gauge wire copper constantan thermocouple pressed against the lower
261 surface of the leaf and attached to a LI-6400 external thermocouple adaptor (LI6400-13, Li-Cor Inc.,
262 Lincoln, NE, USA) that enabled leaf temperature to be recorded by the LI-6400XT. As leaves were
263 heated, net CO₂ exchange was recorded at 30 s intervals using the LI-6400XT portable gas exchange
264 systems fitted with an empty and closed 6 cm² chamber that was plumbed into the airstream exiting
265 the Walz leaf chamber (Fig. S1). A_n was measured as described for the 6 cm² cuvette but using a Walz
266 LED-Panel RGBW-L084 light source (Heinz Walz GmbH, Effeltrich, Germany). A_n was monitored
267 as leaves were heated at 1°C min⁻¹ from 20 to 45°C. A water trap was used to remove water vapour,
268 as transpiration from whole intact leaves was incompatible with Licor instrumentation. Therefore,
269 stomatal conductance (g_s) and associated water parameters were not recorded. For R_{dark} , on separate

270 leaves to those used for measuring A_n , the flow rate was reduced to $300 \mu\text{mol s}^{-1}$, the light source was
271 turned off, and the chamber was covered with a black cloth, before increasing the leaf temperature in
272 steps of 1°C min^{-1} , from 20 to 60°C . In parallel to quantifying the temperature-response of R_{dark} , we
273 measured minimal chlorophyll *a* fluorescence (F_0) in the presence of a low-intensity far-red light pulse
274 (necessary to maintain PSII in the oxidized state) every 30 sec using a Mini-PAM portable chlorophyll
275 fluorometer (Heinz Walz, Effeltrich, Germany) fitted above the glass surface of the leaf chamber. The
276 temperature at which F_0 increased was used as an indication of heat-induced damage to photosystem
277 II, which we hereafter refer to as T_{crit} , calculated using the template of O'Sullivan *et al.* (2013). At the
278 cessation of measurements, leaves were photographed and analysed for leaf area using ImageJ
279 software (Abramoff, Magelhaes, & Ram, 2004). Leaves were stored in paper bags, oven-dried at 70°C
280 for two days and weighed to obtain the dry mass. Quadratic equations were fit to A_n temperature curves
281 and the x- and y-axis values corresponding to the vertex taken as the T -optimum (T_{opt}) and A_n -optimum
282 (A_{opt}) of net assimilation, respectively. For the R_{dark} temperature curves, the x- and y-axis values
283 corresponding to the maximum recorded R_{dark} were taken as the T at which R_{dark} reached a maximum
284 (T_{max}) and the maximum R_{dark} value recorded (R_{max}), respectively.

285

286 *Leaf elongation rates*

287 The leaf elongation rates (LER) of four leaves from separate plants from each temperature regime were
288 measured at five separate time-points over a 24 h period. Measurements were made using a ruler,
289 starting from the ligule of the second youngest leaf to its tip.

290

291 *Statistical analysis*

292 For all T -treatments and collection times, four separate leaves from four separate previously unsampled
293 plants, one plant from each of the four hydroponic tanks (pot replicates) were sampled. One-way
294 Analysis of Variance (ANOVA) was performed on R_{dark} and A_n gas-exchange experiments comparing
295 temperature treatments. Two-way ANOVA was performed on LMA and protein, starch, and sugar
296 ~~contents~~ concentrations comparing time of sampling and temperature treatments. Gas-exchange and
297 leaf biochemical statistical analysis was performed using GraphPad Prism (v 7) software. Statistical
298 analysis of transcript abundance was performed using R statistical software (v 3.6.1) and packages as
299 mentioned above.

300

301 *Data availability*

302 RNA-seq data is available under the GEO identifier GSE136045.

303

304 Results

305

306 *Molecular and biochemical responses of leaves to T*

307 Quantitative PCR was performed on specific genes of interest to elucidate the genetic response of pre-
308 existing (PE) leaves exposed to a change in *T* (Fig. 1). Apart from a sharp rise 6 h into the 40/35°C *T*-
309 transfer, there was a general reduction in transcript abundance of *cytochrome c complex-oxidase* (*cox*),
310 a gene encoding the central respiratory electron transport chain. This reduction occurred in leaves
311 transferred to 25/20°C and 40/35°C, over the seven days post-transfer period, . Two genes encoding
312 respiratory proteins that potentially reduce the production of ATP – *alternative oxidase* (*aox*) and
313 *uncoupling protein* (*ucp*) – both showed an initial increase in expression within the first 24 h of transfer
314 to the hotter 40/35°C, followed by a decline to 30/25°C levels by 48 h. The photosynthetic electron
315 transport gene *ferredoxin NADP reductase* (*fnr*), and the Calvin/Benson cycle gene
316 *phosphoribulokinase* (*prk*) generally showed an increase in expression in the first 48 h at 40/35°C
317 before being suppressed for up to 5 days post-transfer. *Sucrose phosphate synthase* (*sps*), involved in
318 the synthesis of sucrose from its precursors, also initially spiked in the first 24 h following transfer to
319 40/35°C, before being transiently suppressed. Both *sps* and the respiratory and photosynthetic genes –
320 apart from *aox* – followed a similar expression profile when heat-treated, suggesting that assimilate
321 production/consumption and sucrose synthesis were coordinated in response to heat perturbations. In
322 general, the greatest perturbation to gene expression occurred within the first 24 h after transfer.

323 Based on the qPCR results, we conducted RNA-seq at two, six and 24 h after transfer of PE
324 leaves to new *T*. Following data quality control and filtering, transcript abundance of 19,308 rice genes
325 were retained for differential expression testing. Around 20 M reads were obtained per sample, which
326 were aligned to the Os-Nipponbare-Reference-IRGSP-1.0 rice reference genome (Data Set S1).
327 Principal component analysis showed a substantial treatment effect on gene expression for the heat-
328 exposed leaves (40/35°C) during the first six hours after *T*-transfer compared to the other two 30/25°C
329 and 25/20°C growth regimes (Fig. 2). Globally, there was little gene expression variation between the
330 cold (25/20°C) and the warm (30/25°C) control conditions. After 24 h of growth at new *T*-regimes,
331 limited variation in gene expression was observed between all of the three *T*s (Table S3).

332 To assess changes in the expression of individual genes to the hot or cold treatments,
333 differentially expressed genes were identified at each time point by comparison to the warm control
334 expression levels (Data Set S2). There were very few genes differentially expressed under the cold
335 conditions, only six genes in total (Table S3). By contrast, under hot conditions, there were 1,818 and
336 1,465 genes differentially expressed after two and six hours, respectively. After 24 hours, there were

337 no differentially expressed genes under the hot conditions compared to the control plants. There was
338 a significant overlap between the genes differentially expressed after two and six hours of heat
339 treatment, (Fig. 3a, b). In total, 30% of the genes upregulated after six hours were already upregulated
340 by two hours, and 38% of genes downregulated after six hours were already downregulated by two
341 hours. Many of the remaining genes that were significantly different in transcript abundance only after
342 six hours were already trending in the same direction at the two-hour time point, but the difference
343 compared to the controls did not pass the significance threshold (Fig. 3 c). Overall, these results show
344 that there are significant short-term changes in transcript abundance in rice plants exposed to heat
345 stress. The expression profiles of samples exposed for two and six hours show consistent changes;
346 however, some of the changes peak at two hours and others peak at six hours and most changes
347 dissipate within 24 hours.

348 In total, the heat treatment led to the up- and down-regulation of 1,337 and 1,446 genes,
349 respectively. To investigate the extent to which these genes have a photosynthetic or respiratory
350 function, we first examined expression of genes involved in photosynthesis, glycolysis, TCA and
351 mitochondrial electron transport using MapMan pathway annotations (Fig. S2-4) (Thimm et al., 2004).
352 This qualitative analysis revealed that the expression of only a small number of
353 photosynthetic/respiratory genes were affected. To extract a list of high-confidence differentially
354 expressed respiration-related genes, we manually curated a list of rice loci with homology to
355 Arabidopsis respiration genes (Data Set S3). Using this list, we found that eight genes were
356 differentially expressed at high temperature, with two genes downregulated more than 2-fold: *aox* and
357 ATP-dependent *phosphofructokinase* (Table 1). The seemingly conflicting result of an initial increase
358 in *aox* from the qPCR results, but a decline in *aox* during the same period from the RNA-seq results,
359 can be explained by our qPCR primers targeting the *aox1a* isoform while the RNA-seq identified a
360 decline in the *aox1c* isoform (Data Set S3).

361 It is interesting that in addition to the increase in *aox* and *ucp* gene expression, the expression
362 of an external NAD(P)H dehydrogenase also increased, while that of Complex II decreased
363 significantly (Table 1). Together these changes suggest that an increase in non-phosphorylating
364 electron transport occurred in response to exposure to higher *T*, at the expense of electron transport
365 coupled to ATP synthesis, at least in the short term. The increase in external NAD(P)H dehydrogenase
366 gene expression may also indicate an increased need for mitochondrial oxidation of excess reductant
367 produced in the chloroplast at higher *T*.

368 Given the relatively small effect of the heat treatment on the expression of respiration- or
369 photosynthesis-related genes, we next performed Gene Ontology enrichment analysis. This revealed a

370 notable enrichment for genes involved in primary metabolism (eg GO:0044238) and response to
371 abiotic stimuli (eg GO:0050896), as well as in many biosynthetic pathways (Fig 4).

372 Protein abundance (expressed on a leaf area basis) of key mitochondrial electron transport
373 components – CYTOCHROME C OXIDASE (COX) subunit II, ALTERNATIVE OXIDASE (AOX)
374 and UNCOUPLING PROTEIN (UCP) – were determined by Western blots in PE leaves 6 h and one-
375 day after *T*-transfer, and in newly developed (ND) leaves that formed under each prevailing growth *T*
376 (Fig. 5, Fig. S4). The cold (20/25°C) and heat (40/35°C) treatments did not affect the total protein
377 concentration of leaves, at any time after *T*-transfer (Table S4). As was the case for gene expression,
378 there was a significant decline in COX subunit II protein abundance after 24 h. COX subunit II also
379 declined in abundance in ND leaves when grown at 40/35°C compared to 25/20°C (Fig. 5a). We
380 assume the changes observed in COX subunit II reflect changes in abundance of the entire complex.
381 The abundance of AOX and UCP protein did not vary in response to growth *T* or duration of exposure
382 to heat for either PE or ND leaves, despite the initial spike in *aox* and *ucp* gene expression after transfer
383 to 40/35°C (Fig. 1). Interestingly two bands of AOX that varied relative to one another with
384 temperature treatment were evident in the Western blot (Fig. S5). This is consistent with the
385 fluctuations in expression of different *aox* genes noted above. Patterns of protein abundance were
386 similar when the analysis was standardised to dry mass or porin abundance (Fig. S6). Porin is a voltage-
387 dependent channel protein located at the outer membrane of mitochondria and is widely used as a
388 proxy for mitochondrial surface area due to its stability under a wide range of environmental conditions
389 (Noguchi, Taylor, Millar, Lambers, & Day, 2005; Shane et al., 2004). Thus, the matching results using
390 leaf area, dry mass or porin abundance indicate that the decline in COX abundance with increased *T*
391 was not a result of changes in Leaf Mass to Area ratio (LMA) or reduced mitochondria per unit area
392 of leaf. There was a trend for the abundance of Rubisco to decline with the amount of time a leaf
393 developed under 40/35°C (Fig. 5d), although there were no statistically significant *T* or developmental
394 stage effect.

395 LMA and starch, glucose, fructose and sucrose ~~contents~~ concentrations were measured in PE
396 leaves one and seven days after *T*-transfer, and in ND leaves at the prevailing temperature (Table 2).
397 LMA did not change significantly in response to *T*, for either transferred PE leaves or ND leaves,
398 similar to previous observations in rice over a similar *T* range (Nagai & Makino, 2009). However, ND
399 leaves did exhibit significantly greater LMA than PE transferred leaves, suggesting an effect of leaf
400 rank on LMA. Transferred PE and subsequently formed ND leaves exhibited consistently lower starch
401 ~~content~~ concentrations with increasing *T* and significantly lower starch with extended duration of
402 development at the prevailing *T*. Unlike the dynamic responses of leaf starch ~~content~~ concentrations

403 to T change, ~~contents-concentrations~~ of soluble sugars were remarkably stable across both PE and ND
 404 leaves, in terms of both T -regime and exposure time. Negative correlations between R_{dark} and soluble
 405 sugars were observed among leaves within each individual T treatment but not among the three T
 406 treatments (Table S5).

407

408 *CO₂ flux in responses to T*

409 How molecular changes altered the physiological performance of rice carbon metabolism at differing
 410 growth T was investigated through gas-exchange measurements. Rates of A_n and R_{dark} are here
 411 presented on a dry mass (DM) basis, noting that the patterns are similar when expressed on a leaf area
 412 basis (Fig S7), reflecting the fact that growth T had no significant effect on LMA (Table 2). A
 413 significant change in both A_n and R_{dark} (using mid-sections of leaves placed in Licor 6400 3 x 2 cm
 414 chambers) occurred within the first 24 h of transfer to a 40/35°C T -regime for PE leaves, with A_n
 415 falling and R_{dark} increasing when measured at the prevailing growth T (Fig. 6). This was followed by
 416 stabilisation at the new rate over the subsequent six days. By contrast, A_n and R_{dark} remained relatively
 417 constant at both 30/25°C and 25/20°C over a seven-day period monitoring period. Interestingly, rates
 418 of R_{dark} for the 30/25°C treated plants decreased from day 3 to 7, compared to the first three days,
 419 resulting in slightly lower rates of R_{dark} than for the 25/20°C treated plants by day 7. This possibly
 420 reflects temperature-dependent differences in leaf senescence rates. ~~Interestingly~~ As it could not be
 421 controlled, relative humidity in the 40/35°C glasshouse room (Fig. S8) was substantially lower than
 422 the other two rooms, leading to reduced humidity during gas-exchange measurements (Fig. 6c). As a
 423 consequence, the vapour pressure deficit between the leaf and surrounding air (VPD_{Leaf}) increased
 424 ~~consistently~~ over the first seven days in PE leaves transferred to 40/35°C, resulting in a dramatic
 425 difference by day seven (Fig. 6de). ~~This, and the associated reduction in e higher~~ VPD_{Leaf} coincided
 426 with lower stomatal conductance g_s of their 40/35°C treated leaves at days three, five and seven, and
 427 lower intercellular to ambient CO₂ concentration ratios (C_i/C_a) at days five and seven (Fig. 6e, fd).
 428 ~~However, for the first two days post transfer, both the~~ VPD_{Leaf} vapour pressure deficit and g_s stomatal
 429 conductance were similar between the three growth T s, and therefore, the did not explain the
 430 initial 48 h decline in A_n and changes in transcript abundance at within one day of transfer to 40/35°C
 431 were not attributable to water relations, likely contributing to the longer-term limitation in
 432 photosynthesis at this warmer temperature in PE leaves. Over the longer-term, water relations may
 433 have contributed to a slight reduction in C_i/C_a , but not enough to influence A_n , with A_n being stable
 434 from one to seven days after transfer irrespective of changes in g_s and C_i/C_a (Fig. 6b). The changes in
 435 g_s were not substantive enough to change leaf T , which was stable over the seven days, with both air

436 ~~*T* and leaf *T* deviating by less than 2°C from the set room *T* (Fig. S8). However, for the first two days~~
 437 ~~post transfer, the vapour pressure deficit and stomatal conductance was similar between the three~~
 438 ~~growth *T*s, and therefore did not explain the initial 48 h decline in A_n at 40/35°C.~~

439 Short-term temperature response curves of entire ND leaves that formed at each prevailing
 440 growth *T* regime were quantified over a 20 to 60°C range using the Walz large leaf chamber (Fig. 7;
 441 refer to Figure S98 for area-based rates and Table S6 for quadratic equations fit to curves). Over most
 442 of the range of measuring *T*s, leaves developed at 25/20°C exhibited higher rates of R_{dark} than those
 443 developed under the other two *T*-regimes. Rates were lowest in leaves developed at 40/35°C (Fig. 7a).
 444 When normalised to rates at 30°C, differences in R_{dark} were less pronounced (Fig. 7b), indicating that
 445 while R_{dark} at a given measuring *T* was affected by growth *T*, the general shape of the R_{dark} -*T* curves
 446 remained largely similar across the three treatments. These observations are consistent with a Type II
 447 (changes in baseline) rather than Type I (changes in Q_{10} , the increase in R_{dark} with a 10°C increase in
 448 *T*) respiratory acclimation response (Atkin & Tjoelker, 2003). Importantly, while respiratory thermal
 449 acclimation occurred, it was not sufficient to result in R_{dark} being homeostatic across the three growth
 450 *T* treatments. As a result, R_{dark} measured at the growth *T* was significantly ~~faster~~ greater in the leaves
 451 developed under hot conditions than under the other two treatments (Table 3). Growth *T* also had a
 452 significant effect on the measuring *T* at which R_{dark} and A_n reached their maximum rates, with leaves
 453 developed under high *T* exhibiting higher *T*-maxima than control 30/25°C leaves (Table 3). When
 454 measured at the prevailing growth *T* of each treatment, mass-based rates of light-saturated A_n were
 455 stable (i.e. homeostatic), further supporting the occurrence of strong thermal acclimation of A_n in ND
 456 leaves (Fig. 7), contrary to PE leaves (Fig. 6). The temperature at which PSII lost functionality (T_{crit})
 457 ~~also increased~~ tended to increase with growth *T* (being 3.8°C higher in the hot-grown plants compared
 458 to those grown at 25/20°C), although the differences were not statistically significant at $p < 0.05$ (Table
 459 3). The high degree of thermal acclimation exhibited by photosynthesis resulted in the ratio of R_{dark} to
 460 A_n being lowest in the hot-grown plants, particularly at high measuring *T* (Fig. 8a); at a measuring *T*
 461 of 40°C, hot-acclimated plants exhibited R_{dark}/A_n ratios that were 50% lower than those measured for
 462 their cold-grown counterparts. Further evidence that rice acclimated to heat is seen in the fact that leaf
 463 elongation rates – taken over the day and night period – were faster for the 40/35°C grown plants at
 464 all times (Fig. 8b). Interestingly, A_n of PE leaves ranged from 1.2 to 1.8 $\mu\text{mol g}^{-1} \text{DM s}^{-1}$ (Fig. 6),
 465 substantially faster than the 0.6 $\mu\text{mol g}^{-1} \text{DM s}^{-1}$ in ND leaves (Fig. 7). The former were obtained from
 466 measurements on mid-leaf sections placed in a 6 cm² chamber, while the latter were obtained from
 467 whole leaves placed in a 14 x 10 cm Walz chamber. The lower A_n rates in the latter might reflect a

468 lower proportion of mesophyll cells per unit of area or DM across whole blades compared to the mid-
469 blade section.

470

471 Discussion

472

473 Our study investigated the response of photosynthetic and respiratory metabolism to short- and long-
474 term changes in growth T – the highest of which is indicative of heat-wave T s – to explore: (1) the
475 extent of thermal acclimation of photosynthesis and respiration; and, (2) what underlying changes in
476 gene expression and protein abundance occur during the acclimation process. The results demonstrate
477 that the process of acclimation begins with abrupt changes in gene expression in PE leaves within the
478 first 24 h of heat exposure, followed by a return to homeostatic gene expression (Fig. 1). Importantly,
479 the abundance of the key energy-conserving respiratory protein, COX, declines in abundance when
480 pre-existing leaves are heat-treated for 24 hours, with this phenotype being maintained in newly-
481 developed leaves formed at 40/35°C (Fig. 5). This decline in COX was linked to a slight decline in
482 overall rates of R_{dark} (Fig. 7). The results support the hypothesis that acclimation of photosynthesis
483 and dark respiration are asynchronous in rice, but contrary to observations in non-crop species
484 (Campbell et al., 2007), light-saturated A_n acclimated to a greater extent than R_{dark} (Fig. 7; Table 3).
485 This ability to maintain photosynthetic carbon gain at 40°C is likely to be of crucial importance in
486 helping rice maintain growth during heat-wave conditions.

487

488 *Acclimation to changes in T are rapid and involve a multitude of genes*

489 There was a substantial change in the gene expression profile of rice leaves shifted from 30°C to 40°C
490 within the first 24 h of transfer (Figs. 1, 2, 3, and 4). As might be expected, the largest number of gene
491 expression perturbations were in primary and cellular metabolic processes (Fig. 4). This extensive
492 metabolic response aligns with the instability in R_{dark} and A_n fluxes over the initial 24 h post T -transfer
493 (Fig. 6), which would have contributed to a metabolic imbalance through changes in assimilate supply
494 and demand. Interestingly, the most responsive genes to the initial exposure to heat among upregulated
495 genes were genes involved in biosynthetic processes (Fig. 4) suggesting a stimulation of growth. This
496 is supported by the longer-term increase in leaf elongation rates observed in the 40/35°C grown plants.

497 When analysed in more detail, we observed that heat ~~to~~-induced genes linked to energy
498 dissipation (*aox* and *ucp*) over the first 24 h of 40°C heat exposure (Fig. 1, Table 1). AOX and UCP
499 are involved in the diversion of electrons for formation of proton gradients and subsequent ATP
500 synthesis (Krauss, Zhang, & Lowell, 2005; Vanlerberghe, 2013). Past work has shown that

501 overexpressing *aox* in young rice seedlings imparts a benefit on growth under a T of 37°C for eight
502 days, which was attributed to a reduction of excessive proton motive force and reactive oxygen species
503 (Murakami & Toriyama, 2008). Given that AOX and UCP both divert electrons away from ATP
504 synthesis under conditions of high reductant supply, the rapid upregulation of these genes following
505 the initial changes in growth T – with rapid stimulation of R_{dark} and presumably greater reduction of
506 ubiquinone pools (UQ) – indicates that there may have been a temporary imbalance between NAD(P)H
507 supply and demand for ATP. The initial increases in *aox* and *ucp* gene expression (Fig. 1) did not
508 translate into increased total AOX and UCP protein abundance (Fig. 5). However, qPCR results
509 indicate upregulation of the *aox1a* isoform, responsive to abiotic stress in Arabidopsis mitochondria
510 (Clifton, Millar, & Whelan, 2006; Shapiguzov et al., 2019), while over the same period RNA-seq
511 analysis indicated a significant decline in a separate *aox1c* isoform. It is possible that the AOX1C
512 isoform is less tolerant of high temperatures and therefore is partially replaced by the AOX1a isoform.
513 In this context it is interesting that in Arabidopsis AOX1a is the major stress-inducible isoform. Since
514 AOX operates as a non-covalently linked dimer (Siedow & Umbach, 2000), the change in the relative
515 expressions of *aox1a* and *1c* isoforms may also indicate a change in the conformation of the AOX
516 dimer, with a different mix of homo- and hetero-dimers in response to heat. This suggests that AOX
517 may have shifted to a more heat-tolerant conformation at 40/35°C, at least when the initial shock was
518 imposed. This is an illustration that enzyme isoforms can be an important part of abiotic stress
519 responses that can be easily overlooked when only considering total protein abundance.

520 The limited gene induction when leaves were transferred from 30 to 25°C (Fig. 3c) suggests
521 that a shift to this colder growth T did not significantly perturb metabolic processes in rice leaves,
522 consistent with the limited PE leaf response of R_{dark} or A_n when exposed to the cold (Fig. 6). However,
523 cold-responsive transcriptional regulators and associated changes in metabolism expected from cold
524 exposure (Zhu, Dong, & Zhu, 2007) must have been triggered by the colder T s. Regulatory adjustments
525 did indeed occur in ND rather than PE leaves, with R_{dark} at a given T being higher in the cold-grown
526 ND leaves (Fig. 7), and homeostasis of A_n being reached in ND leaves when measured at the prevailing
527 growth T (Table 3, Fig. 7).

528

529 *The most evident longer-term acclimation response is reduced COX abundance*

530 The clearest biochemical response to increasing growth T , both in PE and ND leaves, was a decline in
531 the abundance of COX (Fig. 5). A decline in COX has been reported for rice roots when grown at
532 25°C relative to 15°C (Kurimoto, Millar, Lambers, Day, & Noguchi, 2004). Conversely, COX content
533 increased in *Arabidopsis thaliana* leaves grown at 5°C relative to 21°C (Armstrong et al., 2008). In

534 all these cases, COX protein content and rates of respiration at a common measuring T (including in
535 our study; Fig. 5 and Fig. 7) decreased when plants grew at hotter T , suggesting that thermal
536 acclimation results in changes not only in overall rates of respiration but also in the capacity to produce
537 ATP. The acclimation response was rapid as COX declined in abundance by 24 h after 40°C T transfer
538 in PE leaves (Fig. 5).

539 The decline in COX abundance with hotter growth T is intriguing. If COX activity became
540 rate-limiting, it is likely that more ROS would be produced as the UQ pool would quickly become
541 over-reduced. However, other reports suggest that the UQ redox state is relatively stable, including
542 during changes in T , despite ~~faster~~ higher R_{dark} (Covey-Crump et al., 2007; Wagner & Wagner, 1995).
543 If we assume that UQ redox poise was also stable during the ~~faster~~ greater R_{dark} at the hottest growth
544 T in our experiments, there are two possible explanations. (1) The absolute flux of electrons through
545 COX actually increased despite the decrease in protein abundance. This could be due to COX capacity
546 being far greater than the capacity of the overall mETC. But since increasing T s stimulates the relative
547 activity of enzymes (Copeland, 2000), it is possible that the smaller amount of COX protein had higher
548 activity. In other words, the plants could make do with less COX at hotter T . (2) Alternatively,
549 activation of AOX at the higher T may have occurred to supplement COX activity thereby preventing
550 overload of the UQ pool. Measuring T -dependent *in vivo* ^{18}O fluxes through COX and AOX, as well
551 as leaf ATP content is required to determine terminal oxidase activity and ATP synthesis.
552 Understanding what, if any, biological benefit arises from synthesising less COX at warmer growth T
553 is another important consideration. Alternatively, a reduction in COX might be a consequence of heat
554 directly interfering with its synthesis. In support of this, a recent report shows that COX abundance
555 and capacity in *Arabidopsis* is significantly reduced by knocking out a HSP70 isoform, suggesting that
556 heat in some way interacts with COX formation (Wei et al., 2019).

557

558 *Acclimation of R_{dark} and A_n is asynchronous in rice*

559 The R_{dark}/A_n ratio increased with short-term increases in measuring T (Fig. 8), reflecting the fact that
560 R_{dark} is more temperature dependent than is A_n . R_{dark}/A_n ratios were similar in 25 and 30°C grown leaves,
561 when measured at the prevailing growth T of each treatment (i.e. R_{dark}/A_n was homeostatic). Thus, the
562 acclimation process led to the balance between carbon gain and release being maintained across this
563 moderate range of growth T s (Fig. 8). Acclimation was not, however, sufficient to maintain
564 homeostasis of R_{dark}/A_n in 40°C grown plants (Fig. 8). Similar results of R_{dark}/A_n ratios in leaves and
565 whole plants remaining relatively stable over moderate but not extremely high T have been reported
566 (Atkin, Scheurwater, & Pons, 2006, 2007; Campbell et al., 2007; Drake et al., 2016; Loveys et al.,

2003). Different to past studies, our findings in rice show that homeostasis of R_{dark}/A_n is largely the result of maintenance of A_n more than through a marked reduction in rates of R_{dark} . Our results categorically show A_n acclimates to a greater extent than R_{dark} in rice, supporting previous studies of rice that collectively point to greater A_n than R_{dark} acclimation capacity (Bahuguna et al., 2017; Glaubitz et al., 2014; Kurimoto, Millar, et al., 2004; Mohammed et al., 2013; Nagai & Makino, 2009; Yamori et al., 2010), and field studies that infer limited rice R_{dark} acclimation capacity (Peng et al., 2004; Welch et al., 2010). However, for many plant functional types, including temperate grasses, the opposite occurs; R_{dark} acclimates to a greater extent than A_n (Campbell et al., 2007; Ow, Griffin, Whitehead, Walcroft, & Turnbull, 2008; Way & Oren, 2010; Way & Sage, 2008; Yamori et al., 2005). In this context, it should be noted that the previous studies are of species from temperate rather than tropical habitats, raising the question of whether, beyond rice, tropical grasses generally have asynchronous acclimation favouring A_n . The homeostasis of A_n and superior LER of hot-grown ND rice leaves was more remarkable when viewed alongside evidence that prolonged exposure to drier air was closing stomata and presenting slight reductions in CO_2 availability, at least in PE leaves (Fig. 6). There is evidence that stomata close following a T -dependent increase in VPD_{leaf} , with the mechanism yet uncharacterised but likely involving guard cell sensing of water potential below the epidermis (Peak & Mott, 2010; Shope, Peak, & Mott, 2008). It seems that declining VPD_{leaf} triggers stomatal closure in rice, even with unlimited root water supply.

As noted earlier, in recent years, rice yields have declined in response to increased daily mean T_s , with the decline being more strongly correlated with increasing night rather than day T_s (Peng et al., 2004; Welch et al., 2010). Our finding that A_n is homeostatic across growth T , whereas R_n is not (Table 3) – underpinned by greater acclimation of photosynthesis than respiration – suggests that one reason why yields are declining with increasing night temperatures is because high temperatures stimulate respiratory CO_2 release. This would have a negative effect on daily net carbon gain, and thus the ability to accumulate biomass in the lead up to anthesis.

Potential implications of rice leaf acclimation and starch ~~content~~ concentration on crop yield

We found that soluble sugar ~~contents~~ concentrations of rice leaves were remarkably stable, irrespective of growth T or developmental time at each growth T (Table 2). Maintaining soluble sugar homeostasis is an important physiological requirement for many plant species, achieved through balancing CO_2 uptake and release in source leaves with sugar export to sink tissues (Rolland, Moore, & Sheen, 2002). Homeostasis of sucrose concentrations in rice leaves has been observed even when carbon demand by sink tissues is limited [e.g. reduced partitioning of sugars to grain (Wang et al., 2008)]. In our study, homeostasis of soluble sugar concentrations occurred even at 40°C , where rates of R_{dark} where

601 significantly higher than in plants at the cooler growth T s. Associated with the maintenance of sugar
602 concentrations was a T -dependent decline in starch contentconcentration, both in PE and ND leaves
603 (Table 2). For PE leaves exposed to 40°C, assimilate supply declined, particularly for 40°C transferred
604 leaves, due to a marked increase in R_{dark} and a decline in A_n (Fig. 6). Starch content also significantly
605 declined with developmental duration under high T , contrary to soluble sugar concentrations (Table
606 2). It seems likely, therefore, that the reason soluble sugars did not significantly decline at warmer T
607 for PE leaves – even though assimilate supply fell – was a greater draw-down in the starch pool to
608 maintain soluble sugar contents-concentrations (i.e. a reliance on stored assimilate). Other studies [e.g.
609 on the temperate tree *Populus tremula* (Hüve et al., 2012)] have highlighted the importance of starch
610 degradation in maintaining soluble sugar concentrations, particularly under conditions that stimulate
611 CO₂ release by respiration. Interestingly, in our study, ND leaves exhibited reduced starch content
612 concentrations while also maintaining assimilate supply; one explanation for this might be that the
613 decline in starch and maintenance of sugars of ND leaves was linked to the increased leaf elongation
614 rates we observed for 40°C ND leaves (Fig. 8b), with increased growth (i.e. sink demand) necessitating
615 a greater supply of sugars mediated by the starch pool (Stitt & Zeeman, 2012).

616 The decline in starch content-concentrations for PE and ND leaves at 40°C (Table 2) has
617 interesting implications for rice development and yield. Starch is stored in the stems in the late
618 vegetative stage of rice, and accounts for a large proportion of the carbon accumulated in seeds, a
619 process that is detrimentally affected by heat stress (Blum, Sinmena, Mayer, Golan, & Shpiler, 1994;
620 Impa et al., 2018; Morita & Nakano, 2011; Yang & Zhang, 2005). Other studies using the IR64 cultivar
621 exposed to hot night temperatures have shown an increase in R_{dark} and associated cost to vegetative
622 growth and starch content of panicles, ultimately reducing yield (Bahuguna et al., 2017; Glaubitz et
623 al., 2014). The reduced storage of starch in leaves with increasing T that we observed at the vegetative
624 stage – assuming it did not reflect diversion of starch to stems – would suggest reduced potential for
625 the storage of starch in stems and a penalty to yield of rice growing in warmer environments. This
626 would be particularly true for rice plants exposed to transient extreme T – such as during heat waves –
627 as we postulate the reduction in starch for PE leaves was due to a reduction in assimilate acquisition
628 due to stimulated R_{dark} and suppressed A_n . However, ND leaves did show reduced starch
629 contentconcentration, not as a result of reduced assimilate acquisition, but most likely associated with
630 an increase in growth rates (Table 2; Fig. 8). Thus, it is likely that rice will experience different
631 limitations on yield depending on the duration of thermal changes, with shorter-term exposure to rising
632 T – over a period in which tissue cannot develop anew – likely leading to a greater suppression of yield
633 than leaves developed under the prevailing growth T . Rice may even experience increased yield with

634 sustained mild warming of both night and particularly day T . However, yield potential is dependent on
635 whether heat-dependent changes in growth at the vegetative stage of rice positively contributes to yield,
636 which may be true (Glaubitz et al., 2014; Scafaro et al., 2018), and not simply accelerate development
637 and shorten the time to flowering.

638

639 *Conclusions*

640 Overall, the results we present here demonstrate that both leaf respiration and photosynthesis can
641 acclimate in rice but the extent of acclimation is asynchronous and dependent on the timeframe of T
642 exposure. Warmer growth T of 40°C relative to 25°C will have a greater impact on rice CO₂ flux,
643 metabolic pathways, starch ~~concentration~~ and ultimately growth. Consequently, rice growing
644 in a warmer climate with more extreme heating events will likely experience T -dependent alterations
645 in growth and yield. The duration and intensity of T changes, together with complex interactions
646 between assimilate acquisition, storage and utilisation will determine if this warmer environment will
647 be beneficial or detrimental to rice productivity over the coming decades. We suggest that enhancing
648 the acclimation capacity of R_{dark} for rice at warmer growth T – potentially through COX, AOX and
649 UCP regulation – could be a key target for improving rice productivity in a warmer world.

650

651 **Acknowledgements**

652

653 We thank Assoc. Prof Spencer Whitney for providing Rubisco antibody. The support of the Australian
654 Research Council (ARC) Centre of Excellence in Plant Energy Biology (CE140100008) to OA, BP
655 and JM is acknowledged. The authors have no conflict of interest to declare.

656

657

658 **References**

659

- 660 Abramoff, M. D., Magelhaes, P. J., & Ram, S. J. (2004). Image Processing with ImageJ.
661 *Biophotonics International*, 11(7), 36-42.
- 662 Armstrong, A. F., Badger, M. R., Day, D. A., Barthelet, M. M., Smith, P. M. C., Millar, A. H., . . .
663 Atkin, O. K. (2008). Dynamic changes in the mitochondrial electron transport chain
664 underpinning cold acclimation of leaf respiration. *Plant, Cell & Environment*, 31(8), 1156-
665 1169.
- 666 Atkin, O. K., Bruhn, D., Hurry, V. M., & Tjoelker, M. G. (2005). Evans Review No. 2: The hot and
667 the cold: unravelling the variable response of plant respiration to temperature. *Functional*
668 *Plant Biology*, 32(2), 87-105.

- 669 Atkin, O. K., Scheurwater, I., & Pons, T. L. (2006). High thermal acclimation potential of both
 670 photosynthesis and respiration in two lowland *Plantago* species in contrast to an alpine
 671 congeneric. *Global Change Biology*, *12*(3), 500-515.
- 672 Atkin, O. K., Scheurwater, I., & Pons, T. L. (2007). Respiration as a percentage of daily
 673 photosynthesis in whole plants is homeostatic at moderate, but not high, growth temperatures.
 674 *New Phytologist*, *174*(2), 367-380.
- 675 Atkin, O. K., & Tjoelker, M. G. (2003). Thermal acclimation and the dynamic response of plant
 676 respiration to temperature. *Trends in Plant Science*, *8*(7), 343-351.
- 677 Badger, M. R., Björkman, O., & Armond, P. A. (1982). An analysis of photosynthetic response and
 678 adaptation to temperature in higher plants: temperature acclimation in the desert evergreen
 679 *Nerium oleander* L*. *Plant, Cell & Environment*, *5*(1), 85-99.
- 680 Bahuguna, R. N., Solis, C. A., Shi, W., & Jagadish, K. S. V. (2017). Post-flowering night respiration
 681 and altered sink activity account for high night temperature-induced grain yield and quality
 682 loss in rice (*Oryza sativa* L.). *Physiologia Plantarum*, *159*(1), 59-73.
- 683 Berry, J., & Bjorkman, O. (1980). Photosynthetic response and adaptation to temperature in higher
 684 plants. *Annual Review of Plant Physiology*, *31*(1), 491-543.
- 685 Bhardwaj, A. R., Joshi, G., Kukreja, B., Malik, V., Arora, P., Pandey, R., . . . Agarwal, M. (2015).
 686 Global insights into high temperature and drought stress regulated genes by RNA-Seq in
 687 economically important oilseed crop Brassica juncea. *BMC Plant Biology*, *15*(1), 9.
- 688 Blum, A., Sinmena, B., Mayer, J., Golan, G., & Shpiler, L. (1994). Stem reserve mobilisation
 689 supports wheat-grain filling under heat stress. *Functional Plant Biology*, *21*(6), 771-781.
- 690 Campbell, C., Atkinson, L., Zaragoza-Castells, J., Lundmark, M., Atkin, O., & Hurry, V. (2007).
 691 Acclimation of photosynthesis and respiration is asynchronous in response to changes in
 692 temperature regardless of plant functional group. *New Phytologist*, *176*(2), 375-389.
- 693 Clifton, R., Millar, A. H., & Whelan, J. (2006). Alternative oxidases in Arabidopsis: A comparative
 694 analysis of differential expression in the gene family provides new insights into function of
 695 non-phosphorylating bypasses. *Biochimica et Biophysica Acta (BBA) - Bioenergetics*,
 696 *1757*(7), 730-741.
- 697 Copeland, R. A. (2000). *Enzymes: A Practical Introduction to Structure, Mechanism, and Data*
 698 *Analysis* (Second Edition ed.). New York, NY: JOHN WILEY & SONS.
- 699 Covey-Crump, E. M., Bykova, N. V., Affourtit, C., Hoefnagel, M. H. N., Gardeström, P., & Atkin,
 700 O. K. (2007). Temperature-dependent changes in respiration rates and redox poise of the
 701 ubiquinone pool in protoplasts and isolated mitochondria of potato leaves. *Physiologia*
 702 *Plantarum*, *129*(1), 175-184.
- 703 CSIRO, & BOM. (2018). *State of the Climate 2018*. Retrieved from Canberra, Australia:
 704 [https://www.csiro.au/en/Research/OandA/Areas/Assessing-our-climate/State-of-the-Climite-](https://www.csiro.au/en/Research/OandA/Areas/Assessing-our-climate/State-of-the-Climite-2018)
 705 [2018](https://www.csiro.au/en/Research/OandA/Areas/Assessing-our-climate/State-of-the-Climite-2018)
- 706 Drake, J. E., Tjoelker, M. G., Aspinwall, M. J., Reich, P. B., Barton, C. V. M., Medlyn, B. E., &
 707 Duursma, R. A. (2016). Does physiological acclimation to climate warming stabilize the ratio
 708 of canopy respiration to photosynthesis? *New Phytologist*, *211*(3), 850-863.
- 709 Glaubitz, U., Li, X., Köhl, K. I., van Dongen, J. T., Hinch, D. K., & Zuther, E. (2014). Differential
 710 physiological responses of different rice (*Oryza sativa*) cultivars to elevated night
 711 temperature during vegetative growth. *Functional Plant Biology*, *41*(4), 437-448.
- 712 Godfray, H. C. J., Beddington, J. R., Crute, I. R., Haddad, L., Lawrence, D., Muir, J. F., . . . Toulmin,
 713 C. (2010). Food security: the challenge of feeding 9 billion people. *Science*, *327*(5967), 812-
 714 818.
- 715 Gorsuch, P. A., Pandey, S., & Atkin, O. K. (2010). Temporal heterogeneity of cold acclimation
 716 phenotypes in Arabidopsis leaves. *Plant, Cell & Environment*, *33*(2), 244-258.
- 717 Hartmann, D. L., A.M.G. Klein Tank, M. Rusticucci, L.V. Alexander, S. Brönnimann, Y.
 718 Charabi, . . . Zhai, P. M. (2013). *Observations: Atmosphere and Surface*. In: *Climate Change*

- 719 2013: *The Physical Science Basis. Contribution of Working Group I to the Fifth Assessment*
720 *Report of the Intergovernmental Panel on Climate Change*. Retrieved from Cambridge,
721 United Kingdom and New York, NY, USA:
- 722 Hikosaka, K., Ishikawa, K., Borjigidai, A., Muller, O., & Onoda, Y. (2006). Temperature
723 acclimation of photosynthesis: mechanisms involved in the changes in temperature
724 dependence of photosynthetic rate. *Journal of Experimental Botany*, *57*(2), 291-302.
- 725 Hu, T., Sun, X., Zhang, X., Nevo, E., & Fu, J. (2014). An RNA sequencing transcriptome analysis of
726 the high-temperature stressed tall fescue reveals novel insights into plant thermotolerance.
727 *BMC Genomics*, *15*(1), 1147.
- 728 Hubbart, S., Peng, S., Horton, P., Chen, Y., & Murchie, E. H. (2007). Trends in leaf photosynthesis
729 in historical rice varieties developed in the Philippines since 1966. *Journal of Experimental*
730 *Botany*, *58*(12), 3429-3438.
- 731 Hüve, K., Bichele, I., Ivanova, H., Keerberg, O., Pärnik, T., Rasulov, B., . . . Niinemets, Ü. (2012).
732 Temperature responses of dark respiration in relation to leaf sugar concentration. *Physiologia*
733 *Plantarum*, *144*(4), 320-334.
- 734 Impa, S. M., Sunoj, V. S. J., Krassovskaya, I., Bheemanahalli, R., Obata, T., & Jagadish, S. V. K.
735 (2018). Carbon balance and source-sink metabolic changes in winter wheat exposed to high
736 night-time temperature. *Plant, Cell & Environment*, *0*(ja).
- 737 Krauss, S., Zhang, C.-Y., & Lowell, B. B. (2005). The mitochondrial uncoupling-protein
738 homologues. *Nature Reviews Molecular Cell Biology*, *6*, 248.
- 739 Kurimoto, K., Day, D. A., Lambers, H., & Noguchi, K. (2004). Effect of respiratory homeostasis on
740 plant growth in cultivars of wheat and rice. *Plant, Cell & Environment*, *27*(7), 853-862.
- 741 Kurimoto, K., Millar, A. H., Lambers, H., Day, D. A., & Noguchi, K. (2004). Maintenance of growth
742 rate at low temperature in rice and wheat cultivars with a high degree of respiratory
743 homeostasis is associated with a high efficiency of respiratory ATP production. *Plant and*
744 *Cell Physiology*, *45*(8), 1015-1022.
- 745 Lanning, S. B., Siebenmorgen, T. J., Counce, P. A., Ambardekar, A. A., & Mauromoustakos, A.
746 (2011). Extreme nighttime air temperatures in 2010 impact rice chalkiness and milling
747 quality. *Field Crops Research*, *124*(1), 132-136.
- 748 Law, C. W., Chen, Y., Shi, W., & Smyth, G. K. (2014). voom: precision weights unlock linear model
749 analysis tools for RNA-seq read counts. *Genome Biology*, *15*(2), R29.
- 750 Li, H., Handsaker, B., Wysoker, A., Fennell, T., Ruan, J., Homer, N., . . . Genome Project Data
751 Processing, S. (2009). The Sequence Alignment/Map format and SAMtools. *Bioinformatics*,
752 *25*(16), 2078-2079.
- 753 Liao, Y., Smyth, G. K., & Shi, W. (2013a). featureCounts: an efficient general purpose program for
754 assigning sequence reads to genomic features. *Bioinformatics*, *30*(7), 923-930.
- 755 Liao, Y., Smyth, G. K., & Shi, W. (2013b). The Subread aligner: fast, accurate and scalable read
756 mapping by seed-and-vote. *Nucleic Acids Research*, *41*(10), e108-e108.
- 757 Loveys, B. R., Atkinson, L. J., Sherlock, D. J., Roberts, R. L., Fitter, A. H., & Atkin, O. K. (2003).
758 Thermal acclimation of leaf and root respiration: an investigation comparing inherently fast-
759 and slow-growing plant species. *Global Change Biology*, *9*(6), 895-910.
- 760 McCarthy, D. J., Chen, Y., & Smyth, G. K. (2012). Differential expression analysis of multifactor
761 RNA-Seq experiments with respect to biological variation. *Nucleic Acids Research*, *40*(10),
762 4288-4297.
- 763 Mohammed, R., Cothren, J. T., & Tarpley, L. (2013). High night temperature and abscisic acid affect
764 rice productivity through altered photosynthesis, respiration and spikelet fertility. *Crop*
765 *Science*, *53*(6), 2603-2612.
- 766 Morimoto, R. I. (1998). Regulation of the heat shock transcriptional response: cross talk between a
767 family of heat shock factors, molecular chaperones, and negative regulators. *Genes &*
768 *Development*, *12*(24), 3788-3796.

- 769 Morita, S., & Nakano, H. (2011). Nonstructural carbohydrate content in the stem at full heading
770 contributes to high performance of ripening in heat-tolerant rice cultivar Nikomaru. *Crop*
771 *Science*, *51*(2), 818-828.
- 772 Murakami, Y., & Toriyama, K. (2008). Enhanced high temperature tolerance in transgenic rice
773 seedlings with elevated levels of alternative oxidase, OsAOX1a. *Plant Biotechnology*, *25*(4),
774 361-364.
- 775 Nagai, T., & Makino, A. (2009). Differences Between Rice and Wheat in Temperature Responses of
776 Photosynthesis and Plant Growth. *Plant & Cell Physiology*, *50*(4), 744-755.
- 777 Neilson, K. A., Mariani, M., & Haynes, P. A. (2011). Quantitative proteomic analysis of cold-
778 responsive proteins in rice. *Proteomics*, *11*(9), 1696-1706.
- 779 Noguchi, K. O., Taylor, N. L., Millar, A. H., Lambers, H., & Day, D. A. (2005). Response of
780 mitochondria to light intensity in the leaves of sun and shade species. *Plant, Cell &*
781 *Environment*, *28*(6), 760-771.
- 782 O'Leary, B. M., Asao, S., Millar, A. H., & Atkin, Owen K. (2018). Core principles which explain
783 variation in respiration across biological scales. *New Phytologist*, *0*(0).
- 784 O'sullivan, O. S., Weerasinghe, K. W. L. K., Evans, J. R., Egerton, J. J. G., Tjoelker, M. G., & Atkin,
785 O. K. (2013). High-resolution temperature responses of leaf respiration in snow gum
786 (*Eucalyptus pauciflora*) reveal high-temperature limits to respiratory function. *Plant, Cell &*
787 *Environment*, *36*(7), 1268-1284.
- 788 Ohama, N., Sato, H., Shinozaki, K., & Yamaguchi-Shinozaki, K. (2017). Transcriptional Regulatory
789 Network of Plant Heat Stress Response. *Trends in Plant Science*, *22*(1), 53-65.
- 790 Ow, L. F., Griffin, K. L., Whitehead, D., Walcroft, A. S., & Turnbull, M. H. (2008). Thermal
791 acclimation of leaf respiration but not photosynthesis in *Populus deltoides* × *nigra*. *New*
792 *Phytologist*, *178*(1), 123-134.
- 793 Peak, D., & Mott, K. A. (2010). A new, vapour-phase mechanism for stomatal responses to humidity
794 and temperature. *Plant, Cell & Environment*, *34*(1), 162-178.
- 795 Peng, S., Huang, J., Sheehy, J. E., Laza, R. C., Visperas, R. M., Zhong, X., . . . Cassman, K. G.
796 (2004). Rice yields decline with higher night temperature from global warming. *Proceedings*
797 *of the National Academy of Sciences of the United States of America*, *101*(27), 9971-9975.
- 798 Posch, B. C., Kariyawasam, B. C., Bramley, H., Coast, O., Richards, R. A., Reynolds, M. P., . . .
799 Atkin, O. K. (2019). Exploring high temperature responses of photosynthesis and respiration
800 to improve heat tolerance in wheat. *Journal of Experimental Botany*, *70*(19), 5051-5069.
- 801 Quinlan, A. R., & Hall, I. M. (2010). BEDTools: a flexible suite of utilities for comparing genomic
802 features. *Bioinformatics*, *26*(6), 841-842.
- 803 Ramakers, C., Ruijter, J. M., Deprez, R. H. L., & Moorman, A. F. M. (2003). Assumption-free
804 analysis of quantitative real-time polymerase chain reaction (PCR) data. *Neuroscience*
805 *Letters*, *339*(1), 62-66.
- 806 Reich, P. B., Sendall, K. M., Stefanski, A., Wei, X., Rich, R. L., & Montgomery, R. A. (2016).
807 Boreal and temperate trees show strong acclimation of respiration to warming. *Nature*,
808 *531*(7596), 633-636.
- 809 Robinson, J. T., Thorvaldsdóttir, H., Winckler, W., Guttman, M., Lander, E. S., Getz, G., & Mesirov,
810 J. P. (2011). Integrative genomics viewer. *Nature Biotechnology*, *29*(1), 24-26.
- 811 Robinson, M. D., & Oshlack, A. (2010). A scaling normalization method for differential expression
812 analysis of RNA-seq data. *Genome Biology*, *11*(3), R25.
- 813 Robinson, M. D., & Smyth, G. K. (2007a). Moderated statistical tests for assessing differences in tag
814 abundance. *Bioinformatics*, *23*(21), 2881-2887.
- 815 Robinson, M. D., & Smyth, G. K. (2007b). Small-sample estimation of negative binomial dispersion,
816 with applications to SAGE data. *Biostatistics*, *9*(2), 321-332.
- 817 Rolland, F., Moore, B., & Sheen, J. (2002). Sugar Sensing and Signaling in Plants. *The Plant Cell*,
818 *14*, S185-S205.

- 819 Ruijter, J. M., Ramakers, C., Hoogaars, W. M. H., Karlen, Y., Bakker, O., van den Hoff, M. J. B., &
820 Moorman, A. F. M. (2009). Amplification efficiency: linking baseline and bias in the analysis
821 of quantitative PCR data. *Nucleic Acids Research*, *37*(6), e45-e45.
- 822 Scafaro, A. P., & Atkin, O. K. (2016). The Impact of Heat Stress on the Proteome of Crop Species.
823 In G. H. Salekdeh (Ed.), *Agricultural Proteomics Volume 2: Environmental Stresses* (pp.
824 155-175). Cham: Springer International Publishing.
- 825 Scafaro, A. P., Atwell, B. J., Muylaert, S., Reusel, B. V., Ruiz, G. A., Van Rie, J., & Gallé, A.
826 (2018). A thermotolerant variant of rubisco activase from a wild relative improves growth
827 and seed yield in rice under heat stress. *Frontiers in Plant Science*, *9*, 1663.
- 828 Scafaro, A. P., Xiang, S., Long, B. M., Bahar, N. H. A., Weerasinghe, L. K., Creek, D., . . . Atkin, O.
829 K. (2017). Strong thermal acclimation of photosynthesis in tropical and temperate wet-forest
830 tree species: the importance of altered Rubisco content. *Global Change Biology*, *23*(7), 2783-
831 2800.
- 832 Seck, P. A., Diagne, A., Mohanty, S., & Wopereis, M. C. S. (2012). Crops that feed the world 7:
833 Rice. *Food Security*, *4*(1), 7-24.
- 834 Shane, M. W., Cramer, M. D., Funayama-Noguchi, S., Cawthray, G. R., Millar, A. H., Day, D. A., &
835 Lambers, H. (2004). Developmental physiology of cluster-root carboxylate synthesis and
836 exudation in *harsh hakea*. Expression of phosphoenolpyruvate carboxylase and the
837 alternative oxidase. *Plant Physiology*, *135*(1), 549.
- 838 Shapiguzov, A., Vainonen, J. P., Hunter, K., Tossavainen, H., Tiwari, A., Järvi, S., . . . Kangasjärvi,
839 J. (2019). Arabidopsis RCD1 coordinates chloroplast and mitochondrial functions through
840 interaction with ANAC transcription factors. *eLife*, *8*, e43284.
- 841 Shen, C., Li, D., He, R., Fang, Z., Xia, Y., Gao, J., . . . Cao, M. (2014). Comparative transcriptome
842 analysis of RNA-seq data for cold-tolerant and cold-sensitive rice genotypes under cold
843 stress. *Journal of Plant Biology*, *57*(6), 337-348.
- 844 Shope, J. C., Peak, D., & Mott, K. A. (2008). Stomatal responses to humidity in isolated epidermes.
845 *Plant, Cell & Environment*, *31*(9), 1290-1298.
- 846 Sidaway-Lee, K., Costa, M. J., Rand, D. A., Finkenstadt, B., & Penfield, S. (2014). Direct
847 measurement of transcription rates reveals multiple mechanisms for configuration of the
848 Arabidopsis ambient temperature response. *Genome Biology*, *15*(3), R45.
- 849 Siedow, J. N., & Umbach, A. L. (2000). The mitochondrial cyanide-resistant oxidase: structural
850 conservation amid regulatory diversity. *Biochimica et Biophysica Acta (BBA) -*
851 *Bioenergetics*, *1459*(2), 432-439.
- 852 Smith, N. G., & Dukes, J. S. (2017). Short-term acclimation to warmer temperatures accelerates leaf
853 carbon exchange processes across plant types. *Global Change Biology*, *23*(11), 4840-4853.
- 854 Smyth, G. K., Michaud, J., & Scott, H. S. (2005). Use of within-array replicate spots for assessing
855 differential expression in microarray experiments. *Bioinformatics*, *21*(9), 2067-2075.
- 856 Stitt, M., & Zeeman, S. C. (2012). Starch turnover: pathways, regulation and role in growth. *Current*
857 *Opinion in Plant Biology*, *15*(3), 282-292.
- 858 Strand, A., Hurry, V., Henkes, S., Huner, N., Gustafsson, P., Gardstrom, P., & Stitt, M. (1999).
859 Acclimation of Arabidopsis leaves developing at low temperatures. Increasing cytoplasmic
860 volume accompanies increased activities of enzymes in the calvin cycle and in the sucrose-
861 biosynthesis pathway. *Plant Physiology*, *119*(4), 1387-1398.
- 862 Thimm, O., Bläsing, O., Gibon, Y., Nagel, A., Meyer, S., Krüger, P., . . . Stitt, M. (2004). mapman: a
863 user-driven tool to display genomics data sets onto diagrams of metabolic pathways and other
864 biological processes. *The Plant Journal*, *37*(6), 914-939.
- 865 Tjoelker, M. G., Oleksyn, J., & Reich, P. B. (2001). Modelling respiration of vegetation: evidence
866 for a general temperature-dependent Q₁₀. *Global Change Biology*, *7*(2), 223-230.

- 867 Tjoelker, M. G., Reich, P. B., & Oleksyn, J. (1999). Changes in leaf nitrogen and carbohydrates
868 underlie temperature and CO₂ acclimation of dark respiration in five boreal tree species.
869 *Plant, Cell & Environment*, 22(7), 767-778.
- 870 Vanlerberghe, C. G. (2013). Alternative oxidase: A mitochondrial respiratory pathway to maintain
871 metabolic and signaling homeostasis during abiotic and biotic stress in plants. *International*
872 *Journal of Molecular Sciences*, 14(4).
- 873 Wagner, A. M., & Wagner, M. J. (1995). Measurements of *in vivo* ubiquinone reduction levels in
874 plant cells. *Plant Physiology*, 108(1), 277.
- 875 Wang, E., Wang, J., Zhu, X., Hao, W., Wang, L., Li, Q., . . . He, Z. (2008). Control of rice grain-
876 filling and yield by a gene with a potential signature of domestication. *Nature Genetics*, 40,
877 1370.
- 878 Way, D. A., & Oren, R. (2010). Differential responses to changes in growth temperature between
879 trees from different functional groups and biomes: a review and synthesis of data. *Tree*
880 *Physiology*, 30(6), 669-688.
- 881 Way, D. A., & Sage, R. F. (2008). Thermal acclimation of photosynthesis in black spruce [*Picea*
882 *mariana* (Mill.) B.S.P.]. *Plant, Cell & Environment*, 31(9), 1250-1262.
- 883 Wei, S.-S., Niu, W.-T., Zhai, X.-T., Liang, W.-Q., Xu, M., Fan, X., . . . Li, B. (2019). Arabidopsis
884 mtHSC70-1 plays important roles in the establishment of COX-dependent respiration and
885 redox homeostasis. *Journal of Experimental Botany*, 70(20), 5575-5590.
- 886 Welch, J. R., Vincent, J. R., Auffhammer, M., Moya, P. F., Dobermann, A., & Dawe, D. (2010).
887 Rice yields in tropical/subtropical Asia exhibit large but opposing sensitivities to minimum
888 and maximum temperatures. *Proceedings of the National Academy of Sciences*, 107(33),
889 14562-14567.
- 890 Yamori, W., Noguchi, K., Hikosaka, K., & Terashima, I. (2010). Phenotypic plasticity in
891 photosynthetic temperature acclimation among crop species with different cold tolerances.
892 *Plant Physiology*, 152(1), 388-399.
- 893 Yamori, W., Noguchi, K., & Terashima, I. (2005). Temperature acclimation of photosynthesis in
894 spinach leaves: analyses of photosynthetic components and temperature dependencies of
895 photosynthetic partial reactions. *Plant, Cell & Environment*, 28(4), 536-547.
- 896 Yang, J., & Zhang, J. (2005). Grain filling of cereals under soil drying. *New Phytologist*, 169(2),
897 223-236.
- 898 Yoshida, S. (1972). Physiological aspects of grain yield. *Annual review of Plant Physiology*, 23, 437-
899 464.
- 900 Zhu, J., Dong, C.-H., & Zhu, J.-K. (2007). Interplay between cold-responsive gene regulation,
901 metabolism and RNA processing during plant cold acclimation. *Current Opinion in Plant*
902 *Biology*, 10(3), 290-295.

903
904
905
906
907
908
909
910
911
912

913
914
915
916
917
918
919
920
921
922
923
924
925
926
927
928
929
930
931
932
933

Table 1. Differential expression of respiration genes in leaves after exposure to *T* of 40°C relative to 30°C. Differential expression defined as FDR < 0.05, marked as '*'. Electron transport chain (ETC), Pentose Phosphate Pathway (PPP). No TCA cycle genes were differentially expressed.

Pathway	Gene_name	locus	Log2 fold-change	
			2 hours	6 hours
ETC	Complex II (Succinate dehydrogenase)	LOC_Os08g02640	-0.55*	-0.58*
ETC	External NAD(P)H dehydrogenase	LOC_Os06g47000	0.72*	0.44
ETC	Uncoupling protein	LOC_Os11g48040	0.81*	0.46
ETC	Alternative oxidase	LOC_Os02g47200	-0.99*	-1.91*
glycolysis	ATP-dependent phosphofructokinase	LOC_Os01g53680	-0.11	-1.13*
glycolysis	Phosphoglycerate kinase	LOC_Os02g07260	0.78*	0.39
glycolysis	Enolase	LOC_Os10g08550	0.61*	0.34
PPP	Ribulose 5-phosphate 3-epimerase	LOC_Os09g32810	0.53*	0.87*

934
935
936
937
938
939
940
941
942
943
944
945
946
947
948
949
950
951

Table 2. Leaf mass per unit area (LMA), starch and soluble sugars of pre-existing (PE) leaves transferred from 30/25°C to 25/20°C or 40/35°C for one and seven days, and leaves newly-developed (ND) at the prevailing *T*. Data represents mean of three or four separate leaves from separate previously unsampled plants \pm SE. The *F*-values and *P*-values of a two-way ANOVA comparing *T*, developmental stage (*D*) and any interaction (*T* \times *D*) are reported with asterisks indicating significance at *P*<0.05.

		LMA (g m ⁻²)	Starch (mg g ⁻¹ DM)	Soluble sugar (mg g ⁻¹ DM)
25/20°C	Day 1	20 \pm 3	11.3 \pm 1.9	13.5 \pm 0.2
	Day 7	19 \pm 2	5.5 \pm 0.3	11.2 \pm 0.1
	ND	30 \pm 2	14.4 \pm 3.0	11.1 \pm 0.2
30/25°C	Day 1	19 \pm 2	14.9 \pm 2.1	13.0 \pm 0.5
	Day 7	21 \pm 2	4.9 \pm 1.0	10.5 \pm 0.2
	ND	28 \pm 0.4	9.6 \pm 1.6	11.0 \pm 0.6
40/35°C	Day 1	18 \pm 2	8.5 \pm 0.4	11.9 \pm 0.2
	Day 7	23 \pm 2	3.5 \pm 0.3	10.9 \pm 0.3
	ND	29 \pm 1	6.7 \pm 0.5	11.6 \pm 0.3
<i>T</i> \times <i>D</i>		<i>F</i> =0.7, <i>P</i> =0.6	<i>F</i> =1.7, <i>P</i> =0.14	<i>F</i> =0.01, <i>P</i> =0.99
<i>D</i>		<i>F</i> =28, <i>P</i> <0.001*	<i>F</i> =13, <i>P</i> <0.001*	<i>F</i> =0.14, <i>P</i> =0.94
<i>T</i>		<i>F</i> =0.1, <i>P</i> =0.9	<i>F</i> =4.2, <i>P</i> =0.03*	<i>F</i> =0.01, <i>P</i> =0.99

952
953
954
955
956
957
958
959
960
961
962
963
964
965
966
967
968
969
970
971
972

Table 3. Summary of key photosynthetic and respiratory parameters generated from temperature-response curves. Parameters are: leaf mass per area; the temperature at which R_{dark} and A_n exhibited maximum rates (T_{max} and T_{opt} , respectively); the maximum rates of R_{dark} and A_n reached (R_{max} and A_{opt} , respectively); rates of R_{dark} and A_n at the prevailing growth temperature; and, the temperature at which PSII lost functionality as determined by an increase in basal fluorescence (T_{crit}). Data represents means of three or four separate leaves from separate plants \pm SE and statistical data (F -value and P -value) based on one-way ANOVA of temperature treatment effect. Superscript letters show significant differences between the T treatments according to a Tukey test.

	25/20°C	30/25°C	40/30°C	F -value	P -value
LMA (g m^{-2})	33 \pm 2	30 \pm 2	35 \pm 3	1.4	0.31
T_{max} (°C)	51 \pm 1 ^a	54 \pm 1 ^{a,b}	55 \pm 1 ^b	4.7	0.04*
T_{opt} (°C)	29 \pm 1 ^a	31 \pm 1 ^{a,b}	33 \pm 0.3 ^b	6.1	0.04*
R_{max} ($\mu\text{mol g}^{-1} \text{DM s}^{-1} \times 10^{-3}$)	120 \pm 5	117 \pm 6	121 \pm 2	0.16	0.86
A_{opt} ($\mu\text{mol g}^{-1} \text{DM s}^{-1}$)	0.65 \pm 0.05	0.67 \pm 0.02	0.69 \pm 0.04	0.28	0.76

R_{dark} ($\mu\text{mol g}^{-1} \text{DM s}^{-1} \times 10^{-3}$)	24 \pm 3 ^a	27 \pm 3 ^a	57 \pm 2 ^b	35	<0.001*
A_n ($\mu\text{mol m}^{-2} \text{s}^{-1}$)	0.62 \pm 0.04	0.67 \pm 0.02	0.65 \pm 0.04	0.52	0.62
T_{crit} ($^{\circ}\text{C}$)	46.0 \pm 0.6	46.9 \pm 0.9	49.8 \pm 1.5	3.726	0.089

973

974

975

976

977

978

979

980

981

982

983

984

985

986

987

988

989

990

991 **Figure Legends**

992

993 **Figure 1.** Quantitative PCR analysis of gene expression over the first 168 hours (7 days) after transfer
 994 of leaves from 30/25 $^{\circ}\text{C}$ to 25/20 $^{\circ}\text{C}$ or 40/35 $^{\circ}\text{C}$. Genes analysed were: the respiratory cytochrome *c*
 995 complex (*cox*) subunit II, alternative oxidase complex (*aox*) and uncoupling protein (*ucp*); the
 996 photosynthetic genes ferredoxin NADH reductase (*fnr*) and phosphoribulose kinase (*prk*); and the
 997 sugar metabolism gene sucrose phosphatase synthase (*sps*). Gene expression was revitalised at each
 998 time-point to the non-transferred 30/25 $^{\circ}\text{C}$ control.

999

1000 **Figure 2.** Principal component analysis of normalised RNA-seq expression values for each sample
 1001 following temperature treatment for (a) 2 hours and (b) 6 hours. Samples are coloured by treatment,
 1002 day/night temperatures of 30/25 $^{\circ}\text{C}$ (control), 40/35 $^{\circ}\text{C}$ (hot), and 25/20 $^{\circ}\text{C}$ (cold). The y-axis is principle

component 1 (PC1) and the x axis is principle component 2 (PC2); the percent of variation explained by each axis is indicated. RNA-seq libraries were normalised using *edgeR* (“TMM” method) and *voom* transformation, scaled by unit variance and clustered using singular value decomposition.

Figure 3. Identification of genes differentially expressed during temperature treatments. (a, b) Common and time point specific differentially expressed genes under heat treatment (40/35°C). The overlap between genes differentially expressed at 2 and 6 h under heat treatment for (a) upregulated genes and (b) downregulated genes. ‘*’ indicates significant overlap $p \ll 0.001$, fisher’s one-tailed exact test (hypergeometric). (c) Hierarchical clustering of differentially expressed genes. For each time point (2, 6 and 24 h) differentially expressed genes were determined for both the hot (40/35°C) and cold (25/20°C) temperature treatments relative to the 30/25°C control conditions (FDR < 0.05). For each differentially expressed gene, the relative fold-change under each condition over the time series is then displayed on a log₂ scale: red = upregulated, blue = downregulated.

Figure 4. Gene ontology (GO) term enrichment among genes differentially upregulated (a) or downregulated (b) genes after 2 h at 40°C. Ontological annotations downloaded from MSU and ontology enrichment tests performed with topGO in R using the Fisher standard test (one-tailed fisher’s exact test/ hypergeometric test) with post hoc p value correction for multiple testing using the Benjamini & Hochberg method.

Figure 5. Abundance of mitochondrial electron transport chain proteins and Rubisco determined by Western blot analysis for rice leaves sampled at different developmental stages of; PE leaves six and 24 h after *T* transfer to 25/20°C or 40/35°C, and leaves newly developed (ND) post *T*-transfer. (a) Abundance of CYTOCHROME C OXIDASE (COX) subunit II, (b) ALTERNATIVE OXIDASE (AOX), (c) UNCOUPLING PROTEIN (UCP) and (d) Rubisco large subunit on a leaf area basis with data normalised by adjusting the largest value in each dataset to 100. Data represent mean ± SE of four independent western blots, with each blot representing leaf tissue from a separate plant. The *P*-values of a two-way ANOVA comparing temperature (*T*), developmental stage (*D*) and the interaction between the two (*T*×*D*) are reported on each graph. Representative blots are presented in Figure S5.

Figure 6. Rates of dry mass (DM) based dark respiration (R_{dark} ; a), net photosynthesis (A_n ; b), Relative humidity (RH; c), vapour pressure deficit between the leaf and surrounding air (VPD_{Leaf} ; d), and stomatal conductance (g_s ; e), and ratio of intercellular to ambient CO₂ concentrations (C_i/C_a ; f)

1036 measured at the respective day-time growth temperature of each treatment just prior to (day 0), and 1,
1037 2, 3, 5 and 7-days after transfer of control 30/25°C day/night grown leaves to either 25/20°C, 40/35°C
1038 or maintained at 30/25°C. Values are means of four biological replicates \pm SE.

1039

1040 **Figure 7.** Temperature-response curves (a, b) of dark respiration (R_{dark}) and (c, d) net photosynthesis
1041 (A_n), on a dry mass (DM) basis. Values are absolute (a, c) or normalised to values at 30°C (b, d).
1042 Measurements were made on whole newly-developed (ND) leaves growing for 21 d at day/night
1043 temperatures of 25/20°C, 30/25°C or 40/35°C. Curves fitted to R_{dark} and A_n are quadratic functions.
1044 Calculated acclimation parameters from the curves are presented in Table 3. Rates were recorded every
1045 30 sec as leaves were heated at 1°C per minute. Filled area represent standard error of three to four
1046 biological replicates.

1047

1048 **Figure 8.** The percentage of dark respiration (R_{dark}) relative to light-saturated net assimilation (A_n) (a),
1049 and leaf elongation rates (LER) over a 24 h day/night cycle (b), for ND leaves growing for 21 d at
1050 day/night temperatures of 25/20°C, 30/25°C or 40/35°C. For the R_{dark}/A_n ratio values are calculated
1051 from the absolute means presented in Figure 7. For LER the dark (night) period of the 24 h cycle is
1052 shaded in grey and values are the means \pm SE of four plant replicates.

1053